Numerical Methods for Treating Quasistatic Linear Viscoelastic Problems

A thesis submitted for the degree of Doctor of Philosophy

by

Settapat Chinviriyasit

Department of Mathematical Sciences, Brunel University

October 2001

Acknowledgements

I would like to express my gratitude to my supervisor, Professor J. R. Whiteman for his guidance, supervision and encouragement during this work. Special thanks also go to my second supervisor, Dr. M.K. Warby for his additional help and technical aid.

This is a pleasant opportunity to thank Professor E. H. Twizell for his lectures on numerical analysis and Dr. S. Shaw for some help. I wish to express my gratitude to King Mongkut's University of Technology Thonburi for the scholarship and support provided throughout the duration of this thesis. I also would like to thank the staff in the Department of Mathematical Sciences here at Brunel and my friends both in academia and elsewhere for making my research time enjoyable.

Finally, I would like thank Dr. Wirawan Piyawong for her constant encouragement and support during my study and my sincere thanks also go to my family who have been not only supportive but also encouraging and understanding at all times; this could not have been done without you.

Abstract

In this thesis we study the linear quasistatic compressible viscoelasticity problem described in terms of an elliptic partial differential equation with a Volterra (memory) term. Two mathematical models of the problem based respectively on the works of Janvosky *et al.* [16] and Shaw *et al.* [37] are discussed. These are each discretised to produce numerical schemes for approximating the viscoelasticity problem.

The first model is called an *ODE formulation* and is derived by exploiting the relaxation function, which is quasi-separable, to recast the Volterra equation as a system of ordinary differential equations. For the special case of a linear viscoelastic, homogeneous, non-ageing, synchronous, quasi-separable kernel and a generalized solid, this method results in the decoupling of the space and time dependence. In this case the problem can be solved at each time level by solving first a linear elastic problem in space and then solving a system of ordinary differential equations in time for each point in the spatial mesh at which the viscoelastic displacements are required. The main contribution of this thesis is the implementation of the ODE formulation and applying it to two model viscoelastic test problems. An error indicator, based on that of Zienkiewicz and Zhu [48], [49], is also derived for finite element solutions to a problem of linear elasticity to estimate the errors in the energy norm.

The second model, called a *fully discrete scheme*, is produced by discretization of the Volterra equations using finite element methods in space together with the trapezoidal rule for numerical quadrature in time to treat the history integral. The second model is implemented to provide numerical results for comparison with those of the first model.

The forms of the two numerical algorithms are discussed with particular emphasis on the computational advantage of modelling the viscoelastic relaxation functions with a Dirichlet series. The numerical schemes are tested on problems for which the exact solution is known.

Contents

List of Figures

List of Tables

Chapter 1

Introduction

Many materials may obviously be classed as solid or fluid. There are many others, however, for which the classification is less clear, and their behaviour lies between that of solids and fluids. Examples are silly putty (a silicone), polymer and concrete. Silly putty will fracture cleanly as a solid if subjected to a large suddenly-applied stress, while it will flow freely as a liquid when subjected to a constant stress of low or moderate magnitude (Ronald [32]). Materials which exhibit both viscous fluid and elastic solid characteristics are called *viscoelastic* materials. The study of viscoelastic materials is made more difficult, and more interesting, by the fact that the viscoelastic behaviour combines viscous and elastic properties.

The behaviour of viscoelastic materials is governed by constitutive equations which relate physical properties such as stress and strain. In order to study the behaviour of a viscoelastic material, we need a *constitutive equation* to relate stress to strain. It needs to be recognised that in the case of a real material such equations can be difficult to formulate although constitutive equations describing so called ideal materials may approximately describe the behaviour of real materials quite well over a wide range of conditions. The equations describing ideal materials of the linear viscoelastic type are made up from parts which can be associated with linear elastic elements and linear viscous elements. The basic linear elastic element is a *spring* in which in the one dimensional case stress σ_S and strain ε_S are connected by the relation,

$$\sigma_S = E\varepsilon_S, \tag{1.1}$$

that is, Hooke's law, in which E is *Young's modulus*. The linear viscous element is represented by a *dashpot*. For this element, again in the one dimensional case, the stress σ_D and the strain ε_D are related by

$$\sigma_D = \eta \frac{\mathrm{d}\varepsilon_D}{\mathrm{d}t} := \eta \dot{\varepsilon}_D \tag{1.2}$$

where the constant η is called the coefficient of viscosity. The mixture of the two simple cases described by (1.1) and (1.2) in various ways leads to the constitutive equations in their differential forms. The linear viscoelastic behaviour can also be described by means of hereditary integrals. Shaw *et al.* [36] stated that in the three dimensional context linear viscoelastic media may be characterised by constitutive relationships taking the general form

$$\boldsymbol{\sigma}(t) = \mathbf{D}(0)\boldsymbol{\epsilon}(t) - \int_0^t \mathbf{D}_q(t-q)\boldsymbol{\epsilon}(q)\,\mathrm{d}q, \tag{1.3}$$

$$\boldsymbol{\sigma}(t) = \mathbf{D}(t)\boldsymbol{\epsilon}(0) + \int_0^t \mathbf{D}(t-q)\boldsymbol{\epsilon}_q(q)\,\mathrm{d}q, \tag{1.4}$$

where the subscript q denotes differentiation with respect to the historic time variable q, $\boldsymbol{\sigma}$ is the stress vector, $\boldsymbol{\epsilon}$ is the strain vector and the matrix $\mathbf{D}$ is said to be the stress relaxation matrix. The equivalence of (1.3) and (1.4) can be seen by partial integration. The hereditary relationship or constitutive equation (1.3) shows that the stress at a time does not depend only on the strain at that time, but also on the entire strain history. For this reason, viscoelastic materials are described as having *memory*.

The two forms of the stress in the constitutive equations (1.3) and (1.4) can be used to produce mathematical models for the multidimensional linear viscoelastic problem (Shaw *et al.* [37]). Both models can be discretized in the space domain by using the Galerkin method and a semidiscrete approximating problems can be set up. The discretization in time of these semidiscrete approximating problems by using the trapezoidal rule to approximate the time integrals produces two fully discrete approximating schemes. In 1994, Shaw *et al.* [35] presented numerical techniques for the problem of quasistatic viscoelastic stress analysis based on the constitutive equations (1.3) and (1.4). In that work the numerical results of the linear viscoelastic problem are compared with experimental uniaxial data for a real material.

The objective of this thesis is to present numerical models of linear viscoelastic problems for the case of isotropic, homogeneous, synchronous, non-ageing, quasi-separable kernels and compressible solids. The main contribution is the implementation of a model established by Janovsky *et al.* [16] which is called an *ODE formulation*. A second model, called a *fully discrete formulation* which was initiated by Shaw *et al.* [36] is included for comparison. Numerical algorithms of the discretization of each formulation are defined and the resulting numerical results are compared. To achieve the objective the presentation of the thesis is as follows.

Chapter 2 introduces the function spaces and norms. Weak formulations and the use of the finite element method for elliptic partial differential equations are presented.

Chapter 3 describes linear elasticity and introduces the weak formulation of the problem of linear elasticity derived from the equilibrium equation and Hooke's law. The finite element method is applied to the linear elastic problem via the weak formulation and the Galerkin technique.

Chapter 4 is concerned with the finite element error as a result of the spatial discretization for problems of linear elasticity and in particular it considers the *a posteriori* error estimator which was introduced by Zienkiewicz and Zhu [48], [49] and an adaptive scheme based on using this estimator.

Chapter 5 illustrates the construction of various linear viscoelastic models using elastic springs and viscous dashpots which lead to the idea of internal variables. Such models apply directly to uniaxial states of stress and strain. The hereditary relationship is used to create the viscoelastic model for the quasistatic problems.

Chapter 6 describes the linear viscoelastic problem for the case of isotropic, homogeneous, synchronous, non-ageing, quasi-separable kernels and compressible solids. For this case, the ODE and the fully discrete formulations are produced and the numerical algorithms of both formulations are defined. The ODE formulation results discretizing in decoupled problems of space and time. There are two steps to discretizing the linear viscoelastic problem for the fully discrete formulation. Firstly, the Galerkin method is used to discretize in the space domain. This leads to a semidiscrete approximation problem in the form of a system of Volterra second kind equations. Then full discretization is produced by replacing the Volterra operator with the trapezoidal rule.

Chapter 7 presents and compares the numerical results of the ODE and fully discrete formulations.

Chapter 8 concludes the thesis by summarising the main aspects of the work and presents suggestions for further work that can be done in this area.

Chapter 2

Preliminaries

In this chapter we introduce some of the notation to be used throughout the thesis. In particular we introduce the function spaces (Sobolev spaces) used in the weak formulations of the problems, we outline the procedure for generating a weak formulation for a given elliptic partial differential equation and we outline the finite element method which is the numerical method used in this thesis for obtaining approximate solutions to the weak problems.

2.1 Some Notation

Consider the scalar differentiable functions $u(x, y, z)$ and $v(x, y, z)$, and the vector functions $\mathbf{a} \equiv \mathbf{a}(x, y, z) = a_x\mathbf{i} + a_y\mathbf{j} + a_z\mathbf{k}$ and $\mathbf{b} = b_x\mathbf{i} + b_y\mathbf{j} + b_z\mathbf{k}$, where a_x, a_y, a_z, b_x, b_y and b_z are all functions of x, y and z.

In three dimensional space the Nabla operator ∇ is defined as

$$\nabla \equiv \frac{\partial}{\partial x}\mathbf{i} + \frac{\partial}{\partial y}\mathbf{j} + \frac{\partial}{\partial z}\mathbf{k}. \tag{2.1}$$

When ∇ acts on a continuously differentiable scalar function u, this gives,

$$\nabla u \equiv \operatorname{grad} u = \frac{\partial u}{\partial x}\mathbf{i} + \frac{\partial u}{\partial y}\mathbf{j} + \frac{\partial u}{\partial z}\mathbf{k}. \tag{2.2}$$

Note that ∇ is a linear operator which means that for all u and v and for all constants α we have

$$\nabla(u+v) = \nabla\, u + \nabla\, v, \quad \text{and} \quad \nabla(\alpha u) = \alpha\nabla\, u. \tag{2.3}$$

The Divergence operator $\nabla\cdot$ acting on a continuously differentiable vector function

a is defined as

$$\nabla \cdot \mathbf{a} \equiv \operatorname{div} \mathbf{a} = \frac{\partial a_x}{\partial x} + \frac{\partial a_y}{\partial y} + \frac{\partial a_z}{\partial z}. \tag{2.4}$$

Again, note that for all **a** and **b** and for all constants α we have

$$\nabla \cdot (\mathbf{a} + \mathbf{b}) = \nabla \cdot \mathbf{a} + \nabla \cdot \mathbf{b}, \quad \nabla \cdot (\alpha \mathbf{a}) = \alpha \nabla \cdot \mathbf{a}.$$

The Laplace operator Δ acting on a twice continuously differentiable scalar function u is defined as

$$\Delta u \equiv \nabla \cdot (\nabla u) = \frac{\partial^2 u}{\partial x^2} + \frac{\partial^2 u}{\partial y^2} + \frac{\partial^2 u}{\partial z^2} = \operatorname{div}(\operatorname{grad} u). \tag{2.5}$$

In two-dimensional situations in which $u = u(x, y)$, $v = v(x, y)$, $\mathbf{a} = a_x \mathbf{i} + a_y \mathbf{j}$ etc. we similarly have

$$\nabla \equiv \frac{\partial}{\partial x}\mathbf{i} + \frac{\partial}{\partial y}\mathbf{j}, \quad \nabla u \equiv \frac{\partial u}{\partial x}\mathbf{i} + \frac{\partial u}{\partial y}\mathbf{j}, \quad \nabla \cdot \mathbf{a} = \frac{\partial a_x}{\partial x} + \frac{\partial a_y}{\partial y} \quad \text{and} \quad \Delta u = \frac{\partial^2 u}{\partial x^2} + \frac{\partial^2 u}{\partial y^2}.$$

For deriving the weak formulations in two dimensions the following lemma and theorem are used in later chapters. In both these results $\Omega \subset \mathbb{R}^n, n = 2, 3$, denotes a simply-connected, open, bounded domain with boundary $\partial\Omega$; let $\overline{\Omega} = \Omega \cup \partial\Omega$.

Lemma 2.1 (Identity) If $u, v \in C^2(\overline{\Omega})$, then

$$\nabla \cdot (v \nabla u) = \nabla v \nabla u + v \Delta u.$$

In this relation and in what follows $\nabla v \nabla u = \nabla v \cdot \nabla u$.

Theorem 2.2 (Divergence Theorem)

$$\int_\Omega \operatorname{div} \mathbf{a} \, \mathrm{d}v = \int_{\partial\Omega} \mathbf{a} \cdot \mathbf{n} \, \mathrm{d}s,$$

where **n** is the unit outward normal vector to $\partial\Omega$. The proof of this theorem can be founded in Sobolev [38, p.2].

2.2 Definition of Some Function Spaces

We now define some function spaces for functions defined on an arbitrary open bounded domain $\Omega \subset \mathbb{R}^n, n = 2, 3$, for which the boundary $\partial\Omega$ of Ω is piecewise smooth. We recall that the Lebesgue space $L_p(\Omega)$, $1 \leq p \leq \infty$, is the Banach space of all equivalence classes of real-valued functions u whose pth powers are integrable on Ω such that $\int_\Omega |u|^p \, \mathrm{d}\Omega$ exists and is finite. The norm on $L_p(\Omega)$ is given by

$$\|u\|_{L_p(\Omega)} \equiv \|u\|_{p,\Omega} = \Big(\int_\Omega |u|^p \, \mathrm{d}\Omega \Big)^{1/p}, \quad 1 \leq p < \infty. \tag{2.6}$$

For $p = \infty$, the space $L_\infty(\Omega)$ contains those functions that are bounded in Ω. The norm of this space is defined in the usual way:

$$\|u\|_{L_\infty(\Omega)} \equiv \|u\|_{\infty,\Omega} = \text{ess } \sup_{\mathbf{x}\in\Omega} |u| < \infty. \tag{2.7}$$

An important extension to the L_p spaces are the Sobolev spaces $W_p^r(\Omega)$. These are the spaces of all (equivalence classes of) functions whose generalized derivatives of order less than or equal to r are in $L_p(\Omega)$. To describe this in mathematical symbols we use the multi index symbol $\beta := (\beta_1, \beta_2, \cdots, \beta_n)$ with non-negative integers β_i and we let

$$D^\beta u := \frac{\partial^{|\beta|} u}{\partial x_1^{\beta_1} \partial x_2^{\beta_2} \cdots \partial x_n^{\beta_n}} \tag{2.8}$$

where $|\beta| = \beta_1 + \beta_2 + \cdots + \beta_n$; $D^\beta u$ denotes any of the mixed partial derivatives of u of order β. The Sobolev space $W_p^r(\Omega)$ is thus defined by

$$W_p^r(\Omega) := \{u : D^\beta u \in L_p(\Omega), \ \forall \beta \text{ such that } |\beta| \leq r\}, \tag{2.9}$$

where r is a non-negative integer. Additionally, the corresponding norm for each $u \in W_p^r(\Omega)$ is defined as,

$$\|u\|_{W_p^r(\Omega)} \equiv \|u\|_{r,p,\Omega} = \left(\sum_{|\beta| \leq r} \|D^\beta u\|_{p,\Omega}^p \right)^{1/p}, \quad p \in [1, \infty). \tag{2.10}$$

If $u \in W_\infty^r(\Omega)$ the associated Sobolev norm of u is given by

$$\|u\|_{W_\infty^r(\Omega)} \equiv \|u\|_{r,\infty,\Omega} := \max_{|\beta| \leq r} \|D^\beta u\|_{\infty,\Omega}. \tag{2.11}$$

In particular, the space $L_2(\Omega)$ is the space of square integrable functions. It is well known that $L_2(\Omega)$ is a Hilbert space H with respect to the inner product

$$(u, v)_{L_2(\Omega)} := \int_\Omega uv \, \mathrm{d}\Omega, \quad u, v \in L_2(\Omega) \tag{2.12}$$

and a norm on $L_2(\Omega)$ is defined by

$$\|v\|_{0,\Omega} = ((v,v))^{1/2}, \;\; v \in L_2(\Omega). \tag{2.13}$$

For $p = 2$ the Sobolev spaces $H^r(\Omega) := W_2^r(\Omega)$ are defined as

$$H^r(\Omega) = \{u : D^\beta u \in L_2(\Omega), \; \forall \beta \text{ such that } |\beta| \le r\}. \tag{2.14}$$

We can define the inner product on $H^r(\Omega)$ by

$$(u,v)_{r,\Omega} := \sum_{|\beta|\le r} (D^\beta u, D^\beta v)_{L_2(\Omega)}, \;\; u,v \in H^r(\Omega), \tag{2.15}$$

with the associated norm

$$\|u\|_{H^r(\Omega)} \equiv \|u\|_{r,2,\Omega} := \left(\sum_{|\beta|\le r} \|D^\beta u\|^2_{L_2(\Omega)} \right)^{1/2}. \tag{2.16}$$

Equivalently, $H^r(\Omega)$ is the space of all functions whose generalized derivatives of order less than or equal to r belong to $L_2(\Omega)$. In the definition of $H^r(\Omega)$, there are no conditions imposed on $\partial\Omega$. For the case of homogeneous boundary conditions on $\partial\Omega$, we define the space $\mathring{H}^r(\Omega)$ as

$$\mathring{H}^r(\Omega) := \{v : v \in H^r(\Omega) \text{ and } D^\beta v|_{\partial\Omega} = 0, \quad |\beta| \le r-1\}. \tag{2.17}$$

The semi-norm over $H^r(\Omega)$ defined by

$$|v|_{r,\Omega} := \left(\sum_{|\beta|=r} \|D^\beta v\|^2_{L_2(\Omega)} \right)^{1/2} \tag{2.18}$$

is a norm over $\mathring{H}^r(\Omega)$ which we write $|v|_{\mathring{H}^r(\Omega)}$. We comment on this further in section 2.4 in the case $r = 1$.

For the elasticity and viscoelasticity problems to be described later in the thesis we are dealing with vector quantities such as the displacement vector. When we are dealing with these we will use the product spaces which are defined by

$$(H^r(\Omega))^n := H^r(\Omega) \times \cdots \times H^r(\Omega), \;\; (n \text{ times}), \tag{2.19}$$

which, for $\mathbf{u} := (u_i)_{i=1}^n$, has the product norm

$$\|\mathbf{u}\|_{H^r(\Omega)} \equiv \|\mathbf{u}\|_{r,2,\Omega} := \Big(\sum_{i=1}^n \|u_i\|^2_{H^r(\Omega)}\Big)^{1/2}. \tag{2.20}$$

The L_2 norm of a vector function $\mathbf{u} \in (L_2(\Omega))^n$ is defined as

$$\|\mathbf{u}\|_{L_2(\Omega)} \equiv \|\mathbf{u}\|_{0,2,\Omega} := \Big(\sum_{i=1}^n \|u_i\|^2_{L_2(\Omega)}\Big)^{1/2}. \tag{2.21}$$

2.3 Bilinear Forms

When we reformulate the boundary value problems in weak forms suitable for application of the finite element method we obtain expressions involving bilinear forms. We define these now and also define some properties that are exhibited by the bilinear forms in this thesis.

In the following H denotes a Hilbert space. A mapping $a(\cdot,\cdot) : H \times H \to \mathbb{R}$ is a *bilinear form* on H if for all $u, v, w \in H$ and $\lambda \in \mathbb{R}$ we have

$$a(u, v + \lambda w) = a(u,v) + \lambda a(u,w), \tag{2.22}$$

$$a(u + \lambda v, w) = \lambda a(u,v) + a(u,w) \quad . \tag{2.23}$$

A bilinear form $a(\cdot,\cdot) : H \times H \to \mathbb{R}$ is said to be *continuous* (or *bounded*) if there exists a constant $\mu > 0$ such that

$$|a(u,v)| \leq \mu \|u\|_H \|v\|_H \quad \forall u, v \in H \tag{2.24}$$

and *symmetric* if

$$a(u,v) = a(v,u) \quad \forall u, v \in H. \tag{2.25}$$

A bilinear form $a(\cdot,\cdot) : H \times H \to \mathbb{R}$ is said to be *H-elliptic* (or *coercive*) if there exists a constant $\rho > 0$ such that

$$a(v,v) \geq \rho \|v\|_H^2 \quad \forall v \in H. \tag{2.26}$$

An alternative inner product to that of (2.12) can be defined on H by using a *symmetric* and H-elliptic bilinear form. This is denoted by

$$(u,v)_E := a(u,v). \tag{2.27}$$

and is known as the *energy inner product.* The corresponding *energy norm* is thus defined as

$$\|v\|_E := (a(v,v))^{1/2}. \tag{2.28}$$

For more details about bilinear forms see Fairweather [10], Oden and Reddy [28], Ciarlet [8] and Brenner and Scott [4].

2.4 Remarks about the Spaces H^1 and $\mathring{H}^1$

In section 2.2 we introduced the Hilbert spaces $H^r(\Omega)$ and in section 2.3 we referred to Hilbert spaces when giving the terminology associated with bilinear forms. For the problems considered in this thesis we are mainly concerned only with the spaces $H^1(\Omega)$, $H^0(\Omega) = L_2(\Omega)$ and the subspace $\mathring{H}^1(\Omega) \subset H^1(\Omega)$. For $\Omega \subset \mathbb{R}^2$, and always assuming that Ω is a bounded domain, recall that the norms given in (2.16) are in full

$$\|u\|^2_{L_2} = \int_\Omega u^2 \ \mathrm{d}\Omega \quad \text{and} \quad \|u\|^2_{H^1} = \int_\Omega \left\{ u^2 + \left(\frac{\partial u}{\partial x}\right)^2 + \left(\frac{\partial u}{\partial y}\right)^2 \right\} \mathrm{d}\Omega \tag{2.29}$$

and the semi-norm given in (2.18) is in full

$$|u|^2_{1,\Omega} = \int_\Omega \left\{ \left(\frac{\partial u}{\partial x}\right)^2 + \left(\frac{\partial u}{\partial y}\right)^2 \right\} \mathrm{d}\Omega\ . \tag{2.30}$$

We commented in section 2.2 that this semi-norm (2.30) is actually a norm for the subspace $\mathring{H}^1(\Omega)$. It is in fact the energy norm associated with the bilinear form

$$a(u,v) = \int_\Omega \nabla\, u \,\nabla\, v \ \mathrm{d}\Omega = \int_\Omega \left\{ \frac{\partial u}{\partial x}\frac{\partial v}{\partial x} + \frac{\partial u}{\partial y}\frac{\partial v}{\partial y} \right\} \mathrm{d}\Omega \tag{2.31}$$

and thus we will write $\|u\|_E = \|\nabla\, u\|_{L_2} = |u|_{1,\Omega}$. Hence for a given function $u \in \mathring{H}^1$ we have the usual norm $\|u\|_{H^1}$ and we have the energy norm $\|u\|_E$. From the definitions it is immediately evident that

$$\|u\|^2_{H^1} = \|u\|^2_{L_2} + \|u\|^2_E \geq \|u\|^2_E\ . \tag{2.32}$$

To show that the norms are *equivalent* for functions in $\mathring{H}^1$ we need to show that there exists a constant $\kappa > 0$, depending on Ω but independent of u, such that

$$\kappa\|u\|_{H^1} \leq \|u\|_E \quad \text{for all } u \in \mathring{H}^1(\Omega)\ . \tag{2.33}$$

Fortunately this is a standard result and it is an immediate consequence of the Poincaré-Friedrich inequality, see e.g. [9, p.518–519] and [3, p.30–31]. The Poincaré-Friedrich inequality is a non-trivial result in general but can be much more easily verified in the case considered here in which $u = 0$ on the entire boundary $\partial\Omega$ of Ω. In this special case the inequality result is that there exists a constant $C > 0$ such that for all $u \in \mathring{H}^1(\Omega)$ we have

$$\|u\|_{L_2}^2 \leq C\|\nabla u\|_{L_2}^2 = C|u|_{1,\Omega}^2 = C\|u\|_E^2 \quad \text{for all } u \in \mathring{H}^1(\Omega) \ . \tag{2.34}$$

It is shown in the references [3, 9] that if the domain Ω is contained in a square of side length s then $C = s^2$ is a sufficiently large constant. From this inequality

$$\|u\|_{H^1}^2 = \|u\|_{L_2}^2 + \|u\|_E^2 \leq (1+C)\|u\|_E^2 \tag{2.35}$$

and hence

$$\|u\|_E^2 \geq \frac{1}{1+C}\|u\|_{H^1}^2 \quad \text{giving} \quad \kappa = \frac{1}{\sqrt{1+C}} \ . \tag{2.36}$$

It is this result that establishes the ellipticity property of the particular bilinear form $a(\cdot,\cdot)$ used here.

2.5 Weak Formulation

This section is devoted to the introduction of scalar elliptic boundary-value problems in two dimensions and the related H-elliptic bilinear forms that occur in the weak forms of the problems. We will give examples to demonstrate how a boundary-value problem involving an elliptic partial differential equation can be transformed into a weak form suitable for numerical solution by the finite element method, as described in the next section. For the sake of simplicity, the elliptic partial differential equation considered is the Poisson equation and we consider this for different types of boundary conditions. In the case of an homogeneous Dirichlet boundary conditions the problem is

$$\begin{aligned} -\Delta u(\mathbf{x}) &= f(\mathbf{x}), \quad \mathbf{x} \in \Omega & (2.37)\\ u(\mathbf{x}) &= 0, \qquad \mathbf{x} \in \partial\Omega & (2.38) \end{aligned}$$

where $f \in L_2(\Omega)$, $\Omega \subset \mathbb{R}^2$, $\overline{\Omega} = \Omega \cup \partial\Omega$, and $u \in C^2(\Omega) \cap C^0(\overline{\Omega})$. As usual the spaces $C^0(\overline{\Omega})$ and $C^2(\Omega)$ denote the spaces of continuous functions on $\overline{\Omega}$ and twice continuously differentiable functions in Ω, respectively. We assume that the properties of f and Ω are such that a unique solution u exists to (2.37)-(2.38). Observe that as $u \in C^2(\Omega) \cap C^0(\overline{\Omega})$ and $u = 0$ on $\partial\Omega$ then the solution u to the problem lies in the Sobolev space $\overset{\circ}{H}{}^1(\Omega)$

$$\overset{\circ}{H}{}^1(\Omega) := \{v : v \in H^1(\Omega) \text{ and } v = 0 \text{ on } \partial\Omega\}$$

which we considered in the previous two sections. To create the weak form of this problem we multiply both sides of (2.37) by a test function $v \in \overset{\circ}{H}{}^1(\Omega)$ and integrate over Ω, giving,

$$-\int_\Omega v\Delta u \,\mathrm{d}\mathbf{x} = \int_\Omega f v \,\mathrm{d}\mathbf{x}. \tag{2.39}$$

Use of the vector identity in Lemma 2.1 yields

$$-\int_\Omega v\Delta u \,\mathrm{d}\mathbf{x} = \int_\Omega \nabla v \nabla u \,\mathrm{d}\mathbf{x} - \int_\Omega \nabla \cdot (v\nabla u) \,\mathrm{d}\mathbf{x}. \tag{2.40}$$

Applying the divergence theorem to the second term of the right hand side of (2.40) we obtain

$$-\int_\Omega v\Delta u \,\mathrm{d}\mathbf{x} = \int_\Omega \nabla v \nabla u \,\mathrm{d}\mathbf{x} - \int_{\partial\Omega} v\nabla u \cdot \mathbf{n} \,\mathrm{d}(\partial\Omega). \tag{2.41}$$

Since homogeneous Dirichlet boundary conditions have been assumed, the integral on the boundary will be zero due to the fact that v is zero on the boundary. Then (2.41) becomes

$$-\int_\Omega v\Delta u \,\mathrm{d}\mathbf{x} = \int_\Omega \nabla v \nabla u \;\, \mathrm{d}\mathbf{x}. \tag{2.42}$$

Substituting the above equation into (2.39) gives

$$\int_\Omega \nabla v \nabla u \,\mathrm{d}\mathbf{x} = \int_\Omega f v \,\mathrm{d}\mathbf{x} \tag{2.43}$$

which is called the weak formulation (or the weak problem) of the problem (2.37)–(2.38) which we express in the form

$$a(u, v) = (f, v) \equiv F(v) \quad \forall v \in \overset{\circ}{H}{}^1(\Omega), \tag{2.44}$$

where $a(u, v)$ is the bilinear form

$$a(u, v) := \int_\Omega \nabla u \nabla v \,\mathrm{d}\mathbf{x}, \tag{2.45}$$

and where $F(v)$ is the continuous linear functional

$$F(v) := \int_\Omega f v \, \mathrm{d}\mathbf{x}. \tag{2.46}$$

As $a(u, v)$ only involves integrals of the first partial derivatives of u and v the weak problem makes sense for functions in $\mathring{H}^1(\Omega)$ and the task in solving the weak problem is to seek $u \in \mathring{H}^1(\Omega)$ such that equation (2.44) holds for all $v \in \mathring{H}^1(\Omega)$.

The weak problem (2.44) has to be modified when the boundary conditions are not homogeneous Dirichlet boundary conditions. To illustrate what this involves we consider first the case of non-homogeneous Dirichlet boundary conditions on all of $\partial\Omega$ and we consider next a mixed problem involving a homogeneous Dirichlet condition on part of $\partial\Omega$. In this first case we have

$$-\Delta u(\mathbf{x}) = f(\mathbf{x}), \quad \mathbf{x} \in \Omega \tag{2.47}$$

$$u(\mathbf{x}) = g(\mathbf{x}), \quad \mathbf{x} \in \partial\Omega \tag{2.48}$$

where $g(\mathbf{x})$ is the given boundary data. The weak formulation takes the following form : find $u \in H_g^1$ where

$$H_g^1 \equiv \{u \in H^1(\Omega) \text{ and } u = g \text{ on } \partial\Omega\}$$

such that

$$a(u, v) = F(v) \quad \forall v \in \mathring{H}^1(\Omega), \tag{2.49}$$

where $a(u, v)$ and $F(v)$ are in (2.45) and (2.46). In order to treat (2.47)-(2.48), we transform problem (2.47)-(2.48) into a problem of the type (2.37)-(2.38) by representing $u = u_g + u_0$ where $u_g \in H_g^1$ and $u_0 \in \mathring{H}^1$, i.e. u_0 satisfies the non-homogeneous condition. Substituting into (2.49) we obtain

$$a(u_g + u_0, v) = a(u_g, v) + a(u_0, v) = F(v). \tag{2.50}$$

Defining now

$$\widehat{F}(v) = F(v) - a(u_g, v),$$

the weak formulation (2.49) is to find $u_0 \in \mathring{H}^1$ such that,

$$a(u_0, v) = \widehat{F}(v) \quad \forall v \in \mathring{H}^1(\Omega), \tag{2.51}$$

which is the same type of the problem as given in (2.44).

Next, we discuss Poisson's equation with mixed boundary conditions and for this let $\partial\Omega = \partial\Omega_D \cup \partial\Omega_N$ be a partition of $\partial\Omega$. The problem we consider is

$$\begin{aligned} -\Delta u(\mathbf{x}) &= f(\mathbf{x}), \quad \mathbf{x} \in \Omega && (2.52)\\ u(\mathbf{x}) &= 0, \qquad \mathbf{x} \in \partial\Omega_D && (2.53)\\ \frac{\partial u(\mathbf{x})}{\partial \mathbf{n}} &= \widetilde{G}(\mathbf{x}), \quad \mathbf{x} \in \partial\Omega_N && (2.54) \end{aligned}$$

where $\dfrac{\partial}{\partial \mathbf{n}}$ denotes the outward normal derivative to $\partial\Omega_N$. By considering the previous derivation and in particular (2.41) we see that the equation (2.52) in Ω posed with mixed conditions (2.53)- (2.54) on $\partial\Omega$ again leads to the weak formulation in the form

$$a(u, v) = F(v) \quad \forall v \in V^*, \tag{2.55}$$

where now

$$\begin{aligned} a(u, v) &= \int_\Omega \nabla u \nabla v \, \mathrm{d}\mathbf{x}, && (2.56)\\ F(v) &= \int_\Omega f v \, \mathrm{d}\mathbf{x} + \int_{\partial\Omega_N} \widetilde{G} v \, \mathrm{d}(\partial\Omega), && (2.57) \end{aligned}$$

and the space

$$V^* = \{v \in H^1(\Omega) : v = 0 \text{ on } \partial\Omega_D\}.$$

The above illustrates the general procedures for creating the weak problems corresponding to given boundary-value problems. We just take the inner product of the differential equation with a suitable test function and then re-express this using some form of integration by parts. The numerical solution of the weak problem by the finite element method is presented in the next section using the Galerkin method.

2.6 Finite Element Method

In this section, we describe briefly the finite element method for the numerical solution of the scalar elliptic boundary value problems as given in section 2.5. To keep the description brief we consider first the case of the homogeneous Dirichlet boundary condition on all of $\partial\Omega$ and then we comment at the end how we can deal with the non-homogeneous Dirichlet and mixed boundary conditions. As before let u denote the unknown solution in $\mathring{H}^1(\Omega)$ of the weak problem

$$a(u,v) = F(v) \quad \forall v \in \mathring{H}^1(\Omega). \tag{2.58}$$

The finite element method results in an approximation u_h to the exact solution u of the problem posed. This finite element solution arises from the discretization of the region Ω which is obtained by partitioning Ω into non-overlapping elements $\Omega_i,\ i = 1, \cdots, ne$ (a number of element), the size of which is indicated by a mesh parameter h. In order to solve (2.58) numerically, we choose a finite dimensional subspace $\widetilde{S}^h \subset \mathring{H}^1$ and form the approximating problem which involves seeking $u_h \in \widetilde{S}^h$ such that

$$a(u_h, v_h) = F(v_h) \quad \forall v_h \in \widetilde{S}^h. \tag{2.59}$$

The condition $\widetilde{S}^h \subset \mathring{H}^1$ is known as the *conforming condition*. For the case $\Omega \subset \mathbb{R}^2$ and the case in which the space $\widetilde{S}^h$ is defined using piecewise polynomials we satisfy $\widetilde{S}^h \subset \mathring{H}^1$ when $\widetilde{S}^h \subset C(\bar{\Omega})$, i.e. the piecewise-defined approximations are globally continuous. The problem formulation of (2.59) is called the Galerkin problem corresponding to the problem (2.58) and it is *via* this route that the illustration of the finite element will proceed (see Whiteman [44]).

Suppose that each of the non-overlapping elements Ω_i contains k nodes and suppose that this discretization of Ω involves in total $\mathcal{M}$ nodes $\{\mathbf{z}_i\}_{i=1}^{\mathcal{M}}$ with, for notational convenience, the first $\mathcal{N}$ nodes corresponding to points at which u is unknown and the other nodes $\{\mathbf{z}_i\}_{i=\mathcal{N}+1}^{\mathcal{M}}$ corresponding to where essential boundary conditions are applied (i.e. where Dirichlet boundary conditions are applied in our case). For a given element with its k nodes the finite element method involves constructing in Ω_i a cardinal basis function associated with each node so that the finite element approximation can be expressed in the form

$$u_h(\mathbf{x})|_{\Omega_i} = \sum_{j=1}^{k} (M_j u_h) \phi_j(\mathbf{x}), \tag{2.60}$$

where $(M_j u_h)$ denotes the value of $u_h(\mathbf{x})$ at node j in this local numbering system for the element. All of the functions in $\widetilde{S}^h$ when evaluated at a point $\mathbf{x}$ in the element similarly involve a linear combination of $\phi_1(\mathbf{x}), \cdots, \phi_k(\mathbf{x})$ with the coefficients being the nodal values of $(M_j u_h)$. These cardinal basis functions $\phi_1, \cdots, \phi_k$ are local to each element, but, taken over the totality of elements in the region $\overline{\Omega}$ they together determine a set of (globally defined) linearly independent piecewise polynomials $\{B_i(\mathbf{x})\}_{i=1}^{\mathcal{M}}$ which have the similar cardinal property

$$(M_j B_i)(\mathbf{z}_j) = \delta_{ij}, \quad i, j = 1, 2, \ldots, \mathcal{M}, \tag{2.61}$$

where δ_{ij} is the Kronecker delta. The relations between the globally defined basis functions and the locally defined element basis functions are such that for a point $\mathbf{x}$ in an element and a function B_i which is non-zero at $\mathbf{x}$ we have $B_i(\mathbf{x}) = \phi_j(\mathbf{x})$ for one value of j, $1 \le j \le k$. In terms of these globally defined basis functions the finite element approximation represented in (2.60) can also be written in the form

$$u_h(\mathbf{x}) = \sum_{i=1}^{\mathcal{N}} (M_i u_h) B_i(\mathbf{x}) \tag{2.62}$$

where the sum is only for 1 to $\mathcal{N}$ as Dirichlet boundary conditions give $(M_i u_h) = 0$ for $i = \mathcal{N}+1, \cdots, \mathcal{M}$. Now functions in $\widetilde{S}^h$ are 0 on $\partial\Omega$ and thus a basis for $\widetilde{S}^h$ is given by

$$\widetilde{S}^h = \operatorname{span}\{B_1, \cdots, B_{\mathcal{N}}\}. \tag{2.63}$$

Thus the condition $a(u_h, v_h) = F(v_h)$ for all $v_h \in \widetilde{S}^h$ is satisfied by taking

$$a(u_h, B_j) = F(B_j), \quad j = 1, \cdots, \mathcal{N} \tag{2.64}$$

which gives us $\mathcal{N}$ equations for the unknowns $(M_i u_h)$, $i = 1, \cdots, \mathcal{N}$. In full we have

$$a\left(\sum_{i=1}^{\mathcal{N}} (M_i u_h) B_i, B_j\right) = F(B_j), \quad j = 1, \cdots, \mathcal{N} \tag{2.65}$$

and, by using the bilinear properties of $a(\cdot, \cdot)$ this can be written in matrix form as

$$\mathbf{K}\mathbf{u}_h = \mathbf{F}, \quad \text{where} \quad \mathbf{K} = (a(B_i, B_j)), \quad \mathbf{F} = (F(B_j)) \quad \text{and} \quad \mathbf{u}_h = (M_i u_h). \tag{2.66}$$

The $\mathcal{N} \times \mathcal{N}$ matrix $\mathbf{K}$ is called the *global stiffness matrix*. The vector $\mathbf{u}_h$ is obtained by solving (2.66) and substituting into (2.60) gives the required finite element approximation $u_h(\mathbf{x})$.

We have outlined here the procedure in the case of homogeneous Dirichlet conditions on all of $\partial\Omega$. Next, the procedure for dealing with non-homogeneous or mixed boundary conditions are considered. In all these cases we will again have a finite dimensional test space of the form

$$\widetilde{S}^h = \mathrm{span}\{B_1, \cdots, B_{\mathcal{N}}\}$$

except that now the approximation is of the form

$$u_h(\mathbf{x}) = \sum_{i=1}^{\mathcal{N}} (M_i u_h) B_i(\mathbf{x}) + \sum_{i=\mathcal{N}+1}^{\mathcal{M}} (M_i u_h) B_i(\mathbf{x}) \tag{2.67}$$

with $(M_i u_h)$, $i = \mathcal{N}+1, \cdots, \mathcal{M}$ being known. Thus, although u_h is not now in general in $\widetilde{S}^h$ the 'unknown part' of u_h is in $\widetilde{S}^h$. Again forming (2.65) gives us our linear system for the unknown nodal values $(M_1 u_h), \cdots, (M_{\mathcal{N}} u_h)$.

For further information on finite element methods see Marti [25], Eriksson *et al.* [9], Wait and Mitchell [43], Braess [3] and Strang and Fix [40].

2.7 Comments

All the above has been for scalar elliptic boundary-value problems in two dimensions. The whole scheme will be extended to the vector context of linear elasticity and then to viscoelasticity in Chapters 3 and 5. Clearly in general the weak formulation has to be able to treat the case of homogeneous, non-homogeneous and mixed boundary conditions. Such conditions generalize in the context of elastic and viscoelastic problems to non-zero constraint and traction boundary conditions.

Chapter 3

Basic Solid Mechanics, Linear Elasticity and Finite Elements

As is indicated in the introduction, this thesis is concerned with coupling finite element techniques in space with ODE solvers in time to model the deformation of a certain class of viscoelastic materials under loading regimes. This chapter describes the basic solid mechanics, problems of linear elasticity and the finite element techniques involved in solving linear elastic problems. In fact, in the computations described in Chapters 3, 4 and 6 much of the total computational time is spent in the linear elastic solvers. The purpose of this chapter is thus to introduce a number of terms from the theory of linear elasticity and to collect together the relevant terms and equations needed later in the thesis.

Linear elasticity is the simplest of the constitutive models describing the deformation of solid bodies. It is adequate under the following assumptions

- At each point the stress and hence the strain is sufficiently small.
- Time dependent effects are negligible.
- The stress depends linearly on the strain.

In the remainder of this chapter we consider each of these aspects in a little more detail. We begin, however, by describing first the configuration of a typical solid body, the boundary conditions and the loading. We then introduce the displacement vector, the strain components and the strain–displacement relations, the stress components, the equilibrium equations satisfied by the stress components and Hooke's law which gives the linear relation between stress and strain. To complete the description the weak formulation of the equilibrium statement is then given and the finite element method is described briefly.

3.1 The Basic Set-up and the Displacement Vector

Let G be a compressible solid body with density ρ which in its undeformed state occupies the bounded domain $\Omega \subset \mathbb{R}^n$, $n = 1, 2, 3$. The domain Ω is known as the reference configuration and, as usual, we will let $\partial\Omega$ denote the boundary of Ω. In the problems considered in this thesis, the body is typically fixed on part of its boundary $\partial\Omega$ with a surface traction imposed on the other part. To describe this we will suppose that $\partial\Omega_D$ denotes the part which is fixed and $\partial\Omega_N$ is the part of $\partial\Omega$ which contains the surface traction, with $\partial\Omega_N \cap \partial\Omega_D = \emptyset$. In general at time $t, 0 \leq t \leq T$, the body is acted upon by a body force

$$\mathbf{f}(\mathbf{x}, t) = (f_i(\mathbf{x}, t)), \quad \mathbf{x} \in \Omega, \quad i = 1, 2, \cdots, n,$$

and a surface traction

$$\mathbf{g}(\mathbf{x}, t) = (g_i(\mathbf{x}, t)), \quad \mathbf{x} \in \partial\Omega_N, \quad i = 1, 2, \cdots, n.$$

When $n = 3$ the body force and surface traction have dimensions of respectively force/unit volume and force/unit area. When $n = 2$ the body force and surface traction have dimensions of respectively force/area and force/length. Under the actions of these forces the point $\mathbf{x} \in \Omega$ deforms to the point $\mathbf{x} + \mathbf{u}(\mathbf{x}, t)$ where $\mathbf{u} = (u_i)$, $i = 1, 2, \cdots, n$ is the displacement vector. The basic task for a set-up such as this is to determine the displacement field $\mathbf{u}(\mathbf{x}, t)$, $\mathbf{x} \in \Omega$, $0 \leq t \leq T$.

In the case of linear elasticity time has no meaning and we can simplify the notation slightly here. The displacement field $\mathbf{u}(\mathbf{x}, t)$ at time t depends only on the forcing action at this time and hence we can abbreviate $\mathbf{f}(\mathbf{x}, t)$, $\mathbf{g}(\mathbf{x}, t)$ and $\mathbf{u}(\mathbf{x}, t)$ to simply $\mathbf{f}(\mathbf{x})$, $\mathbf{g}(\mathbf{x})$ and $\mathbf{u}(\mathbf{x})$ respectively.

3.2 Strain and the Strain-displacement Relations

From the displacement field $\mathbf{u}$ we can determine the state of stretch and the state of strain in the body at the point $\mathbf{x} \equiv (x_1, x_2, x_3)$. Both of these are concerned with how line segments in the body change as the body deforms. In one-dimension this is fairly straight forward as there is only one-direction to consider and if l and $\tilde{l}$ denote respectively the undeformed and the deformed lengths then $\tilde{l}/l$ and $(\tilde{l} - l)/l$ are respectively the (engineering) stretch and strain of the segment. In more than one dimension the situation is a bit more complicated as the undeformed and the deformed line segments can have different directions as well as different lengths and to describe completely what is happening at a point we need to consider what happens to line segments in all possible directions. We can do this as follows.

For a given point $\mathbf{x} \in \Omega$ let $\tilde{\mathbf{x}} = \tilde{\mathbf{x}}(\mathbf{x}) = \mathbf{x} + \mathbf{u}(\mathbf{x})$ denote the deformed point and for an infinitesimal change $\Delta\mathbf{x}$ with respect to the undeformed configuration we define

$$\Delta\tilde{\mathbf{x}} = \tilde{\mathbf{x}}(\mathbf{x} + \Delta\mathbf{x}) - \tilde{\mathbf{x}}(\mathbf{x}) = \Delta\mathbf{x} + \mathbf{u}(\mathbf{x} + \Delta\mathbf{x}) - \mathbf{u}(\mathbf{x}) \tag{3.1}$$

as the corresponding change in the deformed configuration. As we are dealing with infinitesimals we have

$$\Delta\tilde{\mathbf{x}} = \mathbf{F}\Delta\mathbf{x}, \tag{3.2}$$

i.e. in components

$$\Delta\tilde{\mathbf{x}} = \begin{bmatrix} \Delta\tilde{x}_1 \\ \\ \Delta\tilde{x}_2 \\ \\ \Delta\tilde{x}_3 \end{bmatrix} = \begin{bmatrix} \dfrac{\partial\tilde{x}_1}{\partial x_1} & \dfrac{\partial\tilde{x}_1}{\partial x_2} & \dfrac{\partial\tilde{x}_1}{\partial x_3} \\ \dfrac{\partial\tilde{x}_2}{\partial x_1} & \dfrac{\partial\tilde{x}_2}{\partial x_2} & \dfrac{\partial\tilde{x}_2}{\partial x_3} \\ \dfrac{\partial\tilde{x}_3}{\partial x_1} & \dfrac{\partial\tilde{x}_3}{\partial x_2} & \dfrac{\partial\tilde{x}_3}{\partial x_3} \end{bmatrix} \begin{bmatrix} \Delta x_1 \\ \\ \Delta x_2 \\ \\ \Delta x_3 \end{bmatrix} \tag{3.3}$$

where $\mathbf{F}$ is the deformation gradient. The matrix $\mathbf{F}$ may be rewritten as,

$$\mathbf{F} = \begin{bmatrix} 1 + \dfrac{\partial u_1}{\partial x_1} & 0 + \dfrac{\partial u_1}{\partial x_2} & 0 + \dfrac{\partial u_1}{\partial x_3} \\ 0 + \dfrac{\partial u_2}{\partial x_1} & 1 + \dfrac{\partial u_2}{\partial x_2} & 0 + \dfrac{\partial u_2}{\partial x_3} \\ 0 + \dfrac{\partial u_3}{\partial x_1} & 0 + \dfrac{\partial u_3}{\partial x_2} & 1 + \dfrac{\partial u_3}{\partial x_3} \end{bmatrix}, \tag{3.4}$$

or

$$\mathbf{F} = \mathbf{I} + \nabla\mathbf{u}, \tag{3.5}$$

where $\mathbf{I}$ is the 3×3 identity matrix and $\nabla\mathbf{u}$ is the gradient of the displacement defined by

$$\nabla\mathbf{u} := \begin{bmatrix} \frac{\partial u_1}{\partial x_1} & \frac{\partial u_1}{\partial x_2} & \frac{\partial u_1}{\partial x_3} \\ \frac{\partial u_2}{\partial x_1} & \frac{\partial u_2}{\partial x_2} & \frac{\partial u_2}{\partial x_3} \\ \frac{\partial u_3}{\partial x_1} & \frac{\partial u_3}{\partial x_2} & \frac{\partial u_3}{\partial x_3} \end{bmatrix}. \tag{3.6}$$

Thus equation (3.2) can also be written as

$$\Delta\tilde{\mathbf{x}} = (\mathbf{I} + \nabla\mathbf{u})\Delta\mathbf{x}, \tag{3.7}$$

The squares of the lengths of the undeformed and the deformed line segments are respectively $\Delta\mathbf{x}^T\Delta\mathbf{x}$ and $\Delta\tilde{\mathbf{x}}^T\Delta\tilde{\mathbf{x}}$ and since $\Delta\tilde{\mathbf{x}} = \mathbf{F}\Delta\mathbf{x}$ we have

$$(\Delta\tilde{\mathbf{x}})^2 := \Delta\tilde{\mathbf{x}}^T\Delta\tilde{\mathbf{x}} = \Delta\mathbf{x}^T\mathbf{F}^T\mathbf{F}\Delta\mathbf{x}. \tag{3.8}$$

This implies that

$$(\Delta\tilde{\mathbf{x}})^2 - (\Delta\mathbf{x})^2 = 2\Delta\mathbf{x}^T\mathbf{E}\Delta\mathbf{x} \quad \text{where} \quad \mathbf{E} = \frac{1}{2}(\mathbf{F}^T\mathbf{F} - \mathbf{I}) \tag{3.9}$$

and in terms of the gradient of the displacement we have

$$\mathbf{E} = \frac{1}{2}((\mathbf{I} + \nabla\mathbf{u})^T(\mathbf{I} + \nabla\mathbf{u}) - \mathbf{I}) = \frac{1}{2}(\nabla\mathbf{u} + (\nabla\mathbf{u})^T + (\nabla\mathbf{u})^T(\nabla\mathbf{u})). \tag{3.10}$$

For a general (i.e. finite) deformation $\mathbf{E}$ is known as the *Lagrangian strain tensor* and we note that the relation giving $\mathbf{E}$ in terms of $\nabla\mathbf{u}$ is non-linear. In many practical situations, however, the situation simplifies as the deformation is small or at least the components of the deformation gradient $\nabla\mathbf{u}$ are small. If we assume the latter then $(\nabla\mathbf{u})^T\nabla\mathbf{u}$ is small in comparison with the other terms in the expression for $\mathbf{E}$ and we get

$$\mathbf{E} \approx \boldsymbol{\epsilon} := \frac{1}{2}(\nabla\mathbf{u} + (\nabla\mathbf{u})^T) \tag{3.11}$$

where $\boldsymbol{\epsilon}$ is known as the *infinitesimal strain tensor*. This relation between the infinitesimal strain $\boldsymbol{\epsilon}$ and the gradient of the displacement $\nabla\mathbf{u}$ is *linear* and this is the strain measure which is used throughout the thesis. To express this in terms of the components we have

$$\boldsymbol{\epsilon} := \begin{pmatrix} \varepsilon_{11} & \varepsilon_{12} & \varepsilon_{13} \\ \varepsilon_{21} & \varepsilon_{22} & \varepsilon_{23} \\ \varepsilon_{31} & \varepsilon_{32} & \varepsilon_{33} \end{pmatrix} \quad \text{where} \quad \varepsilon_{ij} := \frac{1}{2}\Big(\frac{\partial u_i}{\partial x_j} + \frac{\partial u_j}{\partial x_i}\Big), \tag{3.12}$$

and for the finite element implementation it is usual to collect the six independent strain components together to form the so-called strain vector

$$\boldsymbol{\epsilon}(\mathbf{u}) = \begin{bmatrix} \varepsilon_{11} \\ \varepsilon_{22} \\ \varepsilon_{33} \\ 2\,\varepsilon_{12} \\ 2\,\varepsilon_{13} \\ 2\,\varepsilon_{23} \end{bmatrix} = \begin{bmatrix} \frac{\partial u_1}{\partial x_1} \\ \frac{\partial u_2}{\partial x_2} \\ \frac{\partial u_3}{\partial x_3} \\ \frac{\partial u_1}{\partial x_2} + \frac{\partial u_2}{\partial x_1} \\ \frac{\partial u_1}{\partial x_3} + \frac{\partial u_3}{\partial x_1} \\ \frac{\partial u_2}{\partial x_3} + \frac{\partial u_3}{\partial x_2} \end{bmatrix}. \tag{3.13}$$

With this notation we can then write the linear strain displacement relation in matrix form as

$$\boldsymbol{\epsilon} = \mathbf{B}\mathbf{u} \tag{3.14}$$

where, as before, $\mathbf{u} = (u_1, u_2, u_3)^T$ is the displacement vector and $\mathbf{B}$ is the 6×3 matrix differential operator

$$\mathbf{B} = \begin{bmatrix} \frac{\partial}{\partial x_1} & 0 & 0 \\ 0 & \frac{\partial}{\partial x_2} & 0 \\ 0 & 0 & \frac{\partial}{\partial x_3} \\ \frac{\partial}{\partial x_2} & \frac{\partial}{\partial x_1} & 0 \\ \frac{\partial}{\partial x_3} & 0 & \frac{\partial}{\partial x_1} \\ 0 & \frac{\partial}{\partial x_3} & \frac{\partial}{\partial x_2} \end{bmatrix}. \tag{3.15}$$

3.3 State of Stress and the Stress Components

Stress is concerned with describing the force on surface elements interior to a body and it has the dimensions of force/area with the specific stress components depending on the components of the force and the direction of the unit normal to the surface element. The three dimensional state of stress at a point in a stressed body may be described with respect to the stress on three arbitrarily chosen orthogonal planes passing through the point. These planes will be chosen normal to the co-ordinate axes x_1, x_2, x_3 as shown in Figure 3.1. An infinitesimal cube whose sides are parallel to these planes and have lengths Δx_1, Δx_2, Δx_3, respectively, will be considered in what follows. In the most general situation there will be forces $\Delta\mathbf{F}_1$, $\Delta\mathbf{F}_2$, $\Delta\mathbf{F}_3$, see

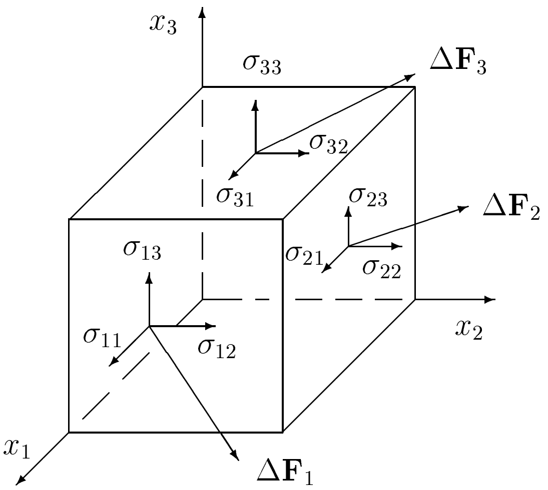

Figure 3.1: Stress component of a general state of stress

Figure 3.1, with each of these forces possibly having components in all directions. To describe these forces and the stress components we have, as the cube is infinitesimal,

$$
\begin{aligned}
\Delta\mathbf{F}_1 &= (\sigma_{11}\mathbf{e}_1 + \sigma_{12}\mathbf{e}_2 + \sigma_{13}\mathbf{e}_3)\Delta x_2 \Delta x_3, \\
\Delta\mathbf{F}_2 &= (\sigma_{21}\mathbf{e}_1 + \sigma_{22}\mathbf{e}_2 + \sigma_{23}\mathbf{e}_3)\Delta x_1 \Delta x_3, \\
\Delta\mathbf{F}_3 &= (\sigma_{31}\mathbf{e}_1 + \sigma_{32}\mathbf{e}_2 + \sigma_{33}\mathbf{e}_3)\Delta x_1 \Delta x_2,
\end{aligned}
$$

where

$$
\mathbf{e}_1 = \begin{bmatrix} 1 \\ 0 \\ 0 \end{bmatrix}, \ \mathbf{e}_2 = \begin{bmatrix} 0 \\ 1 \\ 0 \end{bmatrix}, \ \mathbf{e}_3 = \begin{bmatrix} 0 \\ 0 \\ 1 \end{bmatrix}.
$$

The first subscript of σ_{ij} thus indicates the plane normal to the surface element and the second subscript relates to the force on that plane in the direction of the second subscript. The components $\sigma_{11}, \sigma_{22}, \sigma_{33}$ are known as the *normal stress* components and the components σ_{ij}, $i \neq j$ are known as the *shear stress* components. Thus, considering the right-hand face of the cube in Figure 3.1 σ_{22} is a normal stress component in the x_2 direction, σ_{21} is a shear stress in the x_1 direction, σ_{23} is a shear stress in the x_3 direction and all three components are acting on a plane which is perpendicular to the x_2 axis.

The nine components involved in describing the state of stress, as shown in Figure 3.1, constitute a second order Cartesian tensor, called the stress tensor and it is often convenient to display these in matrix form as follows,

$$\boldsymbol{\sigma} = \sigma_{ij} := \begin{bmatrix} \sigma_{11} & \sigma_{12} & \sigma_{13} \\ \sigma_{21} & \sigma_{22} & \sigma_{23} \\ \sigma_{31} & \sigma_{32} & \sigma_{33} \end{bmatrix}. \tag{3.16}$$

From these nine components we can describe the force on a surface element whose unit normal can be in any direction. Related to this the *traction* vector $\mathbf{g} = (g_i)$ corresponding to the unit vector $\mathbf{n} = (n_i)$ is defined by

$$\begin{bmatrix} g_1 \\ g_2 \\ g_3 \end{bmatrix} = \begin{bmatrix} \sigma_{11} & \sigma_{12} & \sigma_{13} \\ \sigma_{21} & \sigma_{22} & \sigma_{23} \\ \sigma_{31} & \sigma_{32} & \sigma_{33} \end{bmatrix} \begin{bmatrix} n_1 \\ n_2 \\ n_3 \end{bmatrix}. \tag{3.17}$$

As we show in the next subsection, the stress tensor is symmetric, i.e. $\sigma_{ij} = \sigma_{ji}$, and hence there are only six independent components to consider and, as in the case of the strain, it is convenient to gather the six components together to give the stress vector

$$\boldsymbol{\sigma} = [\sigma_{11},\ \sigma_{22},\ \sigma_{33},\ \sigma_{12},\ \sigma_{13},\ \sigma_{23}]^T. \tag{3.18}$$

In what follows it should always be clear from the context whether $\boldsymbol{\sigma}$ refers to the stress tensor or to the stress vector.

3.4 The Equation of Equilibrium

Newton's law of motion states that the rate of change of linear momentum is equal to the resultant of the applied forces and that the rate of change of the moment of momentum with respect to the origin of the co-ordinates is equal to the resultant moment of applied forces about the same origin. This law of motion holds for particles as well as for bodies of all kinds. There are various ways of transforming this law into differential equations for use in the mechanics of deformable bodies. A direct approach is used in the following (see Findley *et al.* [11]).

Consider the static equilibrium state of an infinitesimal parallelepiped of sides Δx_1, Δx_2, Δx_3, with surfaces parallel to the co-ordinate planes. The stresses acting

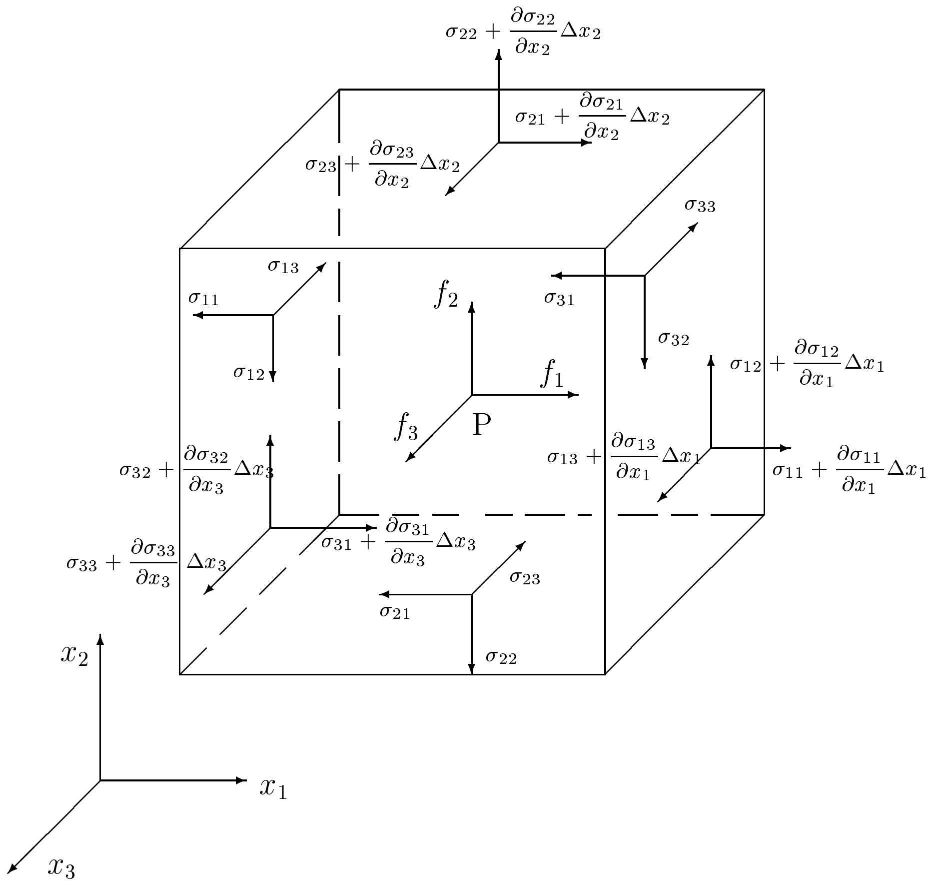

Figure 3.2: Equilibrium stress components

on the various surfaces and the body forces are shown in Figure 3.2, where σ_{11}, σ_{22}, σ_{33} are normal stresses, σ_{12}, σ_{13}, σ_{23}, etc., are shear stresses and f_1, f_2, f_3 are the components of the body force per unit volume in the direction of the co-ordinate axes. The static equilibrium of the body requires that the resultant of all forces is zero. The equilibrium equation along x_1 is then obtained by summing all the forces acting on the element in the x_1 direction. The forces are obtained by multiplying the stress by the area on which the stress acts. The sum of these forces is

$$
\begin{aligned}
& \left(\sigma_{11} + \frac{\partial \sigma_{11}}{\partial x_1} \Delta x_1\right) \Delta x_2 \Delta x_3 - \sigma_{11} \, \Delta x_2 \Delta x_3 \\
+ & \left(\sigma_{21} + \frac{\partial \sigma_{21}}{\partial x_2} \Delta x_2\right) \Delta x_1 \Delta x_3 - \sigma_{21} \, \Delta x_1 \Delta x_3 \\
+ & \left(\sigma_{31} + \frac{\partial \sigma_{31}}{\partial x_3} \Delta x_3\right) \Delta x_1 \Delta x_2 - \sigma_{31} \, \Delta x_1 \Delta x_2 + f_1 \Delta x_1 \Delta x_2 \Delta x_3 = 0 \quad (3.19)
\end{aligned}
$$

The other two equilibrium equations along x_2 and x_3 co-ordinates can be obtained in the same way. Dividing the equations by $\Delta x_1\ \Delta x_2\ \Delta x_3$ yields the following three equilibrium equations oriented along the co-ordinate axes

$$\begin{aligned}
\frac{\partial \sigma_{11}}{\partial x_1} + \frac{\partial \sigma_{21}}{\partial x_2} + \frac{\partial \sigma_{31}}{\partial x_3} + f_1 &= 0, \\
\frac{\partial \sigma_{12}}{\partial x_1} + \frac{\partial \sigma_{22}}{\partial x_2} + \frac{\partial \sigma_{32}}{\partial x_3} + f_2 &= 0, \\
\frac{\partial \sigma_{13}}{\partial x_1} + \frac{\partial \sigma_{23}}{\partial x_2} + \frac{\partial \sigma_{33}}{\partial x_3} + f_3 &= 0.
\end{aligned} \tag{3.20}$$

To write this more compactly it is convenient at this point to introduce the summation convention. When the subscripts express in terms of σ_{ii} or σ_{ij} it is to be understand that these symbols describe the sum of the range of that index, for example,

$$\sigma_{ii} = \sigma_{11} + \sigma_{22} + \sigma_{33}.$$

Hence in the steady state case equation (3.20) can be written compactly in the form

$$-\frac{\partial \sigma_{ij}(\mathbf{x})}{\partial x_j} = f_i(\mathbf{x}) \quad i = 1, 2, 3. \tag{3.21}$$

It is the index j which is repeated here and the range of j is $1, 2, 3$. Boundary conditions considered in this thesis for (3.21) are of the type

$$u_i(\mathbf{x}) = 0, \qquad \mathbf{x} \in \partial\Omega_D \tag{3.22}$$

$$\sigma_{ij} n_j = g_i(\mathbf{x}), \quad \mathbf{x} \in \partial\Omega_N \tag{3.23}$$

where again we have used the summation convention to describe the traction boundary condition on $\partial\Omega_N$. Similarly for quasistatic problems, at time t equation (3.21)-(3.23) hold with σ_{ij}, u_i f_i and g_i now depending on $\mathbf{x}$ and t.

Although not covered in this thesis it is worthwhile at this point to note that the equation of motion under dynamic conditions can be derived in the same way by including the inertia term, i.e. the rate of change of momentum. Thus the right-hand side of (3.20) equals the mass per unit volume times the second derivative of the displacements u_i with respect to time t. The tensor form is

$$\rho \frac{\partial^2 u_i(\mathbf{x}, t)}{\partial t^2} = \frac{\partial \sigma_{ij}(\mathbf{x}, t)}{\partial x_j} + f_i(\mathbf{x}, t), \quad i = 1, 2, 3. \tag{3.24}$$

where u_i are the displacement components along the coordinate axes. The boundary conditions on Ω and initial conditions at $t = 0$ are of the form

$$\begin{aligned} u_i(\mathbf{x}, t) &= 0, & \mathbf{x} \in \partial\Omega_D, \\ \sigma_{ij} n_j &= g_i(\mathbf{x}, t), & \mathbf{x} \in \partial\Omega_N, \\ u_i(\mathbf{x}, 0) &= u_i^0(\mathbf{x}), & \mathbf{x} \in \Omega, \\ \frac{\partial u_i(\mathbf{x}, 0)}{\partial t} &= u_i^1(\mathbf{x}), & \mathbf{x} \in \Omega, \end{aligned} \tag{3.25}$$

where u_i^0 and u_i^1 are given functions.

We have already commented that the stress components are symmetric and to prove this we now show how this is a consequence of the conservation of angular momentum. Consider the moment (vector) about a line through the centre P of the parallelepiped and parallel to the x_1 axis and consider in particular the component of the moment in the x_1 direction. If $\mathbf{f}$ denotes a force on any of the surfaces in the x_2 or x_3 directions then we have to consider the x_1 component in terms of the form $(x_2\mathbf{e}_2 + x_3\mathbf{e}_3) \times \mathbf{f}$. By considering the forces on four of the six sides of the cube shown in Figure 3.2 we get

$$\begin{aligned} &- \left(\sigma_{32} + \frac{\partial \sigma_{32}}{\partial x_3}\Delta x_3\right) \Delta x_1 \Delta x_2 \frac{\Delta x_3}{2} - \sigma_{32}\, \Delta x_1 \Delta x_2 \frac{\Delta x_3}{2} \\ &+ \left(\sigma_{23} + \frac{\partial \sigma_{23}}{\partial x_2}\Delta x_2\right) \Delta x_1 \Delta x_3 \frac{\Delta x_2}{2} + \sigma_{23}\, \Delta x_1 \Delta x_3 \frac{\Delta x_2}{2} = 0. \end{aligned} \tag{3.26}$$

Dividing by $\Delta x_1\ \Delta x_2\ \Delta x_3$ and taking the limit as $\Delta x_1 \longrightarrow 0$, $\Delta x_2 \longrightarrow 0$, and $\Delta x_3 \longrightarrow 0$, the following result is obtained

$$\sigma_{32} = \sigma_{23}. \tag{3.27}$$

The moment of forces about lines through P parallel to x_3, x_2 yields two similar relations

$$\sigma_{12} = \sigma_{21}, \quad \sigma_{13} = \sigma_{31},$$

so in tensor form

$$\sigma_{ij} = \sigma_{ji}. \tag{3.28}$$

Equation (3.28) shows that the stress tensor is symmetric.

3.5 Constitutive Equations for Linear Elastic Materials which are Isotropic and Compressible

The stress and strain tensors were described in the previous sections; we now consider the relation between them. The equations relating stress to strain for a particular material are known as *constitutive equations*. It is intuitively evident that a relationship between stress and strain will be dependent upon the physical properties of the solid body G since different materials will deform in different ways when a force is applied. In the case of a linear elastic material the stress–strain relation is known as Hooke's law, (see Shaw *et al.* [36]), and in the case of the strain vector $\boldsymbol{\epsilon}$ and the stress vector $\boldsymbol{\sigma}$ can be given in the form

$$\boldsymbol{\sigma} = \mathbf{D}\boldsymbol{\epsilon}, \tag{3.29}$$

where $\mathbf{D}$ is the *constitutive matrix*. We consider now the form of this relation when the material is compressible and isotropic. In components the relation can be expressed as

$$\sigma_{ij} = \mu\varepsilon_{ij} + \lambda(\varepsilon_{11} + \varepsilon_{22} + \varepsilon_{33})\delta_{ij}, \quad i, j \leq 1, 2, 3, \tag{3.30}$$

where λ and μ are the Lamé coefficients of the material and δ_{ij} is the Kronecker delta given by

$$\delta_{ij} = \begin{cases} 1 & \text{if } i = j \\ 0 & \text{if } i \neq j. \end{cases} \tag{3.31}$$

Thus (3.30) may be written in the form

$$\begin{bmatrix} \sigma_{11} \\ \sigma_{22} \\ \sigma_{33} \\ \sigma_{12} \\ \sigma_{13} \\ \sigma_{23} \end{bmatrix} = \begin{bmatrix} (\lambda+\mu) & \lambda & \lambda & 0 & 0 & 0 \\ \lambda & (\lambda+\mu) & \lambda & 0 & 0 & 0 \\ \lambda & \lambda & (\lambda+\mu) & 0 & 0 & 0 \\ 0 & 0 & 0 & \mu/2 & 0 & 0 \\ 0 & 0 & 0 & 0 & \mu/2 & 0 \\ 0 & 0 & 0 & 0 & 0 & \mu/2 \end{bmatrix} \begin{bmatrix} \varepsilon_{11} \\ \varepsilon_{22} \\ \varepsilon_{33} \\ 2\varepsilon_{12} \\ 2\varepsilon_{13} \\ 2\varepsilon_{23} \end{bmatrix} \tag{3.32}$$

or equivalently,

$$\boldsymbol{\sigma} = \mathbf{D}\boldsymbol{\epsilon}, \quad \text{where} \quad \mathbf{D} = \begin{bmatrix} (\lambda+\mu) & \lambda & \lambda & 0 & 0 & 0 \\ \lambda & (\lambda+\mu) & \lambda & 0 & 0 & 0 \\ \lambda & \lambda & (\lambda+\mu) & 0 & 0 & 0 \\ 0 & 0 & 0 & \mu/2 & 0 & 0 \\ 0 & 0 & 0 & 0 & \mu/2 & 0 \\ 0 & 0 & 0 & 0 & 0 & \mu/2 \end{bmatrix}.$$

The Lamé coefficients, λ and μ, can be expressed in terms of the *Young's modulus*, E, *Poisson's ratio*, ν, and *Shear modulus*, G, as

$$\lambda = \frac{\nu E}{(1+\nu)(1-2\nu)} \quad \text{and} \quad \mu = \frac{E}{(1+\nu)} = 2G.$$

As a final point, we note that the normal components of the stress are not determined by the strain when the material is incompressible. When a material is incompressible $\nu = 1/2$, so that λ is undefined, and the body can only deform in such a way that $\varepsilon_{11} + \varepsilon_{22} + \varepsilon_{33} = 0$.

For more about elasticity theory we refer to e.g. Hunter [15], Spencer [39], Venkatraman and Patel [42], Oden [26] and Long [22].

3.6 The Weak Formulation in Linear Elasticity

In order to get a weak formulation of the equilibrium problem (3.21) and (3.23), we first define the test space $V \subset (H^1(\Omega))^3$ as

$$V := \{\mathbf{v} : \mathbf{v} \in (H^1(\Omega))^3, \mathbf{v} = \mathbf{0} \text{ on } \partial\Omega_D\}.$$

Now we take the scalar product of the system (3.21) with a test vector function $\mathbf{v} := (v_i)_{i=1}^3 \in V$, and integrate over the domain. This gives,

$$-\int_\Omega \frac{\partial \sigma_{ij}}{\partial x_j} v_i \,\mathrm{d}\mathbf{x} = \int_\Omega f_i v_i \,\mathrm{d}\mathbf{x} \quad \forall\, \mathbf{v} \in V. \tag{3.33}$$

Since

$$\frac{\partial}{\partial x_j}(v_i \sigma_{ij}) = v_i \frac{\partial \sigma_{ij}}{\partial x_j} + \sigma_{ij}\frac{\partial v_i}{\partial x_j},$$

equation (3.33) becomes

$$\int_\Omega \frac{\partial v_i}{\partial x_j}\sigma_{ij} \,\mathrm{d}\mathbf{x} - \int_\Omega \frac{\partial}{\partial x_j}(v_i\sigma_{ij}) \,\mathrm{d}\mathbf{x} = \int_\Omega f_i v_i \,\mathrm{d}\mathbf{x}.$$

Using the divergence theorem we have

$$\int_\Omega \frac{\partial}{\partial x_j}(v_i\sigma_{ij}) \,\mathrm{d}\mathbf{x} = \int_{\partial\Omega} v_i \sigma_{ij} n_j \,\mathrm{d}(\partial\Omega).$$

Hence using the boundary condition on $\partial\Omega_N$, $\sigma_{ij}n_j = g_i(\mathbf{x}) \quad \mathbf{x} \in \partial\Omega_N$, yields,

$$\int_\Omega \frac{\partial v_i}{\partial x_j}\sigma_{ij} \,\mathrm{d}\mathbf{x} = \int_{\partial\Omega_N} v_i g_i \,\mathrm{d}(\partial\Omega) + \int_\Omega v_i f_i \,\mathrm{d}\mathbf{x} \quad \forall\, \mathbf{v} \in V. \tag{3.34}$$

Using the symmetry of the stress (3.28) to get

$$\sigma_{ij}\frac{\partial v_i}{\partial x_j} = \frac{1}{2}\sigma_{ij}\Big(\frac{\partial v_i}{\partial x_j} + \frac{\partial v_i}{\partial x_j}\Big) = \frac{1}{2}\sigma_{ij}\Big(\frac{\partial v_i}{\partial x_j} + \frac{\partial v_j}{\partial x_i}\Big) = \sigma_{ij}\varepsilon_{ij}, \tag{3.35}$$

equation (3.34) can be expressed as

$$\int_\Omega \sigma_{ij}(\mathbf{u})\varepsilon_{ij}(\mathbf{v})\,\mathrm{d}\mathbf{x} = \int_\Omega v_i f_i\,\mathrm{d}\mathbf{x} + \int_{\partial\Omega_N} v_i g_i\,\mathrm{d}(\partial\Omega), \tag{3.36}$$

or in terms of the strain and stress vectors as

$$\int_\Omega \boldsymbol{\epsilon}^T(\mathbf{v})\boldsymbol{\sigma}(\mathbf{u})\,\mathrm{d}\mathbf{x} = \int_\Omega \mathbf{v}^T\mathbf{f}\,\mathrm{d}\mathbf{x} + \int_{\partial\Omega_N} \mathbf{v}^T\mathbf{g}\,\mathrm{d}(\partial\Omega). \tag{3.37}$$

By substituting the Hooke's law relation $\boldsymbol{\sigma} = \mathbf{D}\boldsymbol{\epsilon}$ into (3.37) gives

$$\int_\Omega \boldsymbol{\epsilon}^T(\mathbf{v})\mathbf{D}\boldsymbol{\epsilon}(\mathbf{u})\,\mathrm{d}\mathbf{x} = \int_\Omega \mathbf{v}^T\mathbf{f}\,\mathrm{d}\mathbf{x} + \int_{\partial\Omega_N} \mathbf{v}^T\mathbf{g}\,\mathrm{d}(\partial\Omega). \tag{3.38}$$

This is the weak form for the problem of linear elasticity. The term $\boldsymbol{\epsilon}(\mathbf{v})^T\mathbf{D}\boldsymbol{\epsilon}$ can be written in other ways. Note that

$$[\varepsilon_{11}(\mathbf{v}),\, \varepsilon_{22}(\mathbf{v}),\, \varepsilon_{33}(\mathbf{v})] \begin{bmatrix} 1 & 1 & 1 \\ 1 & 1 & 1 \\ 1 & 1 & 1 \end{bmatrix} \begin{bmatrix} \varepsilon_{11}(\mathbf{u}) \\ \varepsilon_{22}(\mathbf{u}) \\ \varepsilon_{33}(\mathbf{u}) \end{bmatrix} = (\nabla\cdot\mathbf{u})(\nabla\cdot\mathbf{v}) \tag{3.39}$$

so that

$$\boldsymbol{\epsilon}(\mathbf{v})^T\mathbf{D}\boldsymbol{\epsilon}(\mathbf{u}) = \lambda(\nabla\cdot\mathbf{u})(\nabla\cdot\mathbf{v}) + \mu\varepsilon_{ij}(\mathbf{u})\varepsilon_{ij}(\mathbf{v}). \tag{3.40}$$

Hence equation (3.38) may be written as

$$\int_\Omega \lambda(\nabla\cdot\mathbf{u})(\nabla\cdot\mathbf{v}) + \mu\varepsilon_{ij}(\mathbf{u})\varepsilon_{ij}(\mathbf{v})\,\mathrm{d}\mathbf{x} = \int_\Omega f_i v_i\,\mathrm{d}\mathbf{x} + \int_{\partial\Omega_N} g_i v_i\,\mathrm{d}(\partial\Omega). \tag{3.41}$$

We have finally that the weak formulation of (3.21)-(3.23) is to seek $\mathbf{u} \in V$ such that,

$$a(\mathbf{u},\mathbf{v}) = F(\mathbf{v}) \quad \mathbf{v}\in V, \tag{3.42}$$

where,

$$a(\mathbf{u},\mathbf{v}) = \int_\Omega \lambda(\nabla\cdot\mathbf{u})(\nabla\cdot\mathbf{v}) + \mu\varepsilon_{ij}(\mathbf{u})\varepsilon_{ij}(\mathbf{v})\,\mathrm{d}\mathbf{x}, \tag{3.43}$$

and,

$$F(\mathbf{v}) = \int_\Omega f_i v_i\,\mathrm{d}\mathbf{x} + \int_{\partial\Omega_N} g_i v_i\,\mathrm{d}(\partial\Omega). \tag{3.44}$$

3.7 The Finite Element Method in Linear Elasticity

The finite element method is applied to problem (3.21)-(3.23) via the weak formulation (3.42) and the Galerkin technique which was described in section 3.6. To recap, in the weak problem we seek $\mathbf{u} \in V$ such that

$$\int_{\Omega} \boldsymbol{\epsilon}^T(\mathbf{v})\mathbf{D}\boldsymbol{\epsilon}(\mathbf{u})\,\mathrm{d}\mathbf{x} = \int_{\Omega} \mathbf{v}^T\mathbf{f}\,\mathrm{d}\mathbf{x} + \int_{\partial\Omega_N} \mathbf{v}^T\mathbf{g}\,\mathrm{d}(\partial\Omega) \quad \forall\, \mathbf{v} \in V. \tag{3.45}$$

As for the scalar case of section 2.6, the finite element formulation is now to find $\mathbf{u}_h \in S^h$ where $S^h \subset V$ that satisfies (see Whiteman *et al.* [45])

$$\int_{\Omega} \boldsymbol{\epsilon}^T(\mathbf{v}_h)\mathbf{D}\boldsymbol{\epsilon}(\mathbf{u}_h)\,\mathrm{d}\mathbf{x} = \int_{\Omega} \mathbf{v}_h^T\mathbf{f}\,\mathrm{d}\mathbf{x} + \int_{\partial\Omega_N} \mathbf{v}_h^T\mathbf{g}\,\mathrm{d}(\partial\Omega) \quad \forall\, \mathbf{v}_h \in S^h \tag{3.46}$$

where $S^h \subset V$ is a finite dimensional space of vector functions each component of which is a piecewise polynomial function defined over a partition (mesh) of Ω. If N_k, $k = 1, 2, \cdots, M$ are basis functions satisfying the Lagrange conditions then

$$N_k(\mathbf{x}_i) = \begin{cases} 1, & i = k, \\ 0, & i \neq k. \end{cases} \tag{3.47}$$

Then we define the space $\widehat{S}^h$ as the span of the columns of the $3 \times 3M$ matrix,

$$\mathbf{N}(\mathbf{x}) = \begin{pmatrix} N_1 & 0 & 0 & N_2 & 0 & 0 & \cdots & N_M & 0 & 0 \\ 0 & N_1 & 0 & 0 & N_2 & 0 & \cdots & 0 & N_M & 0 \\ 0 & 0 & N_1 & 0 & 0 & N_2 & \cdots & 0 & 0 & N_M \end{pmatrix} \tag{3.48}$$

and we take the space S^h, $S^h \subset \widehat{S}^h$, involving the span of some of the columns of $\mathbf{N}$ which we describe below. Note that S^h is here a space of vector functions this is comparable in the vector context to the space $\widetilde{S}^h$ which was discussed in section 2.6. Using the matrix (3.48), the approximation $\mathbf{u}_h \in S^h$ can be written in the form

$$\mathbf{u}_h(\mathbf{x}) = \mathbf{N}(\mathbf{x})\mathbf{U} \tag{3.49}$$

where $\mathbf{U}$ is a vector of length $3M$ consisting of the nodal parameters of $\mathbf{u}_h$ and note that at the node with index i

$$\mathbf{u}_h(\mathbf{x}_i) = \begin{pmatrix} U_{3i-2} \\ U_{3i-1} \\ U_{3i} \end{pmatrix}.$$

The strain vector associated with $\mathbf{u}_h$ can similarly be written in the form

$$\boldsymbol{\epsilon}(\mathbf{u}_h) = \mathbf{B}\mathbf{U} \tag{3.50}$$

where $\mathbf{B}$ is the $6 \times 3M$ matrix and is given by

$$\mathbf{B} = \begin{pmatrix} \frac{\partial N_1}{\partial x_1} & 0 & 0 & \cdots & \frac{\partial N_M}{\partial x_1} & 0 & 0 \\ 0 & \frac{\partial N_1}{\partial x_2} & 0 & \cdots & 0 & \frac{\partial N_M}{\partial x_2} & 0 \\ 0 & 0 & \frac{\partial N_1}{\partial x_3} & \cdots & 0 & 0 & \frac{\partial N_M}{\partial x_3} \\ \frac{\partial N_1}{\partial x_2} & \frac{\partial N_1}{\partial x_1} & 0 & \cdots & \frac{\partial N_M}{\partial x_2} & \frac{\partial N_M}{\partial x_1} & 0 \\ 0 & \frac{\partial N_1}{\partial x_3} & \frac{\partial N_1}{\partial x_2} & \cdots & 0 & \frac{\partial N_M}{\partial x_3} & \frac{\partial N_M}{\partial x_2} \\ \frac{\partial N_1}{\partial x_3} & 0 & \frac{\partial N_1}{\partial x_1} & \cdots & \frac{\partial N_M}{\partial x_3} & 0 & \frac{\partial N_M}{\partial x_1} \end{pmatrix}. \tag{3.51}$$

Note that if $\mathbf{v}_k$ is the kth column of $\mathbf{N}$ then $\boldsymbol{\epsilon}(\mathbf{v}_k)$ is the kth column of $\mathbf{B}$. Also note that if $\hat{\mathbf{e}}_k$ is the kth column of the $3M \times 3M$ identity matrix then

$$\mathbf{v}_k = \mathbf{N}\hat{\mathbf{e}}_k \quad \text{and} \quad \boldsymbol{\epsilon}(\mathbf{v}_k) = \mathbf{B}\hat{\mathbf{e}}_k. \tag{3.52}$$

Hence by using equations (3.50) and (3.52), we have with the test vector $\mathbf{v}_k = \mathbf{N}\hat{\mathbf{e}}_k$ in (3.46) the equation

$$\hat{\mathbf{e}}_k^T \Big(\int_\Omega \mathbf{B}^T \mathbf{D} \mathbf{B} \, \mathrm{d}\mathbf{x} \Big) \mathbf{U} = \hat{\mathbf{e}}_k^T \int_\Omega \mathbf{N}^T \mathbf{f} \, \mathrm{d}\mathbf{x} + \hat{\mathbf{e}}_k^T \int_{\partial\Omega_N} \mathbf{N}^T \mathbf{g} \, \mathrm{d}(\partial\Omega).$$

We define

$$\begin{aligned} \mathbf{K} &= \int_\Omega \mathbf{B}^T \mathbf{D} \mathbf{B} \, \mathrm{d}\mathbf{x} \\ \mathbf{F} &= \int_\Omega \mathbf{N}^T \mathbf{f} \, \mathrm{d}\mathbf{x} + \int_{\partial\Omega_N} \mathbf{N}^T \mathbf{g} \, \mathrm{d}(\partial\Omega) \end{aligned}$$

with $\mathbf{K}$ known as the *global stiffness matrix* and $\mathbf{F}$ known as the *global force vector*. The finite element equations determining $\mathbf{u}_h$ can now be compactly written in the form

$$\hat{\mathbf{e}}_k^T \mathbf{K} \mathbf{U} = \hat{\mathbf{e}}_k^T \mathbf{F} \tag{3.53}$$

which holds for all k such that the kth column of $\mathbf{N}$ is in S^h. This gives the equations for the unknown values of the vector $\mathbf{U}$.

In the case of a two-dimensional problem all the quantities so far introduced reduce appropriately in size with now $\mathbf{x} \in \mathbb{R}^2$, the displacement $\mathbf{u}$ and its approximation $\mathbf{u}_h, \mathbf{u}_h \in \mathbb{R}^2$, the strain and stress vectors $\boldsymbol{\epsilon}, \boldsymbol{\sigma} \in \mathbb{R}^3$ with $\boldsymbol{\epsilon} = [\varepsilon_{11}, \varepsilon_{22}, 2\varepsilon_{12}]^T$ and $\boldsymbol{\sigma} = [\sigma_{11}, \sigma_{22}, \sigma_{12}]^T$, $\mathbf{D} \in \mathbb{R}^{3,3}$ and correspondingly $\mathbf{N}(\mathbf{x})$ being of size $2 \times 2M$ and $\mathbf{B}(\mathbf{x})$ being of size $3 \times 2M$. To describe the finite element approximation in two dimensions based on piecewise linear functions defined over triangles we refer to the so-called standard triangle

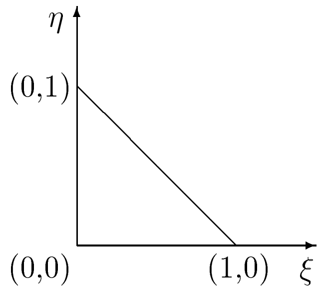

Figure 3.3: A standard triangle

$$0 \le \xi \le 1, \quad 0 \le \eta \le 1, \quad 0 \le 1 - \xi - \eta$$

in the (ξ, η) plane. With respect to this plane we have the following three local basis functions of the Lagrange type, ξ, η and $1 - \xi - \eta$. For a triangle in the (x, y) plane with nodes $\mathbf{x}_i$, $\mathbf{x}_j$, $\mathbf{x}_k$ we have the mapping from the standard triangle given by

$$\mathbf{x} = (1 - \xi - \eta)\mathbf{x}_i + \xi\mathbf{x}_j + \eta\mathbf{x}_k. \tag{3.54}$$

In terms of $\mathbf{x}$ in an actual triangle the basis functions are

$$N_i(\mathbf{x}) = 1 - \xi(\mathbf{x}) - \eta(\mathbf{x}), \quad N_j(\mathbf{x}) = \xi(\mathbf{x}), \quad \text{and} \quad N_k(\mathbf{x}) = \eta(\mathbf{x}).$$

By considering the 2×2 Jacobian J of the mapping (3.54), its inverse J^{-1} and the absolute value of its determinant $|J|$ we can define the local strain matrix $\widehat{\mathbf{B}}$

$$\widehat{\mathbf{B}} = \frac{1}{|J|} \begin{pmatrix} y_j - y_k & 0 & y_k - y_i & 0 & y_i - y_j & 0 \\ 0 & x_k - x_j & 0 & x_i - x_k & 0 & x_j - x_i \\ x_k - x_j & y_j - y_k & x_i - x_k & y_k - y_i & x_j - x_i & y_i - y_j \end{pmatrix} \tag{3.55}$$

where

$$|J| = |(x_j - x_i)(y_k - y_i) - (x_k - x_i)(y_j - y_i)|. \tag{3.56}$$

The matrix $\widehat{\mathbf{B}}$ is such that if $\widehat{\mathbf{U}} = [U_{2i-1},\ U_{2i},\ U_{2j-1},\ U_{2j},\ U_{2k-1},\ U_{2k}]^T$ is the vector of the element nodal displacements, then $\widehat{\mathbf{B}}\widehat{\mathbf{U}}$ gives the 3×1 vector of the strain components. Note that $\widehat{\mathbf{B}}$ is constant over the element. The element stiffness matrix is defined by

$$\widehat{\mathbf{K}} = \int_0^1 \int_0^{1-\eta} \widehat{\mathbf{B}}^T \mathbf{D} \widehat{\mathbf{B}}\, |J|\, \mathrm{d}\xi \mathrm{d}\eta \approx \frac{|J|}{2} \widehat{\mathbf{B}}^T \mathbf{D} \widehat{\mathbf{B}} \tag{3.57}$$

with the right hand side evaluated at the centroid of the triangle. The approximation is exact if $\mathbf{D}$ is constant over the element. The element body force can similarly be defined. With

$$\widehat{\mathbf{N}} = \begin{pmatrix} N_1 & 0 & N_2 & 0 & N_3 & 0 \\ 0 & N_1 & 0 & N_2 & 0 & N_3 \end{pmatrix} \tag{3.58}$$

and with $\mathbf{f} = (f_1, f_2)^T$ denoting the body force on the element

$$\widehat{\mathbf{F}} = \int_0^1 \int_0^{1-\eta} \widehat{\mathbf{N}}^T \mathbf{f}\, |J|\, \mathrm{d}\xi \mathrm{d}\eta \approx \frac{|J|}{6} \begin{pmatrix} f_1 \\ f_2 \\ f_1 \\ f_2 \\ f_1 \\ f_2 \end{pmatrix}. \tag{3.59}$$

If nodes i and j are on the boundary then the basis functions can be described in the form

$$N_i(\mathbf{x}) = 1 - \xi(\mathbf{x}), \qquad N_j(\mathbf{x}) = \xi(\mathbf{x}) \tag{3.60}$$

and the mapping function from local to global co-ordinates is

$$\mathbf{x} = (1 - \xi)\mathbf{x}_i + \xi \mathbf{x}_j. \tag{3.61}$$

Hence the local traction vector may be approximated in a similar way to give

$$\begin{aligned} \widehat{\mathbf{G}} &= \int_0^1 \begin{pmatrix} 1-\xi & 0 \\ 0 & 1-\xi \\ \xi & 0 \\ 0 & \xi \end{pmatrix} \begin{pmatrix} g_1 \\ g_2 \end{pmatrix} |\mathbf{x}_j - \mathbf{x}_i|\, \mathrm{d}\xi \\ &\approx \frac{|\mathbf{x}_j - \mathbf{x}_i|}{2} \begin{pmatrix} g_1 \\ g_2 \\ g_1 \\ g_2 \end{pmatrix}, \end{aligned} \tag{3.62}$$

where the vector $\mathbf{g} = [g_1,\ g_2]^T$ is evaluated at the mid-point of the boundary segment.

All that remains is to apply the boundary conditions, and this is perhaps most conveniently done at the element level. If node i on the triangle is on $\partial\Omega_D$ at which $\mathbf{u}(\mathbf{x}_i) = \mathbf{0}$ we modify $\widehat{\mathbf{K}}$, $\widehat{\mathbf{F}}$ and $\widehat{\mathbf{G}}$ by setting

$$\begin{aligned}
\widehat{\mathbf{K}}_{2i-1,2i-1} &= \widehat{\mathbf{K}}_{2i,2i} = 1, \\
\widehat{\mathbf{K}}_{2i-1,m} &= 0 \quad \forall\, m \in \{1,2,\cdots,6\}/\{2i-1\}, \\
\widehat{\mathbf{K}}_{2i,2m} &= 0 \quad \forall\, m \in \{1,2,\cdots,6\}/\{2i\}, \\
\widehat{\mathbf{F}}_{2i-1} &= \widehat{\mathbf{F}}_{2i} = 0, \\
\widehat{\mathbf{G}}_{2i-1} &= \widehat{\mathbf{G}}_{2i} = 0.
\end{aligned}$$

All the element matrices $\widehat{\mathbf{K}}$ and vectors $\widehat{\mathbf{F}}$ and $\widehat{\mathbf{G}}$, after such modification if necessary, are assembled to form $\widetilde{\mathbf{K}}$ and $\widetilde{\mathbf{F}}$ in a linear system of the form

$$\widetilde{\mathbf{K}}\mathbf{U} = \widetilde{\mathbf{F}}. \tag{3.63}$$

3.8 Summary

The mechanics of continuous media deals with the three kinds of quantities known as displacement, strain and stress. In the case of an undeformed body loaded in some way, the *displacement field* is concerned with the movement (i.e. change in position) of each point in the body, *strain* describes the change of length of line segments (material fibers) and *stress* describes the forces per unit area acting inside the body. The specific displacement, strain and stress fields which are obtained in the body are governed by the laws of nature and various kinematic relations. The kinematic relations relate strain and displacement. The equations of motion are concerned with balancing the forces and the constitutive equation. The forces are the external loading, forces due to the stress and the inertial term. The constitutive equation is specific to the material being deformed and describes the relation between stress and strain. In the simplest case there are six algebraic equations giving the strain components in terms of the stress, or vice versa. If they are linear, they are known as Hooke's law. In many practical situations there are no inertial terms (or at least they are negligible) and the equations of motion reduce to the equations of quasi-static equilibrium which we usually just refer to as the equilibrium equations. The finite element methods can be applied to analyse the stress of elastic structures under the assumption of infinitesimal deformation.

The procedure of finite element methods for the problem of linear elasticity in two dimensions described by a system of differential equations is as follows. The first step is to derive a weak form of the equilibrium equations. The next step is to discretize the domain Ω into the set of finite elements using the three-node triangular element. Then the elements of the stiffness matrix $\mathbf{K}$ and the force vector $\mathbf{F}$ can be calculated. The next procedure after obtaining the element stiffness matrix and the force vector is assembling the global stiffness matrix $\widetilde{\mathbf{K}}$ and the global force vector $\widetilde{\mathbf{F}}$. The finite element solution is then obtained by solving the system $\widetilde{\mathbf{K}}\mathbf{U} = \widetilde{\mathbf{F}}$.

Chapter 4

Error Estimation and Adaptivity in Linear Elasticity

The previous chapter described the equations of linear elasticity together with brief details of the finite element method that we use to compute an approximate solution for problems of linear elasticity. Following on from that the purpose of this chapter is to consider the error in our approximate solutions for problems in two space dimensions. We consider an *a priori* error bound and then describe the *a posteriori* error estimator introduced by Zienkiewicz and Zhu [48, 49] which we use in our adaptive mesh refinement procedures. Hence the estimator and the adaptive procedure enable us to obtain 'accurate' approximate solutions efficiently. This will be an important part of our overall scheme for solving the linear viscoelastic problems in this thesis. Results of how the mesh is adaptively refined based on the estimator are presented in Chapter 7, when results for the overall scheme are given.

4.1 An *a Priori* Error Bound

An *a priori* error bound can be constructed in a standard way which briefly involves the following. We show that the bilinear form $a(\cdot,\cdot)$ in the weak formulation is continuous and elliptic with respect to the usual norm of the space V under consideration. We show that the approximate solution $\mathbf{u}_h$ is the orthogonal projection of the exact solution $\mathbf{u}$ from the approximation space and it is hence the best approximation to $\mathbf{u}$ in the energy norm $\|\cdot\|_E$. As it then follows that $\|\mathbf{u}-\mathbf{u}_h\|_E \leq \|\mathbf{u}-\Pi_h\mathbf{u}\|_E$, where $\Pi_h\mathbf{u}$ is the interpolant to $\mathbf{u}$, we can use standard interpolation estimates to get an *a priori* bound in the energy norm. Continuity and ellipticity lead to an *a priori* bound in the norm of the space V and then the Nitsche lift can be used to get an *a priori* bound in the L_2 norm. We consider some of the details of these steps in what follows.

Recall that for our two-dimensional problem with homogeneous boundary conditions we have $V = (\mathring{H}^1(\Omega))^2$,

$$a(\mathbf{u},\mathbf{v}) = F(\mathbf{v}),\ a(\mathbf{u},\mathbf{v}) = \int_\Omega \lambda(\nabla\cdot\mathbf{u})(\nabla\cdot\mathbf{v}) + \mu\varepsilon_{ij}(\mathbf{u})\varepsilon_{ij}(\mathbf{v})\,\mathrm{d}\mathbf{x}, \quad F(\mathbf{v}) = \int_\Omega f_i v_i\,\mathrm{d}\mathbf{x}, \tag{4.1}$$

the norm of $\mathbf{v} \in V$, $\mathbf{v} = (v_1, v_2)^T$ is given by

$$\|\mathbf{v}\|^2 = \int_\Omega v_1^2 + v_2^2 + |\nabla v_1|^2 + |\nabla v_2|^2\,\mathrm{d}\mathbf{x} \tag{4.2}$$

and the energy norm $\|\cdot\|_E$ is given by

$$\|\mathbf{v}\|_E^2 = a(\mathbf{v},\mathbf{v}). \tag{4.3}$$

In what follows we assume that the Lamé parameters $\lambda = \lambda(\mathbf{x})$ and $\mu = \mu(\mathbf{x})$ satisfy

$$0 \le |\lambda(\mathbf{x})| \le \lambda_1, \quad 0 < \mu_0 \le |\mu(\mathbf{x})| \le \mu_1 \quad \text{for all } \mathbf{x} \in \Omega. \tag{4.4}$$

4.1.1 Continuity of $a(\mathbf{u},\mathbf{v})$

The continuity of a bilinear form was defined in section 2.3. To show that this holds for our bilinear form observe that (4.4) leads to $a(\mathbf{v},\mathbf{v}) \ge 0$ for all $\mathbf{v} \in V$ and from this it follows that we have the Cauchy Schwarz inequality

$$|a(\mathbf{u},\mathbf{v})|^2 \le a(\mathbf{u},\mathbf{u})a(\mathbf{v},\mathbf{v}) = \|\mathbf{u}\|_E^2\|\mathbf{v}\|_E^2. \tag{4.5}$$

It just remains to bound energy norms $\|\cdot\|_E$ in terms of the norms $\|\cdot\|$ of the space V. To do this we first note that by the triangle inequality and the bounds (4.4) again we have

$$a(\mathbf{v},\mathbf{v}) \le \lambda_1 \left|\int_\Omega (\nabla\cdot\mathbf{v})^2\,\mathrm{d}\mathbf{x}\right| + \mu_1 \left|\int_\Omega \sum_{i,j=1}^{2} \varepsilon_{ij}(\mathbf{v})\varepsilon_{ij}(\mathbf{v})\,\mathrm{d}\mathbf{x}\right|. \tag{4.6}$$

We consider each of these terms separately. For the first term we have

$$\begin{aligned}(\nabla\cdot\mathbf{v})^2 &= \left(\frac{\partial v_1}{\partial x}+\frac{\partial v_2}{\partial y}\right)^2 = \left(\frac{\partial v_1}{\partial x}\right)^2 + 2\left(\frac{\partial v_1}{\partial x}\right)\left(\frac{\partial v_2}{\partial y}\right) + \left(\frac{\partial v_2}{\partial y}\right)^2 \\ &\le 2\left(\left(\frac{\partial v_1}{\partial x}\right)^2 + \left(\frac{\partial v_2}{\partial y}\right)^2\right) \le 2\left((\nabla v_1)^2 + (\nabla v_2)^2\right) \qquad (4.7)\end{aligned}$$

and hence

$$\int_\Omega (\nabla\cdot\mathbf{v})^2\,\mathrm{d}\mathbf{x} \le 2\|\mathbf{v}\|^2. \qquad (4.8)$$

For the second term we have

$$\sum_{i,j=1}^{2}\varepsilon_{ij}(\mathbf{v})^2 = \varepsilon_{11}(\mathbf{v})^2 + \varepsilon_{22}(\mathbf{v})^2 + 2\varepsilon_{12}(\mathbf{v})^2.$$

and

$$\begin{aligned}2\varepsilon_{12}(\mathbf{v})^2 &= \frac{1}{2}\left(\frac{\partial v_1}{\partial y}+\frac{\partial v_2}{\partial x}\right)^2 = \frac{1}{2}\left(\left(\frac{\partial v_1}{\partial y}\right)^2 + \left(\frac{\partial v_2}{\partial x}\right)^2 + 2\left(\frac{\partial v_1}{\partial y}\right)\left(\frac{\partial v_2}{\partial x}\right)\right) \\ &\le \left(\frac{\partial v_1}{\partial y}\right)^2 + \left(\frac{\partial v_2}{\partial x}\right)^2. \qquad (4.9)\end{aligned}$$

Thus

$$\sum_{i,j=1}^{2}\varepsilon_{ij}(\mathbf{v})^2 \le (\nabla v_1)^2 + (\nabla v_2)^2 \quad \text{and} \quad \int_\Omega \sum_{i,j=1}^{2}\varepsilon_{ij}(\mathbf{v}(\mathbf{x}))^2\,\mathrm{d}\mathbf{x} \le \|\mathbf{v}\|^2. \qquad (4.10)$$

Hence

$$\|\mathbf{v}\|_E^2 = a(\mathbf{v},\mathbf{v}) \le (2\lambda_1 + \mu_1)\|\mathbf{v}\|^2 \qquad (4.11)$$

and

$$|a(\mathbf{u},\mathbf{v})| \le \gamma\|\mathbf{u}\|\,\|\mathbf{v}\| \quad \text{with } \gamma = 2\lambda_1 + \mu_1. \qquad (4.12)$$

4.1.2 Ellipticity of $a(\mathbf{v},\mathbf{v})$

From the lower bounds in (4.4) we immediately have

$$a(\mathbf{v},\mathbf{v}) \ge \int_\Omega \mu \sum_{i,j=1}^{2}\varepsilon_{ij}(\mathbf{v})^2\,\mathrm{d}\mathbf{x} \ge \mu_0\int_\Omega \sum_{i,j=1}^{2}\varepsilon_{ij}(\mathbf{v})^2\,\mathrm{d}\mathbf{x} \qquad (4.13)$$

with the first inequality being sharp for displacement fields $\mathbf{v}$ which lead to no volume change, i.e. $\nabla\cdot\mathbf{v} = 0$. To bound (4.13) below by a multiple of $\|\mathbf{v}\|$ is a standard result known as Korn's inequality, see Johnson *et al.* [9, p.523–524], and Korn's inequality can be proved using the Poincaré-Friedrich inequality mentioned in section 2.4. We just state the results here.

Theorem 1 *Korn's inequality: There exists a constant $c = C(\Omega) > 0$ such that for all $\mathbf{v} \in (\mathring{H}^1(\Omega))^2$,*

$$\int_\Omega \sum_{i,j=1}^{2} \varepsilon_{ij}(\mathbf{v})^2 \, \mathrm{d}\mathbf{x} \geq c \sum_{i=1}^{2} \|v_i\|^2_{H^1(\Omega)} = c\|\mathbf{v}\|^2. \tag{4.14}$$

Hence

$$a(\mathbf{v}, \mathbf{v}) \geq \rho\|\mathbf{v}\|^2 \quad \text{where } \rho = \mu_0 c. \tag{4.15}$$

4.1.3 Orthogonal Projection and Best Approximation

As the exact solution $\mathbf{u} \in V$ and the approximation solution $\mathbf{u}_h \in S^h \subset V$ satisfy

$$a(\mathbf{u}, \mathbf{v}) = F(\mathbf{v}) \quad \forall\, \mathbf{v} \in V, \tag{4.16}$$

$$a(\mathbf{u}_h, \mathbf{v}_h) = F(\mathbf{v}_h) \quad \forall\, \mathbf{v}_h \in S^h \tag{4.17}$$

the bilinearity and the conforming condition $S^h \subset V$ imply that by taking $\mathbf{v} \in S^h$ in (4.16) and subtracting (4.17) from this restricted form of (4.16) we get

$$a(\mathbf{u} - \mathbf{u}_h, \mathbf{v}) = 0 \quad \mathbf{v} \in S^h. \tag{4.18}$$

This shows that $\mathbf{u}_h$ is the orthogonal projection of $\mathbf{u}$ from S^h in this inner product. The best approximation property in the energy norm then follows almost immediately. If $\mathbf{v} \in S^h$ then $\mathbf{u}_h - \mathbf{v} \in S^h$ and the orthogonality, and the Cauchy Schwarz property gives

$$\|\mathbf{u} - \mathbf{u}_h\|_E^2 = a(\mathbf{u} - \mathbf{u}_h, \mathbf{u} - \mathbf{u}_h) = a(\mathbf{u} - \mathbf{u}_h, \mathbf{u} - \mathbf{u}_h + \mathbf{u}_h - \mathbf{v}) \tag{4.19}$$

$$= a(\mathbf{u} - \mathbf{u}_h, \mathbf{u} - \mathbf{v}) \leq \|\mathbf{u} - \mathbf{u}_h\|_E \|\mathbf{u} - \mathbf{v}\|_E. \tag{4.20}$$

Hence for all $\mathbf{v} \in S^h$

$$\|\mathbf{u} - \mathbf{u}_h\|_E \leq \|\mathbf{u} - \mathbf{v}\|_E \tag{4.21}$$

and hence in particular if $\mathbf{v} = \Pi_h \mathbf{u} \in S^h$ is the interpolant to $\mathbf{u}$ then

$$\|\mathbf{u} - \mathbf{u}_h\|_E \leq \|\mathbf{u} - \Pi_h \mathbf{u}\|_E. \tag{4.22}$$

By using the ellipticity and continuity we similarly have in the usual norm of V

$$\rho\|\mathbf{u} - \mathbf{u}_h\|^2 \leq \gamma\|\mathbf{u} - \Pi_h \mathbf{u}\|^2, \quad \text{i.e. } \|\mathbf{u} - \mathbf{u}_h\|^2 \leq \frac{\gamma}{\rho}\|\mathbf{u} - \Pi_h \mathbf{u}\|^2. \tag{4.23}$$

4.1.4 The Interpolation Error Bound in $\mathbb{R}^2$ with Linear Triangles

For a given mesh of $\Omega \subset \mathbb{R}^2$ involving n triangles the interpolation problem involves

$$\|\mathbf{u}-\Pi_h\mathbf{u}\|^2 = \sum_{i=1}^{2} \|u_i-\Pi_h u_i\|^2 = \sum_{i=1}^{2}\sum_{k=1}^{n} \int_{\Omega_k} (u_i-\Pi_h u_i)^2+(\nabla(u_i-\Pi_h u_i))^2 \,\mathrm{d}\mathbf{x} \quad (4.24)$$

and thus we need only consider the pointwise values of $u_i - \Pi_h u_i$ and the pointwise values of $\nabla(u_i - \Pi_h u_i)$ in the triangle Ω_k. As we will see this depends on the length h_k of the longest of the three sides of Ω_k and on the diameter $\rho_k \le h_k$ of the inscribed circle, i.e. the diameter of the largest circle that can be put inside Ω_k. The value h_k gives the size of the triangle and the value ρ_k relates to the area of the triangle which arises in the relations with the area being bounded below by $h_h \rho_k/2$.

To simplify the notation slightly let $w = u_i$ denote the scalar function under consideration and we abbreviate Π_h to Π. The details that follow correspond approximately to those given in [9, p.334–337]. Let $\mathbf{a}_1, \mathbf{a}_2, \mathbf{a}_3$ denote the three vertices of the triangle and let ϕ_1, ϕ_2, ϕ_3 denote the cardinal basis functions. We write $\phi_1(\xi,\eta) = 1-\xi-\eta$, $\phi_2(\xi,\eta) = \xi$, $\phi_3(\xi,\eta) = \eta$ when we consider these functions on the standard triangle (see Figure 3.3) $0 \le \xi, \eta, 1-\xi-\eta \le 1$ and we write $\phi_1(\mathbf{x}), \phi_2(\mathbf{x}), \phi_3(\mathbf{x})$ when we consider these as functions of $\mathbf{x}$ defined on Ω_k. The relation between (ξ,η) and $\mathbf{x} = (x_1, x_2) = (x, y)$ is

$$\mathbf{x}(\xi,\eta) = \sum_{l=1}^{3} \mathbf{a}_l \phi_l(\xi,\eta) = \mathbf{a}_i + \xi(\mathbf{a}_j - \mathbf{a}_i) + \eta(\mathbf{a}_k - \mathbf{a}_i). \quad (4.25)$$

In the relations to follow it is convenient here to note that

$$\sum_l \phi_l = 1, \quad \sum_l \nabla\phi_l = \mathbf{0}, \quad 0 \le \phi_l(\mathbf{x}) \le 1, \quad (4.26)$$

$$\mathbf{x} = \sum_l \phi_l(\mathbf{x})\mathbf{a}_l, \quad \frac{\partial \mathbf{x}}{\partial x_r} = \sum_l \frac{\partial \phi_l}{\partial x_r}\mathbf{a}_l = r\text{th unit vector in } \mathbb{R}^2 \quad (4.27)$$

$$\sum_l \nabla\phi_l(\mathbf{x})\mathbf{a}_l^T = \begin{pmatrix} 1 & 0 \\ 0 & 1 \end{pmatrix}. \quad (4.28)$$

The interpolant and its error are given by

$$\Pi w(\mathbf{x}) = \sum_{l=1}^{3} w(\mathbf{a}_l)\phi_l(\mathbf{x}) \quad w(\mathbf{x}) - \Pi w(\mathbf{x}) = \sum_{l=1}^{3} (w(\mathbf{x}) - w(\mathbf{a}_l))\phi_l(\mathbf{x}) \quad (4.29)$$

and by considering Taylor's series with finite remainder on the line between $\mathbf{a}_l$ and $\mathbf{x}$ we have (by expanding about $\mathbf{x}$)

$$w(\mathbf{a}_l) - w(\mathbf{x}) = (\nabla w(\mathbf{x}))^T(\mathbf{a}_l - \mathbf{x}) + R_l(\mathbf{x}), \quad \text{where} \quad R_l(\mathbf{x}) = \frac{1}{2}(\mathbf{a}_l - \mathbf{x})^T H_l(\mathbf{x})(\mathbf{a}_l - \mathbf{x}) \tag{4.30}$$

and where $H_l(\mathbf{x})$ is the 2×2 Hessian matrix evaluated at some point between $\mathbf{a}_l$ and $\mathbf{x}$, i.e.

$$H_l(\mathbf{x}) = \left(\frac{\partial^2 w}{\partial x_i \partial x_j}(\hat{\mathbf{a}}_l) \right). \tag{4.31}$$

Now by (4.26) and (4.27)

$$\sum_l (\nabla w(\mathbf{x}))^T(\mathbf{x} - \mathbf{a}_l)\phi_l(\mathbf{x}) = (\nabla w(\mathbf{x}))^T \sum_l (\mathbf{x} - \mathbf{a}_l)\phi_l(\mathbf{x}) = \mathbf{0} \tag{4.32}$$

and we get the representation for the pointwise error

$$w(\mathbf{x}) - \Pi w(\mathbf{x}) = -\sum_l R_l(\mathbf{x})\phi_l(\mathbf{x}). \tag{4.33}$$

To get a representation for the error in the gradient we do not differentiate this relation partially, as then we would have to consider differentiating $R_l(\mathbf{x})$, but instead note that by using (4.30) we get

$$\sum_l (w(\mathbf{a}_l) - w(\mathbf{x}))\nabla\phi_l(\mathbf{x}) = \sum_l (\nabla w(\mathbf{x}))^T(\mathbf{a}_l - \mathbf{x})\nabla\phi_l(\mathbf{x}) + \sum_l R_l(\mathbf{x})\nabla\phi_l(\mathbf{x}). \tag{4.34}$$

By using (4.26) and (4.27) the left hand side simplifies to $\nabla(\Pi w(\mathbf{x}))$. The first term on the right hand side also simplifies by using the (4.26) and (4.27) and the associative property of matrix multiplication. We have

$$(\nabla w(\mathbf{x}))^T(\mathbf{a}_l - \mathbf{x})\nabla\phi_l(\mathbf{x}) = (\nabla\phi_l(\mathbf{x})(\mathbf{a}_l - \mathbf{x})^T)\nabla w(\mathbf{x}) \tag{4.35}$$

and

$$\sum_l (\nabla\phi_l(\mathbf{x})(\mathbf{a}_l - \mathbf{x})^T) = \begin{pmatrix} 1 & 0 \\ 0 & 1 \end{pmatrix} \tag{4.36}$$

so that

$$\sum_l (\nabla\phi_l(\mathbf{x})(\mathbf{a}_l - \mathbf{x})^T)\nabla w(\mathbf{x}) = \nabla w(\mathbf{x}). \tag{4.37}$$

Thus our required representation is

$$\nabla(w(\mathbf{x}) - \Pi w(\mathbf{x})) = -\sum_l R_l(\mathbf{x})\nabla\phi_l(\mathbf{x}). \tag{4.38}$$

Using (4.33) and (4.38) we get our interpolation bounds as follows.

Let

$$M_k = \max_{1\le i,j\le 2} \max_{\mathbf{x}\in\bar{\Omega}_k} \left| \frac{\partial^2 w}{\partial x_i \partial x_j}(\mathbf{x}) \right| . \tag{4.39}$$

The maximum row sum of the Hessian of w is bounded by $2M_k$ (i.e. the ∞ matrix norm is bounded by $2M_k$) and this also bounds the largest eigenvalue of the Hessian over $\bar{\Omega}_k$. Thus

$$|R_l(\mathbf{x})| \le M_k|\mathbf{x} - \mathbf{a}_l|^2 \le M_k h_k^2 \tag{4.40}$$

and using (4.26) again we get

$$|w(\mathbf{x}) - \Pi w(\mathbf{x})| \le M_k h_k^2. \tag{4.41}$$

To bound the error in the gradient we need to consider the size of the gradient of each of the three basis functions. From the mapping $(\xi, \eta) \to (x_1, x_2) = (x, y)$ and its inverse we have the Jacobian

$$\begin{pmatrix} \xi_x & \xi_y \\ \eta_x & \eta_y \end{pmatrix} = \begin{pmatrix} x_\xi & x_\eta \\ y_\xi & y_\eta \end{pmatrix}^{-1} = \frac{1}{\Delta}\begin{pmatrix} y_\eta & -x_\eta \\ -y_\xi & x_\xi \end{pmatrix},$$

where

$$\Delta = x_\xi y_\eta - y_\xi x_\eta$$

with $|\Delta|/2$ being the area of the triangle Ω_k. The partial derivatives of the basis functions with respect to $\mathbf{x}$ are hence

$$\begin{aligned}
\begin{pmatrix} \dfrac{\partial\phi_1}{\partial x} & \dfrac{\partial\phi_2}{\partial x} & \dfrac{\partial\phi_3}{\partial x} \\[2mm] \dfrac{\partial\phi_1}{\partial y} & \dfrac{\partial\phi_2}{\partial y} & \dfrac{\partial\phi_3}{\partial y} \end{pmatrix} &= \begin{pmatrix} \xi_x & \eta_x \\ \xi_y & \eta_y \end{pmatrix}\begin{pmatrix} -1 & 1 & 0 \\ -1 & 0 & 1 \end{pmatrix} \\
&= \begin{pmatrix} -\xi_x - \eta_x & \xi_x & \eta_x \\ -\xi_y - \eta_y & \xi_y & \eta_y \end{pmatrix} = \frac{1}{\Delta}\begin{pmatrix} -y_\eta + y_\xi & y_\eta & -y_\xi \\ x_\eta - x_\xi & -x_\eta & x_\xi \end{pmatrix}.
\end{aligned}$$

From (4.25) and by considering the size of each of the three columns of this matrix we have

$$\max\{|\nabla\phi_1|, |\nabla\phi_2|, |\nabla\phi_3|\} = \frac{1}{|\Delta|}\max\{|\mathbf{a}_2 - \mathbf{a}_3|, |\mathbf{a}_1 - \mathbf{a}_3|, |\mathbf{a}_1 - \mathbf{a}_2|\} = \frac{h_k}{|\Delta|}. \tag{4.42}$$

The area of a triangle is half the length of the base multiplied by the height. If we take the base side of the triangle as the longest side with length h_k and note that the corresponding height is greater than ρ_k, the diameter of the inscribed circle, then $|\Delta| \geq h_k\rho_k/2$. We can now get our bound for the error in the gradients. We have

$$|\nabla(w - \Pi w)(\mathbf{x})| \leq 3M_k h_k^2 \frac{2}{\rho_k} = 6M_k h_k \left(\frac{h_k}{\rho_k}\right). \tag{4.43}$$

The result indicates that when a mesh is constructed we need to construct the triangles in such a way that h_k/ρ_k remains bounded to guarantee that we approximate the gradient to $\mathcal{O}(h_k)$ accuracy. Assuming that this is satisfied, equations (4.41) and (4.43) in conjunction with the interpolation bound (4.24), which applies to all of Ω, we have established the *a priori* convergence of the approximations as $h = \max_k h_k \to 0$.

For any given mesh the size of $\max_k(h_k/\rho_k)$ is an indication of how regular or irregular some of the triangles are. For example if any of the triangles are long and thin (i.e. with small angles) then this could be large. For the above convergence results to hold we thus have to refine the meshes in such a way that h_k/ρ_k remain bounded over all elements considered as $h \to 0$. A sequence of meshes which satisfy the property are said to be *shape regular*. In our implementation we only consider shape-regular meshes and this is achieved in our implementation by ensuring that when we refine all triangles have angles in a range $[\alpha, \beta]$ where $0 < \alpha < \beta < 180°$. In the implementation we take $\alpha = 15°$, $\beta = 130°$.

4.2 *A Posteriori* Error Estimation

It frequently happens in practical problems that due to the nature of the data in certain subdomains, a solution of the linear elasticity problem can have low regularity. In this case it is necessary to increase the local accuracy of the finite element approximation without using too many additional degrees of freedom. One way to do this is to *adaptively* perform *local mesh refinement* in those subdomains where it is needed. Thus the finite element solution will be calculated on a provisional mesh, then an *a posteriori estimate* for the error will be computed on each element. The purpose of this is to indicate what part of the mesh induces large errors. Using this information, we then locally refine the mesh, and repeat the finite element computation. If necessary, the process can be repeated several times.

Assume that the finite element solution $\mathbf{u}_h$ has been calculated and the error function $\mathbf{e}(\mathbf{x})$ has been defined as

$$\mathbf{e}(\mathbf{x}) := \mathbf{u}(\mathbf{x}) - \mathbf{u}_h(\mathbf{x}). \tag{4.44}$$

In order to apply a local refinement strategy based on the knowledge of the finite element solution it is essential to be able to estimate the elemental errors for the current mesh. A quantity ϖ_i which estimates the local discretization error is thus devised. This discretization error is considered in the subdomain occupied by an individual element. Thus each element Ω_i has a calculated ϖ_i associated with it which is called the *error indicator*. The error indicators can be used to determine where the error is large and so that the relevant elements can be refined into smaller elements. The aim of the refinement step is to reduce the *global error estimate*, η, which is defined as

$$\eta^2 = \sum_{i=1}^{NE} \varpi_i^2, \tag{4.45}$$

where NE is the number of elements in the solution domain.

As also stated by Oden *et al.* [27], the construction of an *a posteriori* error estimate is made with the following conditions:

i) The error estimators are computable from given data and an existing finite element solution.

ii) The global error estimate has similar behaviour to the global error in some suitable norm, in the sense that constants C_1 and C_2 exist such that

$$C_1\eta \leq \|\mathbf{e}\| \leq C_2\eta, \tag{4.46}$$

where η is the global error estimate and $\mathbf{e}$ is the actual approximation error. The bounds given in equation (4.46) assure that the actual error and the estimated error decrease (or increase) at the same rate as the mesh is refined or as the order of approximation is altered. In particular, such bounds ensure that if some adaptive procedure is implemented which can be shown to decrease η, then $\|\mathbf{e}\|$ also decreases and at the same rate as η. In order to measure the quality of an error estimator, an effectivity index is employed. This is defined as

$$\theta = \frac{\eta}{||\mathbf{e}||}, \tag{4.47}$$

which is hopefully close to 1 for a given mesh and for a given error estimator. If this estimator tends to 1 as the mesh is refined then the global error estimator η is said to be *asymptotically exact.*

4.2.1 The Zienkiewicz-Zhu Error Estimator

In this section the error estimator developed by Zienkiewicz and Zhu [48], [49] which is referred as Z-Z or Z^2 error estimator, will be introduced. Consider the problem of linear elasticity defined in Chapter 3. The error of the finite element approximation $\mathbf{u}_h$ with respect to the exact solution $\mathbf{u}$ is defined as

$$\mathbf{e} = \mathbf{u} - \mathbf{u}_h \tag{4.48}$$

and the error of the stress (gradients) is defined as

$$\mathbf{e}_\sigma = \boldsymbol{\sigma} - \boldsymbol{\sigma}_h. \tag{4.49}$$

In practical computations the exact solutions $\mathbf{u}$ and $\boldsymbol{\sigma}$ will generally not be known. The basic concept of Z^2 error estimator [49], then, is to replace the exact value of $\mathbf{e}_\sigma$ in equation (4.49) by an approximation $\mathbf{e}^*_\sigma$ which is defined by

$$\mathbf{e}_\sigma \approx \mathbf{e}^*_\sigma = \boldsymbol{\sigma}^* - \boldsymbol{\sigma}_h$$

where $\boldsymbol{\sigma}^*$ is the recovered value of $\boldsymbol{\sigma}_h$ which is interpolated from its nodal values by the same basis functions $\mathbf{N}$ as those used for the variable $\mathbf{u}_h$. To evaluate the error, therefore, the energy norm is used to estimate $\mathbf{e}$ or $\mathbf{e}_\sigma$. The energy norm of the true error $\mathbf{e}$ is written as

$$||\mathbf{e}||_{E(\Omega)} = ||\mathbf{u} - \mathbf{u}_h||_{E(\Omega)} = \Big(\int_\Omega \mathbf{e}^T_\sigma \mathbf{D}^{-1}\mathbf{e}_\sigma \, \mathrm{d}\Omega\Big)^{1/2}, \tag{4.50}$$

where Ω is the domain on which the problem is defined and $\mathbf{D}$ is the elasticity matrix. The approximation of the error measured in the energy norm is thus

$$||\tilde{\mathbf{e}}||_{E(\Omega)} = \Big(\int_\Omega \mathbf{e}^{*T}_\sigma \mathbf{D}^{-1}\mathbf{e}^*_\sigma \, \mathrm{d}\Omega\Big)^{1/2} \tag{4.51}$$

which is known as the error estimator. The quality of the error estimator $||\tilde{\mathbf{e}}||_{E(\Omega)}$ is measured by its effectivity index which is the ratio of the estimated error and the actual error. That is, the effectivity index is given by

$$\theta = \frac{||\tilde{\mathbf{e}}||_{E(\Omega)}}{||\mathbf{e}||_{E(\Omega)}}. \tag{4.52}$$

If θ approaches unity as the true error $||\mathbf{e}||$ tends to zero, this implies that the estimator converges to the exact error. It has been shown in [49] that the following theorem demonstrates how an asymptotically exact error estimator can be achieved.

Theorem 2 *Suppose that* $||\mathbf{e}^*|| = ||\mathbf{u} - \mathbf{u}^*||$ *is some error norm of the recovered solution, then the error estimator* $||\tilde{\mathbf{e}}||$ *is asymptotically exact if*

$$\frac{||\mathbf{e}^*||}{||\mathbf{e}||} \longrightarrow 0 \quad as \quad ||\mathbf{e}|| \longrightarrow 0. \tag{4.53}$$

Proof. The proof of the theorem is straightforward. The error estimator $||\tilde{\mathbf{e}}||$ may be expressed as

$$||\tilde{\mathbf{e}}|| = ||\mathbf{u}^* - \mathbf{u}_h|| := ||(\mathbf{u} - \mathbf{u}_h) - (\mathbf{u} - \mathbf{u}^*)||. \tag{4.54}$$

Using the triangular inequality, we have

$$||\mathbf{u} - \mathbf{u}_h|| - ||\mathbf{u} - \mathbf{u}^*|| \leq ||\tilde{\mathbf{e}}|| \leq ||\mathbf{u} - \mathbf{u}_h|| + ||\mathbf{u} - \mathbf{u}^*|| \tag{4.55}$$

or

$$||\mathbf{e}|| - ||\mathbf{e}^*|| \leq ||\tilde{\mathbf{e}}|| \leq ||\mathbf{e}|| + ||\mathbf{e}^*||. \tag{4.56}$$

Dividing through by $||\mathbf{e}||$ and using the definition of the effectivity index in equation (4.52) we have that,

$$(1 - \frac{||\mathbf{e}^*||}{||\mathbf{e}||}) \leq \ \theta \leq (1 + \frac{||\mathbf{e}^*||}{||\mathbf{e}||}). \tag{4.57}$$

The above shows that the effectivity index θ approaches unity as the ratio $||\mathbf{e}^*||/||\mathbf{e}||$ tends to zero $\Box$

In order for the ratio $||\mathbf{e}^*||/||\mathbf{e}||$ to tend to zero as $||\mathbf{e}||$ tends to zero, $||\mathbf{e}^*||$ has to converge at a higher rate than $||\mathbf{e}||$. It follows that if $||\mathbf{e}^*||$ is superconvergent then asymptotic exactness of the estimator is guaranteed. It may be the case, however, that some sampling points in the recovery procedure may not be superconvergent. In such a scenario the estimator will be still applicable according to [48] providing that the recovered values are more accurate (though not necessarily superconvergent) than those obtained in the finite element computations.

Recovery Procedure

Zienkiewicz and Zhu [48] developed a recovery technique for superconvergent evaluation of derivatives of finite element solutions at nodes. The technique is also often referred to as smoothing procedures which recover more accurate nodal values of derivatives from the original finite element solutions. The exact solution $\mathbf{u}(\mathbf{x})$ and the finite element approximation $\mathbf{u}_h(\mathbf{x})$ at any point $\mathbf{x} \in \Omega$ may be expressed as

$$\mathbf{u}_h = \mathbf{N}\,\overline{\mathbf{u}} \tag{4.58}$$

where $\mathbf{N}$ and $\overline{\mathbf{u}}$ are the array of finite element basis functions and the nodal value of the displacements, respectively. The stress (or gradients) are given by

$$\boldsymbol{\sigma}_h = \mathbf{D}\mathbf{B}\,\mathbf{u}_h. \tag{4.59}$$

Here $\mathbf{D}$ is the elasticity matrix and $\mathbf{B}$ is the differential operator matrix which defines the strain as

$$\boldsymbol{\epsilon}_h = \mathbf{B}\mathbf{u}_h. \tag{4.60}$$

It is clear that the stresses $\boldsymbol{\sigma}_h$ calculated from equation (4.59) are not continuous and have a low accuracy at nodes and element boundaries. Thus the objective of the recovery procedure is to find nodal parameters $\overline{\boldsymbol{\sigma}}^*$ such that the smoothed continuous stress field $\boldsymbol{\sigma}^*$, defined as

$$\boldsymbol{\sigma}^* = \mathbf{N}\overline{\boldsymbol{\sigma}}^*, \tag{4.61}$$

where $\mathbf{N}$ are again the same basis functions which were used for interpolation of the nodal displacements, is more accurate than $\boldsymbol{\sigma}_h$. In the recovery process it is assumed that the nodal values $\overline{\boldsymbol{\sigma}}^*$ belong to a polynomial expansion $\boldsymbol{\sigma}_p^*$ of the same order p as that present in the basis functions $\mathbf{N}$ and which is valid over an element patch surrounding the particular assembly node considered. Such a patch represents a union of elements containing this vertex node which is shown in Figure 4.1. The polynomial expansion will be used for each component of $\boldsymbol{\sigma}_p^*$ (or the derivatives) and for each may be expressed as,

$$\sigma_p^* = \mathbf{Pa}, \tag{4.62}$$

where $\mathbf{P}$ contains the appropriate polynomial terms and $\mathbf{a}$ is a set of unknown parameters. For one dimensional elements of order p we can write, for instance,

$$\mathbf{P} = [1, x, x^2, \ldots, x^p] \tag{4.63}$$

and

$$\mathbf{a} = [a_1, a_2, a_3, \ldots, a_{p+1}]^T. \tag{4.64}$$

In the case of two dimensions we have, in addition to the complete polynomials, a term involving x and y. Thus for two dimensions and linear expansion we have

$$\mathbf{P} = [1, x, y]. \tag{4.65}$$

The task is thus to determine the unknown parameters $\mathbf{a}$ of the expansion given in equation (4.62) for each component of $\boldsymbol{\sigma}_p^*$ (or the derivatives). This is done by ensuring a least square fit of this to the set of superconvergent or at least high

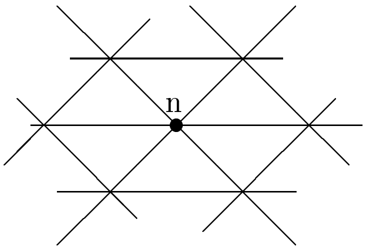

Figure 4.1: Example of a general patch assembly point, n for regular mesh.

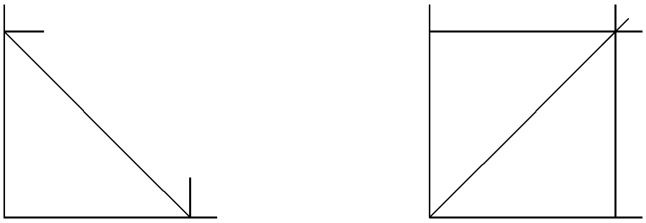

Figure 4.2: Patch of one and two elements

accuracy sampling points existing on the element patch considered. In order to do this we minimize

$$\begin{aligned} F(\mathbf{a}) &= \sum_{i=1}^{NS} \Big(\sigma_h(x_i, y_i) - \sigma_p^*(x_i, y_i) \Big)^2 \\ &= \sum_{i=1}^{NS} \Big(\sigma_h(x_i, y_i) - \mathbf{P}(x_i, y_i)\, \mathbf{a} \Big)^2, \end{aligned}$$

where (x_i, y_i) are the coordinates of a group of sampling points and NS is the total number of sampling points. The minimization condition of $F(\mathbf{a})$ implies that $\mathbf{a}$ satisfies

$$\sum_{i=1}^{NS} \mathbf{P}^T(x_i, y_i)\, \mathbf{P}(x_i, y_i)\, \mathbf{a} = \sum_{i=1}^{NS} \mathbf{P}^T(x_i, y_i)\, \sigma_h(x_i, y_i).$$

This can be solved in matrix form

$$\mathbf{a} = \mathbf{A}^{-1}\, \mathbf{b},$$

where

$$\mathbf{A} = \sum_{i=1}^{NS} \mathbf{P}^T(x_i, y_i)\, \mathbf{P}(x_i, y_i) \quad \text{and} \quad \mathbf{b} = \sum_{i=1}^{NS} \mathbf{P}^T(x_i, y_i)\, \sigma_h(x_i, y_i).$$

For a linear triangular element it is known that the optimal sampling point lies at the element centroid (Zienkiewicz and Zhu [48]). Thus, for the patch shown in Figure 4.1, the same sampling points are used for each component of $\boldsymbol{\sigma}_p^*$ and it is clear that the same matrix $\mathbf{A}$ will result for a given patch. Once the parameters $\mathbf{a}$ are obtained, the recovered nodal values of $\overline{\boldsymbol{\sigma}}^*$ are calculated by insertion of the appropriate coordinates into the expression for σ_p^* in equation (4.62). It is expected [48] that all values of $\boldsymbol{\sigma}_p^*$ in the domain of the patch are superconvergent as it fits closely to local sampling points which exhibit this property and is also of the correct polynomial order.

For the case of boundary nodes, the patch may contain only one element or two elements as shown in Figure 4.2. In such cases it is not difficult to show that the resulting matrix $\mathbf{A}$ will be a singular matrix and thus we cannot solve the linear system for $\mathbf{a}$. In order to cope with this undesirable effect, the nodes adjacent to the boundary node will be used. Of these adjacent nodes, the node with the greatest number of elements surrounding it is selected as the substitute patch assembly node. The patch is then constructed around this substitute node and the recovered gradients can be evaluated by using the co-ordinates from the original boundary nodes.

4.3 Adaptive Scheme

It has been seen that the error estimators provide the user with a global error estimate over Ω. These global error estimates are obtained by summing elemental contributions which are known as error indicators. As mentioned in section 4.2, the global error estimate η is given by

$$\eta^2 = \sum_{i=1}^{NE} \varpi_i^2. \tag{4.66}$$

The true global error can be approximated by the error estimates. For the energy norm measure of the true error, $\mathbf{u} - \mathbf{u}_h$, it is required that

$$\eta^2 \approx \| \mathbf{u} - \mathbf{u}_h \|_{E(\Omega)}^2 := \| \mathbf{e} \|_{E(\Omega)}^2 . \tag{4.67}$$

We define the *relative energy norm error* (percentage) as

$$R = \frac{\| \mathbf{e} \|_{E(\Omega)}}{\| \mathbf{u} \|_{E(\Omega)}} \times 100\%. \tag{4.68}$$

The norm $\| \mathbf{u} \|_{E(\Omega)}$ will not be known in practice and so this norm can be estimated by (see Ludwig [24])

$$\| \mathbf{u} \|_{E(\Omega)}^2 \approx \| \mathbf{u}_h \|_{E(\Omega)}^2 + \| \mathbf{e} \|_{E(\Omega)}^2 . \tag{4.69}$$

Using this approximation in (4.68) we obtain

$$R = \frac{\| \mathbf{e} \|_{E(\Omega)}}{\sqrt{\| \mathbf{u}_h \|_{E(\Omega)}^2 + \| \mathbf{e} \|_{E(\Omega)}^2}} \times 100\%. \tag{4.70}$$

Applying (4.70) in (4.66) gives

$$\eta^2 = \sum_{i=1}^{NE} \varpi_i^2 \approx \left(\frac{R}{100}\right)^2 \Big(\| \mathbf{u}_h \|_{E(\Omega)}^2 + \| \mathbf{e} \|_{E(\Omega)}^2 \Big). \tag{4.71}$$

In order to get an optimal mesh it is desirable that the distribution of energy norm error should be equal for all elements. Thus we could impose a local *tolerance* that the error in any element i should be

$$\eta \leq \left(\frac{R}{100}\right)\left(\frac{\| \mathbf{u}_h \|^2_{E(\Omega)} + \| \mathbf{e} \|^2_{E(\Omega)}}{NE}\right)^{1/2}. \tag{4.72}$$

Elements in which the above is not satisfied are obvious candidates for refinement.

As detailed by Li and Wiberg [19], it is very difficult to achieve the target tolerance level through a sequence of mesh refinements. Thus an empirical correction factor K is introduced in equation (4.71) which has a value in the range 1.0-1.5. The empirical correction factor K depends on the elements used and is typically set to 1.3 and 1.4 for linear elements and quadratic elements respectively (see Zienkiewicz and Zhu [47]). Dividing this into the right-hand side of equation (4.71) has the effect of lowering the local tolerance level requirement and causes more elements to be refined. However, in this thesis, there was no such difficulty observed to reach the tolerance and as a consequence it was not necessary to use the empirical correction factor K in the error estimation. For more on adaptive schemes we refer to, e.g., Lee and Lo [18] or Zhu and Zienkiewicz [46].

4.3.1 Practical Refinement

This section introduces methods for the actual geometrical aspects arising in the mesh refinement of linear triangular elements, and the red-green refinement strategy of Bank [2] is presented.

In the practical refinement procedure, the element S (see Figure 4.3) which needs to be refined is split into four elements by connecting the midpoints of the parent triangle in a process known as the red refinement stage. Such a refinement is illustrated in Figure 4.4a. This gives rise to hanging nodes. The three neighbouring elements of the element S will be bisected in what is termed the green refinement stage to produce two elements each as shown in Figure 4.4b, and to remove the hanging nodes.

A difficulty which may occur with this adaptive process arises in the case where more than one neighbour of an element has been red refined. In such a case this

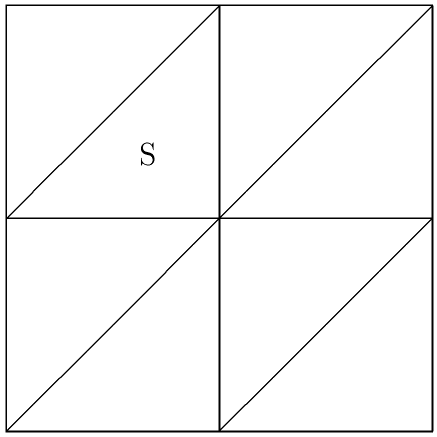

Figure 4.3: The element S is required to refine

will lead to the element having more than one mid-side node as is indicated in the element T in Figure 4.5a. The solution to this problem is simple and can be constructed immediately by adopting red refinement for element T itself, with all neighbours consequently green refined, and leading to the mesh shown in Figure 4.5b.

Many other refinement algorithms exist for triangular elements such as *Delaunay triangulation* (see for example Kirby [17]) and the *bisection method* in which the triangular element is bisected by connecting the midpoint of the longest side with the appropriate opposite node. (see for example Ludwig [23], Rivara [30] and [31]).

(a) red refinement of parent element

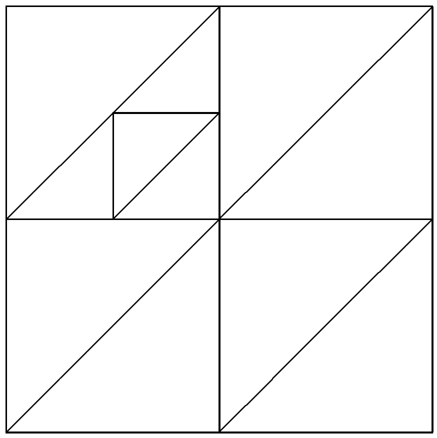

(b) red and green refinements complete

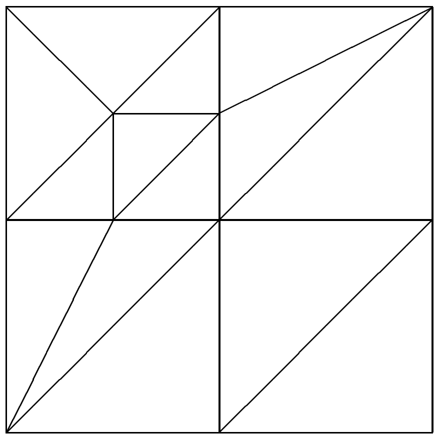

Figure 4.4: Illustration of red-green refinement on a general triangulation.

(a) element T with two mid-side nodes

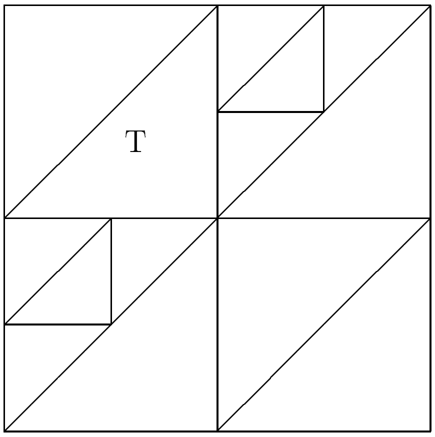

(b) Final red-green refined mesh

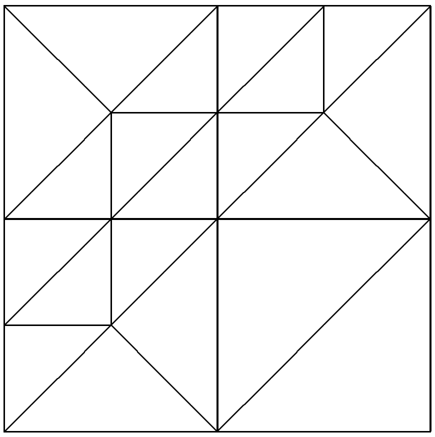

Figure 4.5: Red refinement of element T having two mid-side nodes

Chapter 5

Linear Viscoelasticity

5.1 Introduction

As was said in Chapter 1, materials can exhibit many forms of deformation behaviour; the three most common forms being elastic, plastic and viscoelastic. Elastic behaviour (which may be linear or non-linear, see Figure 5.1) involves recoverable deformations. Plastic behaviour involves non-recoverable deformation. Typically the deformation may be recoverable up to a certain point known as the yield point but after that point a non-recoverable deformation takes place. Specifically, the material is left with a permanent strain and on unloading the material does not return to its original state, as illustrated in Figure 5.2. For the third type of deformation, viscoelasticity, we now give more details and further develop the discussion of Chapter 1. As was said there *viscoelasticity* is a combination of elastic deformation and

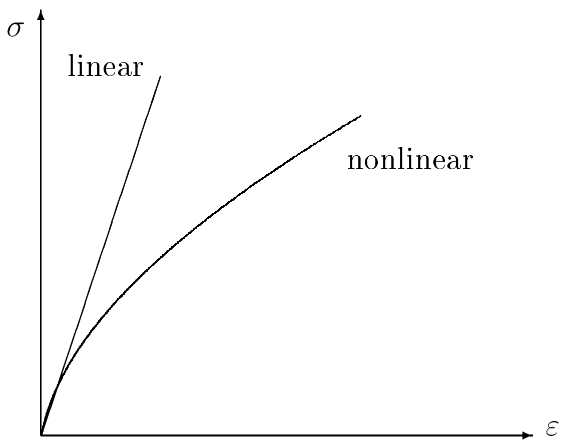

Figure 5.1: Elastic

viscous flow. In order to illustrate this we consider the case where a constant stress is applied to a one-dimensional solid bar at time $t = 0$, and removed at $t = t_1$. The viscoelastic material responds with non-linear strain. As shown in Figure 5.3, at $t = 0$ there results a more or less instantaneous deformation (strain) AB, after which during the time interval $(0, t_1)$ the material *creeps* (BC) and then, when the stress is removed, it creeps back to its original position CD. If, alternatively, an

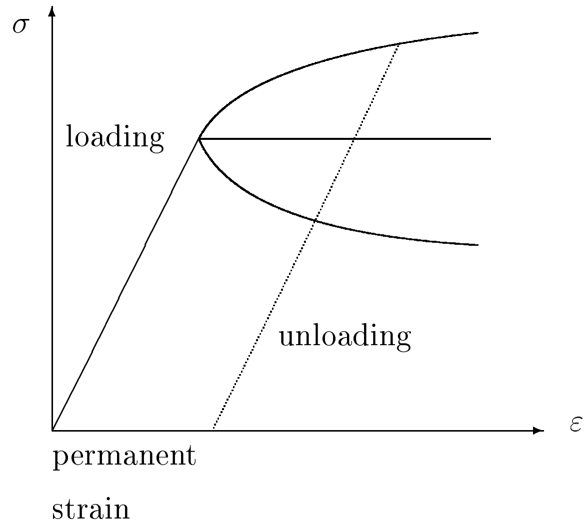

Figure 5.2: Plastic

instantaneous strain (displacement) is applied at $t = 0$ and maintained constant, the viscoelastic material responds with an *instantaneous* stress which is finite for a solid. When the displacement is removed, the viscoelastic material *relaxes* at a finite rate as shown in Figure 5.4.

The description of the response of materials which exhibit combined viscous and elastic properties is based upon an analogy with the response of certain mechanical elements. This involves the construction of viscoelastic models by the combining mechanical elements which represent purely viscous and purely elastic properties. Such models are, of course, idealized and purely hypothetical, and useful for representing the behaviour of real materials only to the extent that the observed response of the real material can be approximated by that of the model.

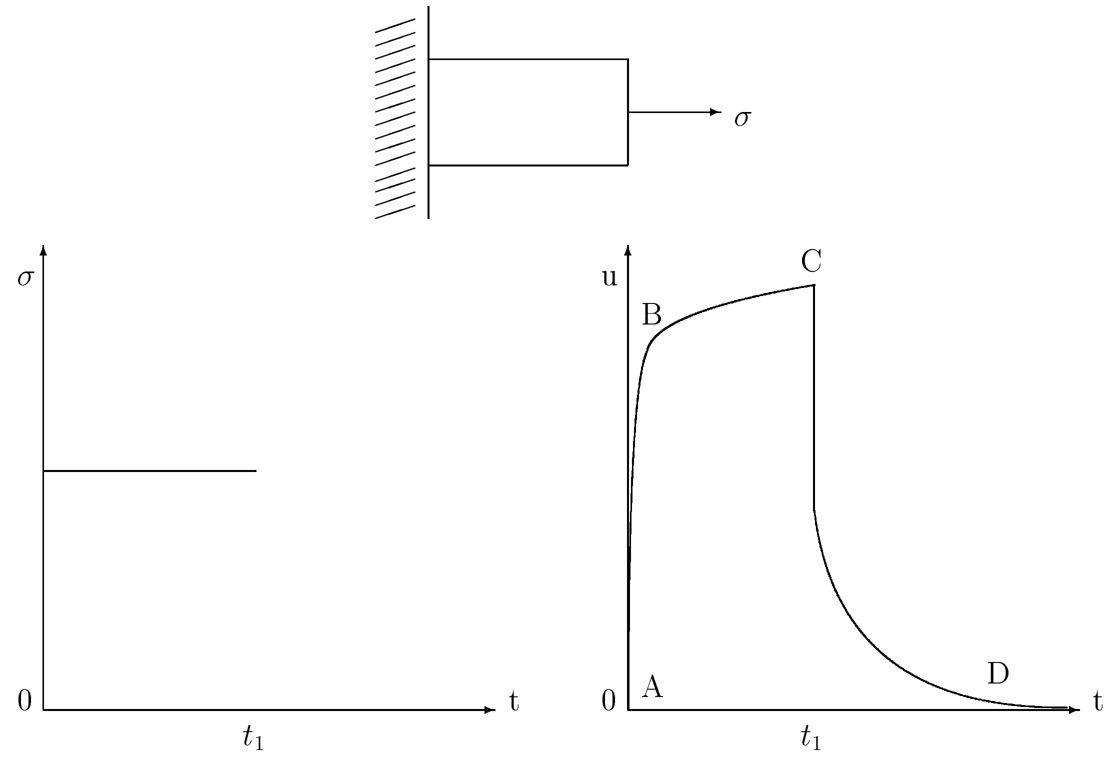

Figure 5.3: Creep

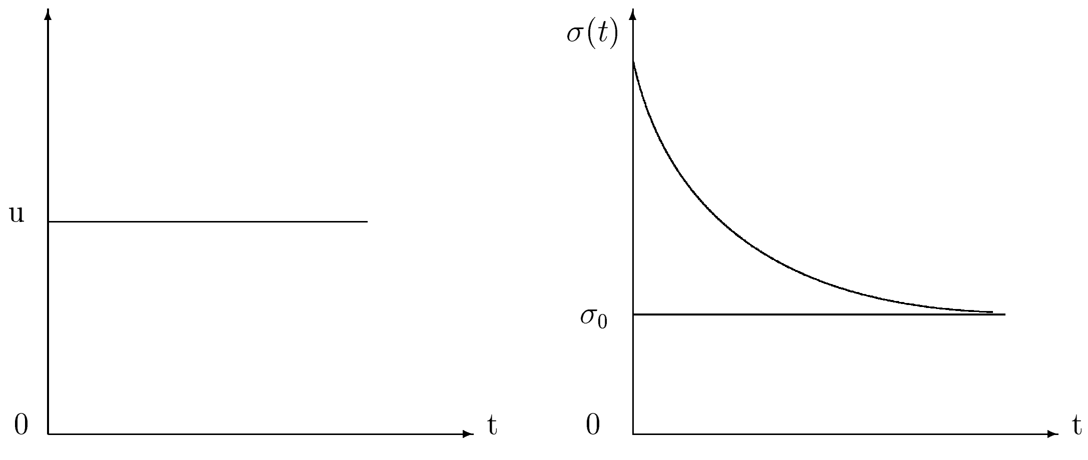

Figure 5.4: Stress relaxation

We now discuss again the analogy made between mechanical spring and dashpot models and constitutive linear viscoelastic behaviour. Repeating the relations given in Chapter 1 (Shaw *et al.* [36]) are repeated here, namely that linear viscoelastic medium may be characterized by constitutive relationships taking the general forms

$$\begin{aligned} \boldsymbol{\sigma}(t) &= \mathbf{D}(0)\boldsymbol{\epsilon}(t) - \int_0^t \mathbf{D}_q(t-q)\boldsymbol{\epsilon}(q)\,\mathrm{d}q, && (5.1)\\ \boldsymbol{\sigma}(t) &= \mathbf{D}(t)\boldsymbol{\epsilon}(0) + \int_0^t \mathbf{D}(t-q)\boldsymbol{\epsilon}_q(q)\,\mathrm{d}q, && (5.2)\end{aligned}$$

where the subscript q denotes differentiation with respect to the historical time variable q and $\mathbf{x}$ dependence has been suppressed. In more general relations involving ageing materials we need to replace $\mathbf{D}(t-q)$ by $\mathbf{D}(t,q)$ in (5.1) and (5.2). The equations (5.1) and (5.2), respectively, can be expressed as

$$\begin{aligned} \sigma_{ij}(t) &= \lambda(t,t)\nabla\cdot\mathbf{u}(t)\delta_{ij} + \mu(t,t)\varepsilon_{ij}\Big(\mathbf{u}(t)\Big)\\ &- \int_0^t \lambda_q(t,q)\nabla\cdot\mathbf{u}(q)\delta_{ij} + \mu_q(t,q)\varepsilon_{ij}\Big(\mathbf{u}(q)\Big)\ \mathrm{d}q, && (5.3)\end{aligned}$$

and

$$\begin{aligned} \sigma_{ij}(t) &= \lambda(t,0)\nabla\cdot\mathbf{u}(0)\delta_{ij} + \mu(t,0)\varepsilon_{ij}\Big(\mathbf{u}(0)\Big)\\ &+ \int_0^t \lambda(t,q)\nabla\cdot\mathbf{u}_q(q)\delta_{ij} + \mu(t,q)\varepsilon_{ij}\Big(\mathbf{u}_q(q)\Big)\ \mathrm{d}q. && (5.4)\end{aligned}$$

The matrix $\mathbf{D}$ is said to be the *constitutive* or *stress relaxation matrix* and the *stress relaxation functions* λ and μ are viscoelastic analogues of the Lamé coefficients of linear elasticity. Based on these constitutive laws we then derive a weak formulation of the quasistatic problem. Everything contained in this chapter may be found in texts such as Shaw *et al.* [36] or Findley *et al.* [11] and for more viscoelasticity we refer to Pipkin [29], Flügge [12], Christensen [7], Tscgoegl [41] and Lockett [21].

5.2 Basic Elements:Spring and Dashpot

Linear viscoelastic models can be constructed in term of linear springs and linear viscous dashpots. Inertia effects are neglected in such models. The linear spring (Figure 5.5) is an ideal elastic element obeying the linear force extension relation

$$\sigma = E\varepsilon, \tag{5.5}$$

that is, Hooke's law, in which E is *Young's modulus*. This is Hooke's law in one-dimension, see (3.29).

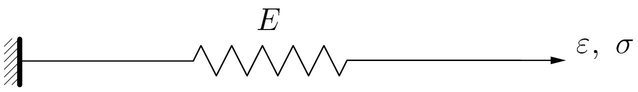

Figure 5.5: A Hookean (linear) spring

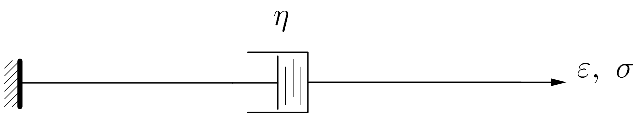

Figure 5.6: A Newtonian (linear) dashpot

The dashpot is an ideal viscous element that extends at a rate proportional to the applied force, see Figure 5.6. By Newton's law of viscosity, we have

$$\sigma = \eta \frac{\mathrm{d}\varepsilon}{\mathrm{d}t} := \eta \dot{\varepsilon} \tag{5.6}$$

where the constant η is called the coefficient of viscosity.

Models of linear viscoelastic behaviour can be constructed in terms of combinations of (5.5) and (5.6) in series or parallel, or amalgamations of both. We shall now proceed to build up models by combining springs and dashpots, in various ways and to derive from them possible patterns of viscoelastic behaviour.

5.3 The Maxwell Model (Fluid)

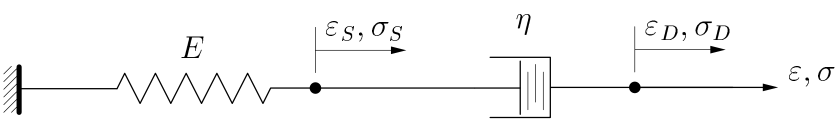

Figure 5.7: The Maxwell model

The Maxwell model is one of the simplest models that can be constructed by connecting a spring and dashpot in series, as shown in Figure 5.7. The stress-strain relations of spring and dashpot follow from (5.5) and (5.6), respectively, and are given by

$$\sigma_S = E\varepsilon_S, \tag{5.7}$$

$$\sigma_D = \eta\frac{\mathrm{d}\varepsilon_D}{\mathrm{d}t}, \tag{5.8}$$

where σ_S and ε_S denote respectively stress and strain in the spring, whilst σ_D and ε_D denote the same effect in the dashpot.

Since both elements are connected in series, the total stress is given by

$$\sigma = \sigma_S = \sigma_D \tag{5.9}$$

and the total strain is

$$\varepsilon = \varepsilon_S + \varepsilon_D. \tag{5.10}$$

Differentiating (5.10) with respect to time gives

$$\frac{\mathrm{d}\varepsilon}{\mathrm{d}t} = \frac{\mathrm{d}\varepsilon_S}{\mathrm{d}t} + \frac{\mathrm{d}\varepsilon_D}{\mathrm{d}t}. \tag{5.11}$$

Equations (5.7),(5.8) and (5.11) contain four unknowns $\sigma, \varepsilon, \varepsilon_S, \varepsilon_D$. Among these ε_S and ε_D are internal variables and σ and ε are the external variables. Therefore the stress-strain relation of the model can be obtained by eliminating ε_S and ε_D from these equations. Inserting (5.8) and the time derivative of (5.7) into (5.11) ε_S and ε_D can be eliminated and the following stress-strain rate relation for the Maxwell model is obtained

$$\frac{\mathrm{d}\varepsilon}{\mathrm{d}t} = \frac{1}{E}\frac{\mathrm{d}\sigma}{\mathrm{d}t} + \frac{\sigma}{\eta},$$

or

$$\frac{\mathrm{d}\sigma}{\mathrm{d}t} + \frac{E}{\eta}\sigma = E\frac{\mathrm{d}\varepsilon}{\mathrm{d}t}.$$

The above equation can be expressed as

$$\frac{\mathrm{d}\sigma}{\mathrm{d}t} + \frac{\sigma}{\tau} = E\frac{\mathrm{d}\varepsilon}{\mathrm{d}t}, \tag{5.12}$$

where, clearly, $\sigma = \sigma(t)$, $\varepsilon = \varepsilon(t)$ and $\tau := \frac{\eta}{E}$ is the *relaxation time*. In order to produce a constitutive relation between σ and ε for this Maxwell model, we must solve (5.12), and for this we use the integrating factor $e^{t/\tau}$ in the normal way for ODE's. Multiplying (5.12) by this integrating factor we get

$$e^{t/\tau}\frac{\mathrm{d}\sigma}{\mathrm{d}t}+\frac{\sigma}{\tau}e^{t/\tau}=E\frac{\mathrm{d}\varepsilon}{\mathrm{d}t}e^{t/\tau}$$

or

$$\frac{\mathrm{d}}{\mathrm{d}t}(\sigma e^{t/\tau})=E\frac{\mathrm{d}\varepsilon}{\mathrm{d}t}e^{t/\tau}.$$

By integrating this, we obtain

$$\left[\sigma(q)e^{\frac{q}{\tau}}\right]_0^t=E\int_o^t\frac{\mathrm{d}\varepsilon(q)}{\mathrm{d}q}e^{q/\tau}\;\mathrm{d}q.$$

Using the fact that $\sigma(0)=E\varepsilon(0)$ gives

$$\sigma(t)=E\varepsilon(0)e^{-t/\tau}+E\int_0^t e^{-(t-q)/\tau}\frac{\mathrm{d}\varepsilon(q)}{\mathrm{d}q}\;\mathrm{d}q. \tag{5.13}$$

The integral term in the above equation can be expressed as

$$\int_0^t e^{-(t-q)/\tau}\frac{\mathrm{d}\varepsilon(q)}{\mathrm{d}q}\;\mathrm{d}q=\varepsilon(t)-e^{-t/\tau}\varepsilon(0)-\int_0^t\frac{\varepsilon(q)}{\tau}e^{-(t-q)/\tau}\;\mathrm{d}q. \tag{5.14}$$

Substituting (5.14) into (5.13), we obtain

$$\sigma(t)=E\varepsilon(t)-E\int_0^t\frac{1}{\tau}e^{-(t-q)/\tau}\varepsilon(q)\;\mathrm{d}q \tag{5.15}$$

which is the *hereditary integral* constitutive relation for the Maxwell (fluid) model.

To understand why this model describes a viscoelastic fluid and is not a viscoelastic solid, consider what happens in a standard stress relaxation test. If a strain ε_0 is instantaneously applied at time $t=0$ and then kept constant, as shown in Figure 5.8, the resulting stress response is shown in Figure 5.9. At time $t=0$ we immediately get the stress $\sigma_0=E\varepsilon_0$ but for $t>0$ the stress decreases according to

$$\sigma(t)=\sigma_0\exp(-t/\tau). \tag{5.16}$$

It is because the stress tends to 0 as $t\to\infty$ that the material is classified as a fluid.

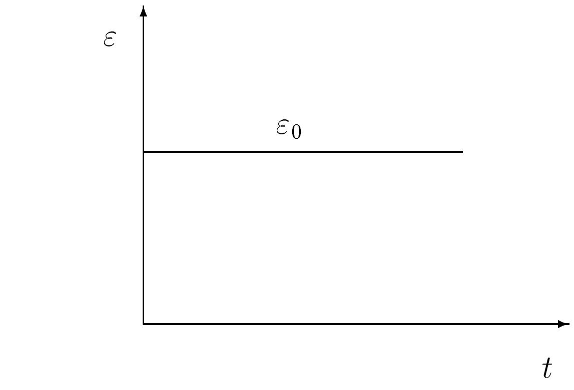

Figure 5.8: Applied strain for stress relaxation test

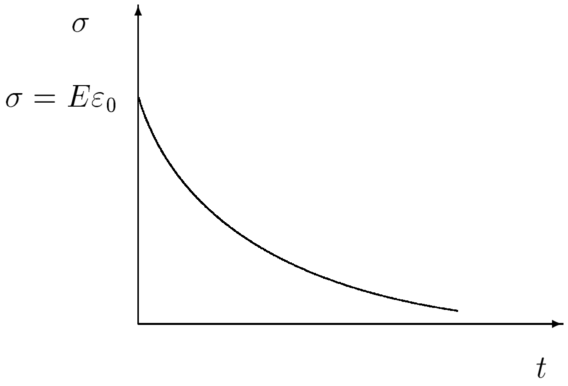

Figure 5.9: Response to stress relaxation test

5.4 The Voigt Model

Connecting a spring and dashpot in parallel represents the simplest possible model for a viscoelastic solid, and this model is called the Voigt or sometimes the Kelvin, solid (see Figure 5.10).

Since both elements are connected in parallel, we have

$$\varepsilon = \varepsilon_S = \varepsilon_D \tag{5.17}$$

and the total stress is

$$\sigma = \sigma_S + \sigma_D. \tag{5.18}$$

Replacing σ_S and σ_D by (5.5) and (5.6), respectively, gives

$$\sigma = E\varepsilon_S + \eta \frac{\mathrm{d}\varepsilon_D}{\mathrm{d}t}. \tag{5.19}$$

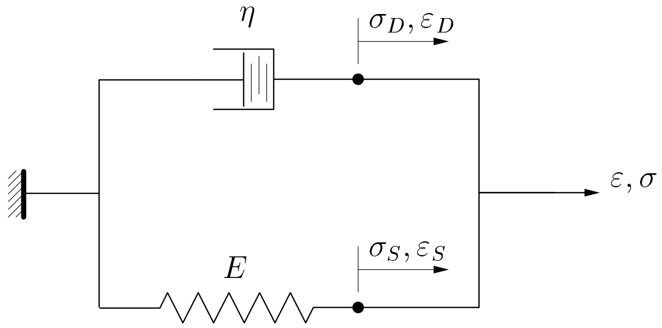

Figure 5.10: The Voigt model

Using (5.17), we get

$$\sigma = E\varepsilon + \eta \frac{\mathrm{d}\varepsilon}{\mathrm{d}t} \tag{5.20}$$

or

$$\frac{\mathrm{d}\varepsilon(t)}{\mathrm{d}t} + \frac{\varepsilon(t)}{\tau} = \frac{\sigma(t)}{\eta}, \tag{5.21}$$

where, again, $\tau = \frac{\eta}{E}$ is the relaxation time. Solving (5.21) gives the constitutive law in hereditary form as

$$\varepsilon(t) = \varepsilon(0)e^{-t/\tau} + \frac{1}{\eta}\int_0^t e^{-(t-q)/\tau}\sigma(q)\ \mathrm{d}q. \tag{5.22}$$

Note that equation (5.22) is in *compliance form.*

5.5 The Maxwell Solid

To generalize the Maxwell (fluid) and Voigt models, respectively, we combine springs and dashpots in series and in parallel. For the Maxwell solid, we connect a Maxwell element in parallel with a spring as shown in Figure 5.11, where E_0 and E_1, are the spring stiffnesses and σ^*, ε^* are known as the *internal stress* and *strain variables.* In this model, we have

$$\sigma^* = \sigma_D, \tag{5.23}$$

$$\sigma = \sigma_S + \sigma^*, \tag{5.24}$$

$$\varepsilon = \varepsilon_S = \varepsilon^* + \varepsilon_D. \tag{5.25}$$

Substituting (5.6) into (5.23) and replacing ε_D by (5.25) yields

$$\sigma^* = \eta\Big(\frac{\mathrm{d}\varepsilon}{\mathrm{d}t} - \frac{\mathrm{d}\varepsilon^*}{\mathrm{d}t}\Big). \tag{5.26}$$

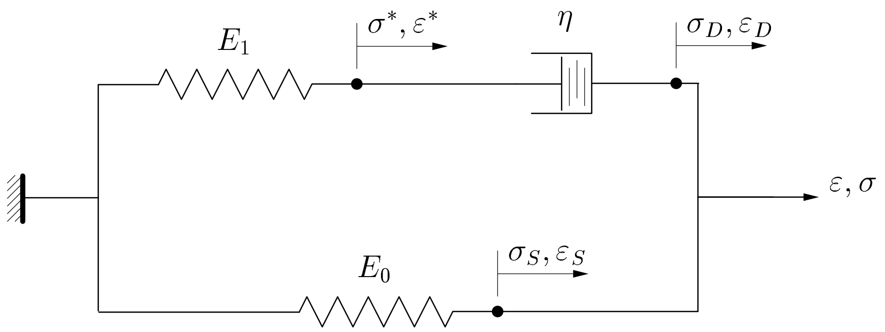

Figure 5.11: The Maxwell solid

Substituting for $\sigma^* = E_1\varepsilon^*$, gives

$$E_1\varepsilon^* = \eta\Big(\frac{\mathrm{d}\varepsilon}{\mathrm{d}t} - \frac{\mathrm{d}\varepsilon^*}{\mathrm{d}t}\Big). \tag{5.27}$$

Hence, the linear ODE which relates the internal strain $\varepsilon^*(t)$ to the total strain is given by

$$\frac{\mathrm{d}\varepsilon^*(t)}{\mathrm{d}t} + \frac{\varepsilon^*(t)}{\tau} = \frac{\mathrm{d}\varepsilon(t)}{\mathrm{d}t}, \tag{5.28}$$

where now $\tau = \frac{\eta}{E_1}$. This can be solved again by multiplying it by an integrating factor, $e^{t/\tau}$, and then integrating over $(0, t)$ to obtain

$$\varepsilon^*(t) = e^{-t/\tau}\varepsilon^*(0) + \int_0^t e^{-(t-q)/\tau}\frac{\mathrm{d}\varepsilon(q)}{\mathrm{d}q}\ \mathrm{d}q. \tag{5.29}$$

Replacing for σ_S and σ^* in (5.24), gives

$$\begin{aligned}\sigma(t) &= \sigma_S(t) + \sigma^*(t)\\ &= E_0\varepsilon_S(t) + E_1\varepsilon^*(t),\end{aligned}$$

and using (5.25) and (5.29), it follows that

$$\sigma(t) = E_0\varepsilon(t) + E_1e^{-t/\tau}\varepsilon^*(0) + E_1\int_0^t e^{-(t-q)/\tau}\frac{\mathrm{d}\varepsilon(q)}{\mathrm{d}q}\ \mathrm{d}q. \tag{5.30}$$

Integrating by parts gives

$$\int_0^t e^{-(t-q)/\tau}\frac{\mathrm{d}\varepsilon(q)}{\mathrm{d}q}\ \mathrm{d}q = \Big[e^{-(t-q)/\tau}\varepsilon(q)\Big]_0^t - \int_0^t \frac{\varepsilon(q)}{\tau}e^{-(t-q)/\tau}\ \mathrm{d}q; \tag{5.31}$$

with the use of $\varepsilon^*(0) = \varepsilon(0)$, we obtain

$$\sigma(t) = (E_0 + E_1)\varepsilon(t) - E_1\int_0^t \frac{\varepsilon(q)}{\tau}e^{-(t-q)/\tau}\mathrm{d}q. \tag{5.32}$$

The stress relaxation function is defined by

$$D(t) := E_0 + E_1 e^{-t/\tau}, \tag{5.33}$$

and consider

$$\begin{aligned} D(0) &= E_0 + E_1, \\ D(t-q) &= E_0 + E_1 e^{-(t-q)/\tau}, \\ D_q(t-q) &:= \frac{\mathrm{d}D(t-q)}{\mathrm{d}q} = \frac{E_1}{\tau} e^{-(t-q)/\tau}, \end{aligned}$$

which, when substituted in (5.32), gives

$$\sigma(t) = D(0)\varepsilon(t) - \int_0^t D_q(t-q)\varepsilon(q)\ \mathrm{d}q. \tag{5.34}$$

Further integration of (5.34) leads to the alternative form

$$\sigma(t) = D(t)\varepsilon(0) + \int_0^t D(t-q)\frac{\mathrm{d}\varepsilon(q)}{\mathrm{d}q}\ \mathrm{d}q, \tag{5.35}$$

which is the constitutive relation for the Maxwell solid. Equations (5.34) and (5.35) are the scalar analogues of (5.1) and (5.2), respectively, with $D(t)$ as given above.

5.6 Internal Variables

In this section, a Hookean spring connected in parallel to a sequence of N spring-dashpot components will be used to form the *generalized Maxwell solid* as shown in Figure 5.12. In this model, states of uniaxial stress and strain are assumed and we have

$$\varepsilon_0 = \varepsilon,\ \sigma_0 = E_0\varepsilon \text{ and } \sigma_i^* = E_i\varepsilon_i^*.$$

Balancing the stresses carried by each of the spring-dashpot pairs we get for each $i \in \{1, \cdots, N\}$ that

$$\frac{\mathrm{d}\varepsilon_i^*(t)}{\mathrm{d}t} + \frac{\varepsilon_i^*(t)}{\tau_i} = \frac{\mathrm{d}\varepsilon}{\mathrm{d}t}, \tag{5.36}$$

and by solving (5.36) we get

$$\varepsilon_i^*(t) = \varepsilon(0)e^{-t/\tau_i} + \int_0^t e^{-(t-q)/\tau_i}\varepsilon_q(q)\ \mathrm{d}q, \tag{5.37}$$

where $\tau_i := \frac{\eta_i}{E_i}$. The total stress is therefore given by

$$\begin{aligned}
\sigma(t) &= \sigma_0(t) + \sigma_1(t) + \cdots + \sigma_N(t) \\
&= E_0\varepsilon(t) + E_1\varepsilon_1^*(t) + \cdots + E_N\varepsilon_N^*(t) \\
&= E_0\varepsilon(0) + E_0\Big(\varepsilon(t) - \varepsilon(0)\Big) + \sum_{i=1}^N E_i e^{-t/\tau_i}\varepsilon(0) + \sum_{i=1}^N \int_0^t E_i e^{-(t-q)/\tau_i}\varepsilon_q(q)\ \mathrm{d}q \\
&= E_0\varepsilon(0) + \sum_{i=1}^N E_i e^{-t/\tau_i}\varepsilon(0) + E_0\Big(\varepsilon(t) - \varepsilon(0)\Big) + \sum_{i=1}^N \int_0^t E_i e^{-(t-q)/\tau_i}\varepsilon_q(q)\ \mathrm{d}q \\
&= \Big(E_0 + \sum_{i=1}^N E_i e^{-t/\tau_i}\Big)\varepsilon(0) + \int_0^t \Big(E_0 + \sum_{i=1}^N E_i e^{-(t-q)/\tau_i}\Big)\varepsilon_q(q)\ \mathrm{d}q \\
&= E(t)\varepsilon(0) + \int_0^t E(t-q)\varepsilon_q(q)\ \mathrm{d}q \qquad (5.38)
\end{aligned}$$

where

$$E(t) := E_0 + \sum_{i=1}^N E_i e^{-t/\tau_i}.$$

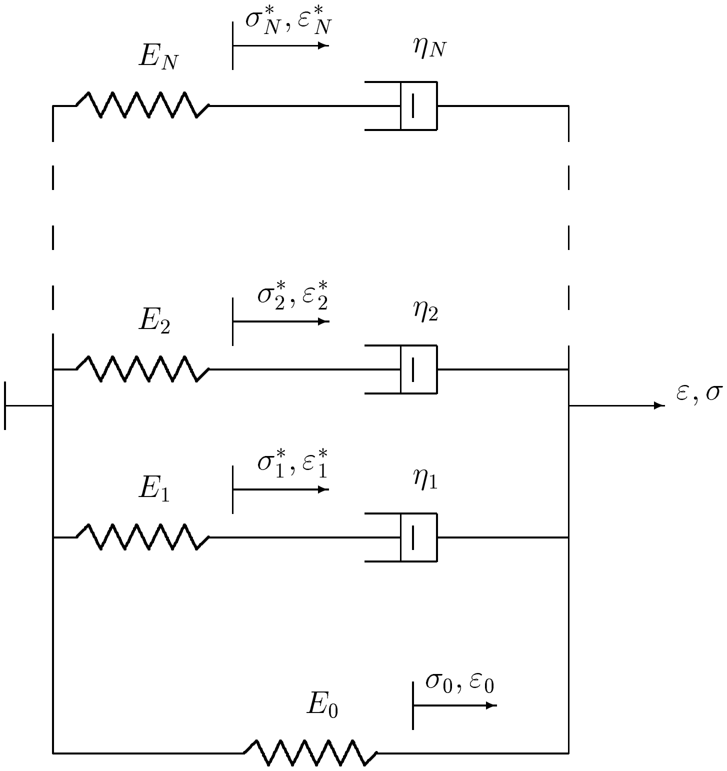

Figure 5.12: The generalized Maxwell solid

Equation (5.38) is the constitutive relation for the generalized Maxwell solid which is the scalar analogue of (5.2) with the analogue of $\mathbf{D}(t-q)$ given by $E(t-q)$.

5.7 The Quasistatic Displacement Model

The concept described in section 3.6, involving the weak formulation in elasticity, will be applied with the constitutive equation (5.3) to produce the weak formulation of the quasistatic linear viscoelasticity problem. Here we use the summation convention. The subscript q denotes differentiation with respect to the history variable q and the $\mathbf{x}$ dependence has been suppressed. The elements of $\mathbf{D}$, λ and μ which are depicted in section 5.1 are examples of stress relaxation functions. To describe them, it is appropriate at this stage to state the assumptions for a generic stress relaxation function $\phi(t,q)$ and what we say about ϕ will apply to any of the other stress relaxation functions.

Assumption 1 [relaxation functions] For $T > 0$, let $\mathcal{J} := [0,T]$. Assume that the time dependent part of the generic stress relaxation function $\phi(t,q)$ defined for $t, q \in \mathcal{J}$ satisfies the following:

1. **Regularity**: $\phi(t,q) \in C^\infty \quad (0 \leq q < t \leq T)$.
2. **Positivity**: $\phi(t,t) > 0 \quad \forall t \in \mathcal{J} \quad \text{and} \quad \phi(t,q) \geq 0 \quad \forall t,q \in \mathcal{J}$.
3. **Causality**: $\phi(t,q) := 0 \quad \forall q > t \quad \text{such that} \quad t,q \in \mathcal{J}$.
4. **Fading memory**: for every fixed $t \in \mathcal{J}$, $\phi_q(t,q) > 0$ when $q \in [0,t]$.

It is understood that these assumptions also hold for (time dependent parts of the) specific relaxation functions, $\lambda(t,q)$ and $\mu(t,q)$. Also we assume spatial regularity by

$$\lambda(\mathbf{x}),\ \mu(\mathbf{x}) \in L_\infty(\Omega) \quad \text{and} \quad \lambda(\mathbf{x}), \mu(\mathbf{x}) > 0 \quad \forall \mathbf{x} \in \Omega.$$

Assuming $\mathbf{f} \in L_\infty\Big(\mathcal{J}; (L_2(\Omega))^n\Big)$ and $\mathbf{g} \in L_\infty\Big(\mathcal{J}; (L_2(\partial\Omega_N))^n\Big)$, we consider the weak problem : find $\mathbf{u} \in L_\infty(\mathcal{J}; V)$ such that

$$\int_\Omega \sigma_{ij}(\mathbf{u})\varepsilon_{ij}(\mathbf{v})\, \mathrm{d}\Omega = \int_\Omega f_i v_i \,\mathrm{d}\Omega + \int_{\partial\Omega_N} g_i v_i \,\mathrm{d}(\partial\Omega) \quad \forall \mathbf{v} \in V. \tag{5.39}$$

Applying the constitutive equation (5.3) into the left-hand side of (5.39) gives

$$\begin{aligned}\int_\Omega \lambda\nabla\cdot\mathbf{u}\,\delta_{ij}\,\varepsilon_{ij}(\mathbf{v}) + \mu\varepsilon_{ij}(\mathbf{u})\varepsilon_{ij}(\mathbf{v})\,\mathrm{d}\Omega \\ -\int_\Omega\int_0^t \lambda_q\nabla\cdot\mathbf{u}\,\delta_{ij}\varepsilon_{ij}(\mathbf{v}) +\ \mu_q\varepsilon_{ij}(\mathbf{u})\varepsilon_{ij}(\mathbf{v})\ \mathrm{d}q\,\mathrm{d}\Omega \\ = \int_\Omega f_i v_i\,\mathrm{d}\Omega + \int_{\partial\Omega_N} g_i v_i\ \mathrm{d}(\partial\Omega).\end{aligned}$$

We assume that it is permissible to interchange the order of integration, thus

$$\begin{aligned}\int_\Omega \lambda\nabla\cdot\mathbf{u}\nabla\cdot\mathbf{v} + \mu\varepsilon_{ij}(\mathbf{u})\varepsilon_{ij}(\mathbf{v})\ \ \mathrm{d}\Omega \\ -\int_0^t\int_\Omega \lambda_q\nabla\cdot\mathbf{u}\nabla\cdot(\mathbf{v}) + \mu_q\varepsilon_{ij}(\mathbf{u})\varepsilon_{ij}(\mathbf{v})\,\mathrm{d}\Omega\mathrm{d}q. \\ = \int_\Omega f_i v_i\,\mathrm{d}\Omega + \int_{\partial\Omega_N} g_i v_i\ \mathrm{d}(\partial\Omega).\end{aligned} \tag{5.40}$$

This leads to the weak formulation for $\mathbf{u}\in L_\infty(\mathcal{J};V)$ such that

$$a(t,t;\mathbf{u}(t),\mathbf{v}) + \int_0^t b(t,q;\mathbf{u}(q),\mathbf{v})\ \mathrm{d}q = L(t;\mathbf{v}) \quad \forall\mathbf{v}\in V,\ t\in\mathcal{J}, \tag{5.41}$$

where $a(t,t;\cdot,\cdot)$ and $b(t,q;\cdot,\cdot)$ are time-dependent bilinear forms, mapping $V\times V$ into $\mathbb{R}$, and defined for all $\mathbf{v}$, $\mathbf{w}\in V$ by

$$a(t,q;\mathbf{w},\mathbf{v}) \ := \ \int_\Omega \lambda(t,q)\nabla\cdot\mathbf{w}\nabla\cdot\mathbf{v} + \mu(t,q)\varepsilon_{ij}(\mathbf{w})\varepsilon_{ij}(\mathbf{v})\,\mathrm{d}\Omega, \tag{5.42}$$

$$b(t,q;\mathbf{w},\mathbf{v}) \ := \ -\int_\Omega \lambda_q(t,q)\nabla\cdot\mathbf{w}\nabla\cdot\mathbf{v} + \mu_q(t,q)\varepsilon_{ij}(\mathbf{w})\varepsilon_{ij}(\mathbf{v})\,\mathrm{d}\Omega. \tag{5.43}$$

Also $L(t;\cdot): V\to\mathbb{R}$ is a time-dependent linear form defined by

$$L(t;\mathbf{v}) := \int_\Omega f_i(t)v_i\,\mathrm{d}\Omega + \int_{\partial\Omega_N} g_i(t)v_i\ \mathrm{d}(\partial\Omega). \tag{5.44}$$

The weak formulation (5.41) is called the *quasistatic displacement model.*

Chapter 6

The Quasistatic Displacement Formulations

In Chapter 5 we described the model and formulation of the problem of quasistatic linear viscoelasticity. We now specialise further by considering viscoelastic models which involve quasi-separable kernels which, as we will show, enable special schemes to be used. In particular in this chapter two displacement formulations for the case of the quasistatic problem, (5.41)-(5.44), with a non-ageing, synchronous, homogeneous, quasi-separable kernel and generalized solid will be produced. The first formulation introduced by Janovsky *et al.* [16] is called an Ordinary Differential Equation (ODE) formulation. This formulation makes use of the quasi-separable property of the kernel and a major contribution of this thesis is the construction of an algorithm for implementing the ODE formulation and for testing it on two model problems. The second formulation which is described is a fully discrete formulation, and has been presented by Shaw [34] and has been programmed here simply to produce results for comparison. The numerical results of both formulations will be shown in Chapter 7, where the results of the fully discrete formulation will be used for comparison.

6.1 An Ordinary Differential Equation Formulation

We now define the ODE formulation in the case of the quasistatic problem for a non-ageing, synchronous, homogeneous, quasi-separable kernel and generalized solid.

Before studying the ODE formulation of the problem, it is appropriate to outline some of the special cases which, when they occur, render the problem simple (see Janovsky *et al.* [16]).

i) A viscoelastic material is called *synchronous* if there exist the time independent functions λ_0 and μ_0, and a generic *stress relaxation function*, ϕ, such that

$$\phi(\mathbf{x}, t, q) = \frac{\lambda(\mathbf{x}, t, q)}{\lambda_0(\mathbf{x})} = \frac{\mu(\mathbf{x}, t, q)}{\mu_0(\mathbf{x})}. \tag{6.1}$$

In this case λ and μ have exactly the same temporal behaviour and the material has a constant Poisson ratio. Otherwise the material is called *asynchronous.* We will also restrict further to the case when the body under consideration is homogeneous so that ϕ is independent of $\mathbf{x}$ and we just write $\phi(t, q)$.

ii) The relaxation function ϕ is said to be *separable* if it can be expressed as the product of two functions, each depending only upon one variable, time. Specifically: the generic stress relaxation function $\phi(t, q)$ is separable if the functions $y(t)$ and $z(q)$ exist such that

$$\phi(t, q) := y(t)z(q). \tag{6.2}$$

Or, more generally, ϕ can be expressed as a finite series of $y(t)z(q)$

$$\phi(t, q) = \sum_{j=0}^{N_\phi} y_j(t)z_j(q), \tag{6.3}$$

the function $\phi(t, q)$ is said to be quasi-separable.

iii) For non-ageing materials, the material properties are assumed not to change with time (at least within the time scale of interest, $[0, T]$). In this case the generic stress relaxation function ϕ remains unchanged under any overall time translation, that is

$$\phi(t + \tau, q + \tau) = \phi(t, q) \quad \text{for all } \tau. \tag{6.4}$$

The value of the function ϕ only depends on the time difference $t - q$ and thus in what follows we will write $\phi(t - q)$ instead of $\phi(t, q)$.

iv) A common form for the relaxation functions (see e.g. Christensen [7]) for non-ageing materials is the truncated Dirichlet series given by

$$\phi(t) = \sum_{j=0}^{N_\phi} \phi_j \, \exp(-\alpha_j t). \tag{6.5}$$

In order to satisfy the four properties in Assumption 1 in Chapter 5, it is sufficient that the coefficients $\phi_0, \phi_1, \cdots, \phi_{N_\phi}$ and $\alpha_0, \alpha_1, \cdots, \alpha_{N_\phi}$ satisfy

$$\sum_{j=0}^{N_\phi} \phi_j > 0, \quad \alpha_j \geq 0 \quad \forall i \in \{0, 1, \ldots, N_\phi\}. \tag{6.6}$$

For convenience we suppose that $0 \leq \alpha_0 < \alpha_1 < \cdots < \alpha_{N_\phi}$. The relaxation corresponds to a solid when $\alpha_0 = 0$ and $\phi_0 > 0$ and it corresponds to a fluid if $0 < \alpha_0$ as then $\phi(t) \to 0$ as $t \to \infty$.

For a general quasi-separable relaxation function, which covers the case of the truncated Dirichlet series in (6.5), we now show how the quasi-static displacement problem (5.41)-(5.44) can be re-expressed in terms of time-dependent elastic problem in space coupled with ODE systems in time. To do this consider again the quasistatic displacement problem which involves finding $\mathbf{u} \in L_\infty(\mathcal{J}; V)$ such that

$$a(t, t; \mathbf{u}(t), \mathbf{v}) + \int_o^t b(t, q; \mathbf{u}(q), \mathbf{v}) \, \mathrm{d}q = L(t; \mathbf{v}), \quad \forall \mathbf{v} \in V, \ t \in \mathcal{J}, \tag{6.7}$$

where $T > 0$, $\mathcal{J} = (0, T]$ and $V = \{\mathbf{v} \in (H^1(\Omega))^3 : \mathbf{v} = 0 \text{ on } \partial\Omega_D\}$, and where $a(t, t; \cdot, \cdot)$ and $b(t, q; \cdot, \cdot)$ are time bilinear forms, mapping $V \times V$ into $\mathbb{R}$, and defined for all $\mathbf{v}$, $\mathbf{w} \in V$ by

$$\begin{aligned} a(t, q; \mathbf{w}, \mathbf{v}) &= \int_\Omega \lambda(t, q) \nabla \cdot \mathbf{w} \nabla \cdot \mathbf{v} + \mu(t, q) \varepsilon_{ij}(\mathbf{w}) \varepsilon_{ij}(\mathbf{v}) \ \mathrm{d}\Omega, & (6.8) \\ b(t, q; \mathbf{w}, \mathbf{v}) &= -\int_\Omega \dot{\lambda}(t, q) \nabla \cdot \mathbf{w} \nabla \cdot \mathbf{v} + \dot{\mu}(t, q) \varepsilon_{ij}(\mathbf{w}) \varepsilon_{ij}(\mathbf{v}) \ \mathrm{d}\Omega. & (6.9) \end{aligned}$$

The overdot denotes differentiation with respect to the history variable q. Also $L(t; \cdot) : V \to \mathbb{R}$ is a time-independent linear form and is defined by

$$L(t; \mathbf{v}) = \int_\Omega \mathbf{f}(t) \mathbf{v} \, \mathrm{d}\Omega + \int_{\partial\Omega_N} \mathbf{g}(t) \mathbf{v} \, \mathrm{d}(\partial\Omega). \tag{6.10}$$

If the material is both synchronous and homogeneous then the resulting simplification is readily established. From (6.1)

$$\begin{aligned} \lambda(t,q) &= \lambda_0\phi(t,q), && (6.11)\\ \mu(t,q) &= \mu_0\phi(t,q). && (6.12) \end{aligned}$$

Substituting equations (6.11) and (6.12) into equation (6.8) gives

$$a(t,q;\mathbf{w},\mathbf{v}) = \int_\Omega \lambda_0\phi(t,q)\nabla\cdot\mathbf{w}\nabla\cdot\mathbf{v} + \mu_0\phi(t,q)\varepsilon_{ij}(\mathbf{w})\varepsilon_{ij}(\mathbf{v})\ \mathrm{d}\Omega. \tag{6.13}$$

As the material is homogeneous, $\phi(t,q)$ does not depend on $\mathbf{x} \in \Omega$, and

$$a(t,q;\mathbf{w},\mathbf{v}) = \phi(t,q)\int_\Omega \lambda_0\nabla\cdot\mathbf{w}\nabla\cdot\mathbf{v} + \mu_0\varepsilon_{ij}(\mathbf{w})\varepsilon_{ij}(\mathbf{v})\ \mathrm{d}\Omega. \tag{6.14}$$

Choosing $\lambda_0 = \lambda(0,0)$ and $\mu_0 = \mu(0,0)$ gives $\phi(0,0) = 1$. Thus equation (6.14) may be expressed as

$$\begin{aligned} a(t,q;\mathbf{w},\mathbf{v}) &= \phi(t,q)\int_\Omega \lambda(0,0)\nabla\cdot\mathbf{w}\nabla\cdot\mathbf{v} + \mu(0,0)\varepsilon_{ij}(\mathbf{w})\varepsilon_{ij}(\mathbf{v})\ \mathrm{d}\Omega\\ &= \phi(t,q)a(0,0;\mathbf{w},\mathbf{v}). && (6.15) \end{aligned}$$

In a similar process, equation (6.9) can be written as

$$b(t,q;\mathbf{w},\mathbf{v}) = -\dot\phi(t,q)\int_\Omega \lambda_0\nabla\cdot\mathbf{w}\nabla\cdot\mathbf{v} + \mu_0\varepsilon_{ij}(\mathbf{w})\varepsilon_{ij}(\mathbf{v})\ \mathrm{d}\Omega. \tag{6.16}$$

Using, again, $\lambda_0 = \lambda(0,0)$ and $\mu_0 = \mu(0,0)$, equation (6.16) becomes

$$\begin{aligned} b(t,q;\mathbf{w},\mathbf{v}) &= -\dot\phi(t,q)\int_\Omega \lambda(0,0)\nabla\cdot\mathbf{w}\nabla\cdot\mathbf{v} + \mu(0,0)\varepsilon_{ij}(\mathbf{w})\varepsilon_{ij}(\mathbf{v})\ \mathrm{d}\Omega\\ &= -\dot\phi(t,q)a(0,0;\mathbf{w},\mathbf{v}). && (6.17) \end{aligned}$$

Using the linearity of $a(t,q;\cdot,\cdot)$ and substituting the expression (6.15) and (6.17) into (6.7) we obtain

$$\begin{aligned} \phi(t,t)a(0,0;\mathbf{u}(t),\mathbf{v}) - \int_0^t \dot\phi(t,q)a(0,0;\mathbf{u}(q),\mathbf{v})\,\mathrm{d}q &= L(t;\mathbf{v})\\ a(0,0;\phi(t,t)\mathbf{u}(t),\mathbf{v}) - \int_0^t a(0,0;\dot\phi(t,q)\mathbf{u}(q),\mathbf{v})\,\mathrm{d}q &= L(t;\mathbf{v})\\ a\Big(0,0;\phi(t,t)\mathbf{u}(t) - \int_0^t \dot\phi(t,q)\mathbf{u}(q)\,\mathrm{d}q,\mathbf{v}\Big) &= L(t;\mathbf{v}). && (6.18) \end{aligned}$$

The equation (6.18) can be written as

$$a(0,0;\mathbf{u}_E(t),\mathbf{v}) = L(t;\mathbf{v}), \tag{6.19}$$

where

$$\mathbf{u}_E(t) = \phi(t,t)\mathbf{u}(t) - \int_0^t \dot{\phi}(t,q)\mathbf{u}(q)\,\mathrm{d}q. \tag{6.20}$$

The equation (6.19) is called the *time-dependent elasticity problem* for an elastic displacement field $\mathbf{u}_E(t)$, and a Volterra equation for the viscoelastic displacement field $\mathbf{u}(t)$. The physical reason for separation of space and time is that the synchronous and homogeneous assumptions imply that the material relaxes in the same way in all directions and at all points in the body and thus the viscoelastic response of the body is related to elastic responses of associated bodies.

The ODE formulation of viscoelasticity is available in the case of quasi-separable relaxation functions and is, in fact, quite closely related to the differential form of the constitutive relation (6.5) in the case of a generalized standard linear solid (Janovsky *et al.* [16]). Janovsky *et al.* showed that, in that case, the solution can be decomposed into *creep modes* and that creep modes satisfy systems of ODE. Based on their scheme outlined, the ODE formulation is again repeated here. The numerical implementation of the scheme will be reported in Chapter 7. We begin by considering the case of separable, $\phi(t,q)$, which now denotes the $\mathbf{x}$ independent relaxation function which can be expressed as the product of two functions,

$$\phi(t,q) = \sum_{j=0}^{N_\phi} y_j(t)z_j(q). \tag{6.21}$$

Substituting equation (6.21) into (6.20), we obtain

$$\mathbf{u}_E(t) = \sum_{j=0}^{N_\phi} y_j(t)z_j(t)\mathbf{u}(t) - \int_0^t \sum_{j=0}^{N_\phi} y_j(t)\dot{z}_j(q)\mathbf{u}(q)\,\mathrm{d}q. \tag{6.22}$$

Using the normalization

$$\phi(t,t) = \sum_{j=0}^{N_\phi} y_j(t)z_j(t) = 1, \tag{6.23}$$

equation (6.22) becomes

$$\mathbf{u}_E(t) = \mathbf{u}(t) - \sum_{j=0}^{N_\phi} y_j(t)\int_0^t \dot{z}_j(q)\mathbf{u}(q)\,\mathrm{d}q. \tag{6.24}$$

This may be written as

$$\mathbf{u}_E(t) = \mathbf{u}(t) - \sum_{j=0}^{N_\phi} \mathbf{w}_j(t) \tag{6.25}$$

or

$$\mathbf{u}(t) = \mathbf{u}_E(t) + \sum_{j=0}^{N_\phi} \mathbf{w}_j(t), \tag{6.26}$$

where

$$\mathbf{w}_j(t) = y_j(t) \int_0^t \dot{z}_j(q)\mathbf{u}(q)\, \mathrm{d}q, \quad j = 0, 1, \cdots, N_\phi. \tag{6.27}$$

Next, we will show that the function $\mathbf{w}_j(t)$ satisfies a system of first-order linear ODEs. Differentiating equation (6.27) with respect to t yields

$$\begin{aligned}
\dot{\mathbf{w}}_j(t) &= y_j(t)\dot{z}_j(t)\mathbf{u}(t) + \dot{y}_j(t) \int_0^t \dot{z}_j(q)\mathbf{u}(q)\, \mathrm{d}q \\
&= \dot{y}_j(t)\frac{y_j(t)}{y_j(t)} \int_0^t \dot{z}_j(q)\mathbf{u}(q)\, \mathrm{d}q + y_j(t)\dot{z}_j(t)\mathbf{u}(t) \\
&= \frac{\dot{y}_j(t)}{y_j(t)}\mathbf{w}_j(t) + y_j(t)\dot{z}_j(t)\mathbf{u}(t) \\
\dot{\mathbf{w}}_j(t) &= \beta_j \mathbf{w}_j(t) + C_j \mathbf{u}(t), \quad j = 0, 1, \cdots, N_\phi,
\end{aligned} \tag{6.28}$$

where

$$\beta_j = \beta_j(t) = \frac{\dot{y}_j(t)}{y_j(t)}, \qquad C_j = y_j(t)\dot{z}_j(t), \quad j = 0, 1, \cdots N_\phi. \tag{6.29}$$

Substituting equation (6.26) into equation (6.28) yields

$$\dot{\mathbf{w}}_j(t) = \beta_j \mathbf{w}_j(t) + C_j\Big(\sum_{k=0}^{N_\phi} \mathbf{w}_k(t)\Big) + C_j \mathbf{u}_E(t), \quad j = 0, 1, \cdots, N_\phi. \tag{6.30}$$

The displacement in elasticity problem, $\mathbf{u}_E$, given by

$$\mathbf{u}_E = [u_{E1}, u_{E2}]^T \tag{6.31}$$

represents horizontal and vertical movements of a typical point within the element. Hence (6.30) can be expressed in full matrix form as

$$\begin{bmatrix} \dot{w}_{01} \\ \dot{w}_{11} \\ \vdots \\ \dot{w}_{N_\phi 1} \\ \\ \dot{w}_{02} \\ \dot{w}_{12} \\ \vdots \\ \dot{w}_{N_\phi 2} \end{bmatrix} = \begin{bmatrix} \beta_0 & 0 & \cdots & 0 & 0 & 0 & \cdots & 0 \\ 0 & \beta_1 & \cdots & 0 & 0 & 0 & \cdots & 0 \\ \vdots & \vdots & \ddots & \vdots & \vdots & \vdots & \ddots & \vdots \\ 0 & 0 & \cdots & \beta_{N_\phi} & 0 & 0 & \cdots & 0 \\ \\ 0 & 0 & \cdots & 0 & \beta_0 & 0 & \cdots & 0 \\ 0 & 0 & \cdots & 0 & 0 & \beta_1 & \cdots & 0 \\ \vdots & \vdots & \ddots & \vdots & \vdots & \vdots & \ddots & \vdots \\ 0 & 0 & \cdots & 0 & 0 & 0 & \cdots & \beta_{N_\phi} \end{bmatrix} \begin{bmatrix} w_{01} \\ w_{11} \\ \vdots \\ w_{N_\phi 1} \\ \\ w_{02} \\ w_{12} \\ \vdots \\ w_{N_\phi 2} \end{bmatrix}$$

$$+\begin{bmatrix} C_0 & C_0 & \cdots & C_0 & 0 & 0 & \cdots & 0 \\ C_1 & C_1 & \cdots & C_1 & 0 & 0 & \cdots & 0 \\ \vdots & \vdots & \ddots & \vdots & \vdots & \vdots & \ddots & \vdots \\ C_{N_\phi} & C_{N_\phi} & \cdots & C_{N_\phi} & 0 & 0 & \cdots & 0 \\ 0 & 0 & \cdots & 0 & C_0 & C_0 & \cdots & C_0 \\ 0 & 0 & \cdots & 0 & C_1 & C_1 & \cdots & C_1 \\ \vdots & \vdots & \ddots & \vdots & \vdots & \vdots & \ddots & \vdots \\ 0 & 0 & \cdots & 0 & C_{N_\phi} & C_{N_\phi} & \cdots & C_{N_\phi} \end{bmatrix} \begin{bmatrix} w_{01} \\ w_{11} \\ \vdots \\ w_{N_\phi 1} \\ w_{02} \\ w_{12} \\ \vdots \\ w_{N_\phi 2} \end{bmatrix}$$

$$+\begin{bmatrix} C_0 u_{E1} \\ C_1 u_{E1} \\ \vdots \\ C_{N_\phi} u_{E1} \\ C_0 u_{E2} \\ C_1 u_{E2} \\ \vdots \\ C_{N_\phi} u_{E2} \end{bmatrix} \tag{6.32}$$

or we can write the above equation for each component as

$$\begin{bmatrix} \dot{w}_{0i} \\ \dot{w}_{1i} \\ \vdots \\ \dot{w}_{N_\phi i} \end{bmatrix} = \begin{bmatrix} \beta_0 & 0 & \cdots & 0 \\ 0 & \beta_1 & \cdots & 0 \\ \vdots & \vdots & \ddots & \vdots \\ 0 & 0 & \cdots & \beta_{N_\phi} \end{bmatrix} \begin{bmatrix} w_{0i} \\ w_{1i} \\ \vdots \\ w_{N_\phi i} \end{bmatrix} + \begin{bmatrix} C_0 \\ C_1 \\ \vdots \\ C_{N_\phi} \end{bmatrix} [1, 1, \cdots, 1] \begin{bmatrix} w_{0i} \\ w_{1i} \\ \vdots \\ w_{N_\phi i} \end{bmatrix} + \begin{bmatrix} C_0 u_{Ei} \\ C_1 u_{Ei} \\ \vdots \\ C_{N_\phi} u_{Ei} \end{bmatrix}, \ i = 1, 2. \tag{6.33}$$

Therefore, the ODE formulation in this case is given by

$$\dot{\mathbf{w}}(t) \ = \ J(t)\mathbf{w}(t) + \mathbf{b}(t), \tag{6.34}$$

where

$$\mathbf{w} \ = \ [w_{0i}, w_{1i} \cdots, w_{N_\phi i}]^T, \ i = 1, 2, \tag{6.35}$$

$$\mathbf{b} \ = \ [C_0 u_{Ei}, C_1 u_{Ei}, \cdots, C_{N_\phi} u_{Ei}]^T, \ i = 1, 2, \tag{6.36}$$

and the matrix J is given by

$$J(t) = D(t) + \mathbf{c}(t)\mathbf{e}^T, \tag{6.37}$$

where

$$D = \mathrm{diag}(\beta_j),\ j = 0, 1, \cdots, N_\phi, \quad \mathbf{c} = [C_0, \cdots, C_{N_\phi}]^T,\ \mathbf{e} = [1, \cdots, 1]^T. \tag{6.38}$$

The schemes outlined above exploited the relaxation functions being quasi-separable. In this case a classical method allows the Volterra equation (6.20) to be recast as the system of ODE problems (6.34)-(6.38). We solve a problem of linear elasticity at each time level to get $\mathbf{u}_E$ and need only apply an ODE solver to the system (6.34). As we will see, a Dirichlet series for ϕ leads to a matrix J which is constant in time. It is known that the properties of the solution of the system (6.34) depend on the eigenvalues of J. If $\{\lambda_1, \lambda_2 \cdots, \lambda_{N_\phi}\}$ denote the eigenvalues with corresponding eigenvectors $\{\mathbf{v}_1, \mathbf{v}_2, \cdots, \mathbf{v}_{N_\phi}\}$, then for an eigenvalue λ and corresponding eigenvector $\mathbf{v} \neq \mathbf{0}$ we have

$$\mathbf{0} = (\lambda I - J)\mathbf{v},$$

where I is an identity matrix. Using equation (6.37), the above equation becomes

$$\begin{aligned} \mathbf{0} &= (\lambda I - D - \mathbf{c}\mathbf{e}^T)\mathbf{v} \\ &= (\lambda I - D)\mathbf{v} - (\mathbf{e}^T\mathbf{v})\mathbf{c} \\ &= (\lambda I - D)[\mathbf{v} - (\mathbf{e}^T\mathbf{v})(\lambda I - D)^{-1}\mathbf{c}]. \end{aligned}$$

As $(\lambda I - D)$ is non-singular, then

$$\mathbf{v} - (\mathbf{e}^T\mathbf{v})(\lambda I - D)^{-1}\mathbf{c} = \mathbf{0}. \tag{6.39}$$

Multiplying (6.39) by $\mathbf{e}^T$ we obtain

$$\begin{aligned} \mathbf{e}^T\Big(\mathbf{v} - (\mathbf{e}^T\mathbf{v})(\lambda I - D)^{-1}\mathbf{c}\Big) &= 0 \\ (\mathbf{e}^T\mathbf{v})\{1 - \mathbf{e}^T(\lambda I - D)^{-1}\mathbf{c}\} &= 0. \end{aligned}$$

It is assumed that $\mathbf{e}^T\mathbf{v} \neq 0$ so that

$$1 - \mathbf{e}^T(\lambda I - D)^{-1}\mathbf{c} = 0. \tag{6.40}$$

Substituting (6.38) into (6.40), gives

$$0 = 1 - [1, \ldots, 1] \begin{bmatrix} (\lambda - \beta_0)^{-1} & 0 & \cdots & 0 \\ 0 & (\lambda - \beta_1)^{-1} & \cdots & 0 \\ \vdots & \vdots & \ddots & \vdots \\ 0 & 0 & \cdots & (\lambda - \beta_{N_\phi})^{-1} \end{bmatrix} \begin{bmatrix} C_0 \\ C_1 \\ \vdots \\ C_{N_\phi} \end{bmatrix}. \tag{6.41}$$

Thus the eigenvalues λ of matrix J are the solutions of the equation

$$1 - \sum_{j=0}^{N_\phi} \frac{C_j}{\lambda - \beta_j} = 1 - \sum_{j=0}^{N_\phi} \frac{C_j}{\lambda + \alpha_j} = 0. \tag{6.42}$$

For the case of a generalized standard linear solid (see (6.5)), the stress relaxation is given by

$$\phi(t,q) = \sum_{j=0}^{N_\phi} \phi_j \exp(-\alpha_j(t-q)) = \sum_{j=0}^{N_\phi} y_j(t) z_j(q). \tag{6.43}$$

The functions y_j and z_j can be taken as

$$y_j(t) = \phi_j \exp(-\alpha_j t) \;\text{ and }\; z_j(t) = \exp(\alpha_j t), \tag{6.44}$$

so that

$$\beta_j = \frac{\dot{y}_j(t)}{y_j(t)} = -\frac{\alpha_j \phi_j \exp(-\alpha_j t)}{\phi_j \exp(-\alpha_j t)} = -\alpha_j\,, \tag{6.45}$$

$$C_j = y_j(t)\dot{z}_j(t) = \alpha_j \phi_j e^{-\alpha_j t} e^{\alpha_j t} = \alpha_j \phi_j. \tag{6.46}$$

To model a solid, it is usual to take $\alpha_0 = 0$, which gives $\beta_0 = 0, C_0 = 0$ and $\dot{\mathbf{w}}_0 = \mathbf{0}$. It follows that equation (6.30) may be written in matrix form as

$$\dot{\mathbf{w}}(t) = J(t)\mathbf{w}(t) + \mathbf{b}(t), \tag{6.47}$$

where now the vectors are of length N_ϕ with specifically

$$\mathbf{w} = [w_{1i}, w_{2i} \cdots, w_{N_\phi i}]^T, \tag{6.48}$$

$$\mathbf{b} = [C_1 u_{Ei}, C_2 u_{Ei}, \cdots, C_{N_\phi} u_{Ei}]^T \tag{6.49}$$

and the matrix J is given by

$$J(t) = D(t) + \mathbf{c}(t)\mathbf{e}^T \tag{6.50}$$

and now

$$D = \operatorname{diag}(\beta_j),\; j = 1, 2, \cdots, N_\phi, \quad \mathbf{c} = [C_1, \cdots, C_{N_\phi}]^T, \;\; \mathbf{e} = [1, \cdots, 1]^T. \tag{6.51}$$

In full, in matrix form, we have

$$\begin{bmatrix} \dot{w}_{1i} \\ \dot{w}_{2i} \\ \vdots \\ \dot{w}_{N_\phi i} \end{bmatrix} = \begin{bmatrix} \beta_1 & 0 & \cdots & 0 \\ 0 & \beta_2 & \cdots & 0 \\ \vdots & \vdots & \ddots & \vdots \\ 0 & 0 & \cdots & \beta_{N_\phi} \end{bmatrix} \begin{bmatrix} w_{1i} \\ w_{2i} \\ \vdots \\ w_{N_\phi i} \end{bmatrix}$$

$$+\begin{bmatrix} C_1 \\ C_2 \\ \vdots \\ C_{N_\phi} \end{bmatrix} [1,1,\cdots,1] \begin{bmatrix} w_{1i} \\ w_{2i} \\ \vdots \\ w_{N_\phi i} \end{bmatrix}$$
$$+\begin{bmatrix} C_1 u_{Ei} \\ C_2 u_{Ei} \\ \vdots \\ C_{N_\phi} u_{Ei} \end{bmatrix}, \ i = 1, 2. \tag{6.52}$$

The eigenvalues λ of matrix J in equation (6.47) satisfy

$$1 - \sum_{j=1}^{N_\phi} \frac{C_j}{\lambda - \beta_j} = 1 - \sum_{j=1}^{N_\phi} \frac{C_j}{\lambda + \alpha_j} = 0. \tag{6.53}$$

We use these eigenvalues for solving the fundamental ODE system (6.47). We now describe how this will be done.

6.1.1 ODE Solver

In this section, we discuss a procedure for obtaining the solution of the ODE formulation

$$\dot{\mathbf{w}}(t) = J(t)\mathbf{w}(t) + \mathbf{b}(t) \tag{6.54}$$

where $\mathbf{b}(t)$ and $J(t)$ are as in (6.49) and (6.50), respectively. This is subject to the initial condition

$$\mathbf{w}_j(0) = \mathbf{0}, \quad j = 1, 2, \cdots, N_\phi.$$

The eigenvalues $\lambda \in \{\lambda_1, \cdots, \lambda_{N_\phi}\}$ of matrix J are determined by solving

$$0 = 1 - \sum_{j=1}^{N_\phi} \frac{C_j}{\lambda + \alpha_j}. \tag{6.55}$$

Let $\{\mathbf{v}_1, \mathbf{v}_2, \ldots, \mathbf{v}_{N_\phi}\}$ be the corresponding eigenvectors of J. To find an eigenvector $\mathbf{v}$ corresponding to an eigenvalue λ we must solve

$$J\mathbf{v} = \lambda\mathbf{v}. \tag{6.56}$$

Rearranging terms in equation (6.56) we find that

$$(J - \lambda I)\mathbf{v} \ = \ 0. \tag{6.57}$$

Substituting for J in the above equation, gives

$$\begin{aligned}(D + \mathbf{c}\mathbf{e}^T - \lambda I)\mathbf{v} &= 0 \\ (D - \lambda I)\mathbf{v} + (\mathbf{e}^T\mathbf{v})\mathbf{c} &= 0 \\ (\lambda I - D)\mathbf{v} &= (\mathbf{e}^T\mathbf{v})\mathbf{c} \\ \mathbf{v} &= (\mathbf{e}^T\mathbf{v})(\lambda I - D)^{-1}\mathbf{c}. \end{aligned} \tag{6.58}$$

Using the normalization $\mathbf{e}^T\mathbf{v} = 1$, equation (6.58) becomes

$$\mathbf{v} = (\lambda I - D)^{-1}\mathbf{c}. \tag{6.59}$$

Thus if $\lambda = \lambda_k$ and $\mathbf{v} = \mathbf{v}_k = ((\mathbf{v}_k)_j)$ we have

$$(\mathbf{v}_k)_j = \frac{C_j}{\lambda_k - \beta_j}, \quad j, k = 1, \cdots, N_\phi. \tag{6.60}$$

Hence, equation (6.59) gives the eigenvectors associated with the eigenvalues in equation (6.55). The equation (6.56) can be expressed as

$$\begin{aligned} J[\mathbf{v}_1, \mathbf{v}_2, \cdots, \mathbf{v}_{N_\phi}] &= [\lambda_1\mathbf{v}_1, \lambda_2\mathbf{v}_2, \cdots, \lambda_{N_\phi}\mathbf{v}_{N_\phi}] \\ &= [\mathbf{v}_1, \mathbf{v}_2, \cdots, \mathbf{v}_{N_\phi}] \begin{bmatrix} \lambda_1 & 0 & \cdots & 0 \\ 0 & \lambda_2 & \cdots & 0 \\ \vdots & \vdots & \ddots & \vdots \\ 0 & 0 & \cdots & \lambda_{N_\phi} \end{bmatrix}. \end{aligned} \tag{6.61}$$

Let $\mathbf{X} := [\mathbf{v}_1, \mathbf{v}_2, \cdots, \mathbf{v}_{N_\phi}]$ and $\widetilde{D} := \begin{bmatrix} \lambda_1 & 0 & \cdots & 0 \\ 0 & \lambda_2 & \cdots & 0 \\ \vdots & \vdots & \ddots & \vdots \\ 0 & 0 & \cdots & \lambda_{N_\phi} \end{bmatrix}$, we have

$$J\mathbf{X} = \mathbf{X}\widetilde{D} \tag{6.62}$$

then the matrix J may be written as

$$J = \mathbf{X}\widetilde{D}\mathbf{X}^{-1}. \tag{6.63}$$

Substituting for J in equation (6.47) we obtain

$$\dot{\mathbf{w}} = (\mathbf{X}\widetilde{D}\mathbf{X}^{-1})\mathbf{w} + \mathbf{b}. \tag{6.64}$$

Since $\mathbf{X}$ is non-singular it follows that

$$\mathbf{X}^{-1}\dot{\mathbf{w}} = \widetilde{D}(\mathbf{X}^{-1}\mathbf{w}) + \mathbf{X}^{-1}\mathbf{b}. \tag{6.65}$$

Now we consider the initial-value problem consisting of the differential equation (6.65) and the initial condition

$$\mathbf{w}_j(0) = \mathbf{0}, \quad j = 1, 2, \cdots, N_\phi. \tag{6.66}$$

The solution of the initial-value problem, $\{(6.65),(6.66)\}$, will be determined as follows.

Let $\mathbf{P} = \mathbf{X}^{-1}\mathbf{w}$ and $\mathbf{Q} = \mathbf{X}^{-1}\mathbf{b}$, then equation (6.65) can be written as

$$\dot{\mathbf{P}} = \widetilde{D}\mathbf{P} + \mathbf{Q}, \;\; \mathbf{P}(0) = \mathbf{0}. \tag{6.67}$$

Firstly, equation (6.67) is solved by using the fourth-order Runge Kutta method for the vector $\mathbf{P}$. Next, the vector $\mathbf{w}$ is obtained by

$$\mathbf{w} = \mathbf{X}\mathbf{P}. \tag{6.68}$$

Finally, the viscoelastic solution, $\mathbf{u}(t)$, is determined by

$$\mathbf{u}(t) = \mathbf{u}_E(t) + \sum_{j=1}^{N_\phi} \mathbf{w}_j(t). \tag{6.69}$$

In practical computations the exact solutions in the linear elasticity problem, $\mathbf{u}_E$, will generally not be known and will be approximated by finite element solutions $\mathbf{u}_{Eh}$. The finite element solutions are employed to determine the vector $\mathbf{b}$ in equation (6.49) which is used for solving $\mathbf{w}_j(t)$ in (6.54).

6.2 The Discrete Formulation

In this section we derive the *discrete formulation*, referred to in the previous section. The result of this formulation will be used for comparison with these of the ODE formulation.

As detailed in Shaw [34], there are two steps to discretize the quasistatic problem. Firstly, the Galerkin finite element method as outlined in Chapter 3 is employed to discretize in the space domain. This constructs a semidiscrete approximation problem as a system of Volterra second kind equations. Finally, a fully discretization is produced by replacing the Volterra operator with a suitable numerical quadrature rule (for e.g. see Linz [20]) and we shall use the trapezoidal rule.

The semidiscrete finite element approximation to the quasistatic displacement model, (6.7), is stated as the problem: find $\mathbf{u}_h \in L_\infty(\mathcal{J}; V^h)$, $V^h \subset V$, such that (Shaw [34])

$$a(t,t;\mathbf{u}_h(t),\mathbf{v}) + \int_0^t b(t,q;\mathbf{u}_h(q),\mathbf{v})\,\mathrm{d}q = L(t;\mathbf{v}), \quad \forall \mathbf{v} \in V^h,\ t \in \mathcal{J}, \tag{6.70}$$

where $a(t,t;\cdot,\cdot)$, $b(t,q;\cdot,\cdot)$ and $L(t;\cdot)$ are as in (6.8), (6.9) and (6.10), respectively. By following the methodology outlined in section 3.7 of Chapter 3 we can write this as the Volterra system:

$$\mathbf{A}(t,t)\mathbf{U}(t) + \int_0^t \mathbf{B}(t,q)\mathbf{U}(q)\,\mathrm{d}q = \mathbf{F}(t), \quad t \in \mathcal{J}, \tag{6.71}$$

where the time-dependent vector $\mathbf{F}(t)$ contains the body forces and surface tractions, $\mathbf{A}(t,t)$ and $\mathbf{B}(t,q)$ are the stiffness matrix and history matrix, respectively. Both $\mathbf{A}(t,t)$ and $\mathbf{B}(t,q)$ can be given by assembling the element matrices $\mathbf{A}_i(t,t)$ and $\mathbf{B}_i(t,q)$, given, respectively, by,

$$\mathbf{A}_i(t,t) = \int_0^1 \int_0^{1-\eta} \widehat{\mathbf{B}}^T \mathbf{D}(t,t) \widehat{\mathbf{B}} \quad |J| \mathrm{d}\xi \mathrm{d}\eta, \tag{6.72}$$

$$\mathbf{B}_i(t,q) = -\int_0^1 \int_0^{1-\eta} \widehat{\mathbf{B}}^T \dot{\mathbf{D}}(t,q) \widehat{\mathbf{B}} \quad |J| \mathrm{d}\xi \mathrm{d}\eta, \tag{6.73}$$

where $\widehat{\mathbf{B}}$ is the matrix as in (3.55) and $\mathbf{D}(t,q)$ is the stress relaxation matrix which in two space dimensions has the form,

$$\mathbf{D}(t,q) = \begin{pmatrix} \lambda+\mu & \lambda & 0 \\ \lambda & \lambda+\mu & 0 \\ 0 & 0 & \mu/2 \end{pmatrix} (t,q). \tag{6.74}$$

The elements of this matrix, $\lambda = \lambda(t,q)$ and $\mu = \mu(t,q)$, are examples of stress relaxation functions; in this case these are the viscoelastic analoguos to the Lamé coefficients that appear in linear elasticity theory (see e.g. Hunter [15]).

A fully discrete problem can be obtained by replacing the hereditary integral in (6.71) by the trapezoidal rule. Initially, for a positive integer N, let

$$\mathcal{J}^k := \{0 = t_0, t_1, \ldots, t_N = T \in \mathbb{R} : t_{i-1} < t_i \text{ for } i = 1,2,\ldots,N\} \tag{6.75}$$

denote a partition of the time interval $\mathcal{J}$ and we set

$$u_i := u(t_i) \text{ for } t_i \in \mathcal{J}^k, \tag{6.76}$$

$$h_i := t_i - t_{i-1} \text{ for } 1 \leq i \leq N, \tag{6.77}$$

$$h := \max_{1 \leq i \leq N} h_i. \tag{6.78}$$

Now, the fully discrete approximation to the quasistatic displacement model can be defined to find, for each $t_i \in \mathcal{J}^k$, a function $\mathbf{u}_{h,i} \in V^h$ such that

$$a(t_i, t_i; \mathbf{u}_{h,i}, \mathbf{v}) + \sum_{j=0}^{i} w_{ij} b(t_i, t_j, ; \mathbf{u}_{h,j}, \mathbf{v}) = L(t_i; \mathbf{v}) \quad \forall \mathbf{v} \in V^h. \tag{6.79}$$

Here the w_{ij} denote the weights and $w_{00} := 0$. This may be written as the computational problem

$$\mathbf{A}(t_i, t_i)\mathbf{U}_i + \sum_{j=0}^{i} w_{ij} \mathbf{B}(t_i, t_j)\mathbf{U}_j = \mathbf{F}_i. \tag{6.80}$$

Using the trapezoidal rule and rearranging (6.80) yield

$$\begin{aligned}\Big(\mathbf{A}(t_i, t_i) + \frac{h_i}{2}\mathbf{B}(t_i, t_i)\Big)\mathbf{U}_i = \mathbf{F}_i - \frac{h_i}{2}\mathbf{B}(t_i, t_{i-1})\mathbf{U}_{i-1} \\ - \sum_{j=1}^{i-1} \frac{h_j}{2}\Big(\mathbf{B}(t_i, t_{i-1})\mathbf{U}_{j-1} + \mathbf{B}(t_i, t_{j-1})\mathbf{U}_j\Big).\end{aligned} \tag{6.81}$$

For h small enough, this represents a deterministic algorithm for finding the vectors $\mathbf{U}_i \in V^h$ for each $t_i \in \mathcal{J}^k$, $i = 1, 2, \ldots, N$. The above equation requires a starting value $\mathbf{U}_0$ which is obtained by solving the linear elasticity problem,

$$\mathbf{A}(0, 0)\mathbf{U}_0 = \mathbf{F}_0. \tag{6.82}$$

It can be seen that there is an accumulation of history terms on the right-hand-side of equation (6.81) as time increases. Thus the demand on computer storage and computer time required at each time step will increase with time. This is true for a general Volterra problem but in the special case of viscoelasticity considered here this difficulty can be overcome. This will be explained in what follows as we consider what is involved in implementing the scheme when ϕ is given by a Dirichlet series.

For the synchronous case we have

$$\lambda(t, q) = \lambda_0 \phi(t, q), \tag{6.83}$$

$$\mu(t, q) = \mu_0 \phi(t, q). \tag{6.84}$$

Using the above equations in (6.74), gives

$$\mathbf{D}(t,q) = \begin{pmatrix} \lambda_0+\mu_0 & \lambda_0 & 0 \\ \lambda_0 & \lambda_0+\mu_0 & 0 \\ 0 & 0 & \mu_0/2 \end{pmatrix} \phi(t,q) := \mathbf{D}_0\phi(t,q). \tag{6.85}$$

Substituting (6.85) into (6.72) and (6.73) we obtain

$$\mathbf{A}_i(t,t) = \int_0^1\int_0^{1-\eta} \widehat{\mathbf{B}}^T\mathbf{D}_0\widehat{\mathbf{B}} \quad |J|\mathrm{d}\xi\mathrm{d}\eta \tag{6.86}$$

$$\mathbf{B}_i(t,q) = -\int_0^1\int_0^{1-\eta} \widehat{\mathbf{B}}^T\mathbf{D}_0\dot{\phi}(t,q)\widehat{\mathbf{B}} \quad |J|\mathrm{d}\xi\mathrm{d}\eta \tag{6.87}$$

$$= -\dot{\phi}(t,q)\mathbf{A}_i(t,t). \tag{6.88}$$

The equation (6.88) leads to

$$\mathbf{B}(t,q) = -\dot{\phi}(t,q)\mathbf{A}(t,t). \tag{6.89}$$

Thus equation (6.71) becomes

$$\mathbf{A}(t,t)\Big[\mathbf{U}(t) - \int_0^t \dot{\phi}(t,q)\mathbf{U}(q)\,\mathrm{d}q\Big] = \mathbf{F}(t), \quad t\in\mathcal{J}. \tag{6.90}$$

In order to obtain the general fully discrete formulation at each time step $t = t_i$, $i = 1, 2, \cdots, N_\phi$, we begin considering a fully discrete formulation at $t = t_1 > 0$,

$$\mathbf{A}(t_1,t_1)\Big[\mathbf{U}(t_1) - \int_0^{t_1} \dot{\phi}(t_1,q)\mathbf{U}(q)\,\mathrm{d}q\Big] = \mathbf{F}(t_1), \quad t_1\in\mathcal{J}^k. \tag{6.91}$$

Now let

$$\boldsymbol{\gamma}(t_1) := \int_0^{t_1} \dot{\phi}(t_1,q)\mathbf{U}(q)\,\mathrm{d}q, \tag{6.92}$$

since

$$\dot{\phi}(t,q) = \sum_{j=1}^{N_\phi} \alpha_j\phi_j e^{-\alpha_j(t-q)}, \tag{6.93}$$

then

$$\boldsymbol{\gamma}(t_1) = \int_0^{t_1}\sum_{j=1}^{N_\phi} \alpha_j\phi_j e^{-\alpha_j(t_1-q)}\mathbf{U}(q)\,\mathrm{d}q \tag{6.94}$$

$$= \sum_{j=1}^{N_\phi} \mathbf{r}_j(t_1), \tag{6.95}$$

where

$$\mathbf{r}_j(t_1) := \int_0^{t_1} \alpha_j \phi_j e^{-\alpha_j(t_1-q)} \mathbf{U}(q)\, \mathrm{d}q, \quad j = 1, 2, \cdots, N_\phi. \tag{6.96}$$

The integral (6.94) is approximated by the trapezoidal rule and setting $h_1 = t_1$ we obtain

$$\boldsymbol{\gamma}(t_1) = \sum_{j=1}^{N_\phi} \mathbf{r}_j(t_1) = \Big(\frac{h_1}{2}\Big)\Big[\sum_{j=1}^{N_\phi} \alpha_j \phi_j \Big\{e^{-\alpha_j t_1}\mathbf{U}(0) + \mathbf{U}(t_1)\Big\}\Big]. \tag{6.97}$$

By using (6.97) in (6.91) and rearranging leads to a fully discrete formulation at $t = t_1$,

$$\mathbf{A}(t_1, t_1)\Big[1 - \frac{h_1}{2}\sum_{j=1}^{N_\phi} \alpha_j \phi_j\Big]\mathbf{U}(t_1) = \mathbf{F}(t_1) + \mathbf{A}(t_1, t_1)\frac{h_1}{2}\sum_{j=1}^{N_\phi} \alpha_j \phi_j e^{-\alpha_j t_1}\mathbf{U}(0). \tag{6.98}$$

This is solved for $\mathbf{U}(t_1)$ and then $\mathbf{r}_j(t_1)$, $j = 1, 2, \cdots N_\phi$ is computed. These values will be used in the next time step. Next, for $t = t_2$ from (6.71) we have that

$$\mathbf{A}(t_2, t_2)\Big[\mathbf{U}(t_2) - \int_0^{t_2} \dot{\phi}(t_2, q)\mathbf{U}(q)\, \mathrm{d}q\Big] = \mathbf{F}(t_2), \quad t_2 \in \mathcal{J}^k. \tag{6.99}$$

In order to show that $\boldsymbol{\gamma}(t_2)$ can be written in terms of $\mathbf{r}_j(t_1)$, we define

$$\begin{aligned} \boldsymbol{\gamma}(t_2) &:= \int_0^{t_2} \dot{\phi}(t_2, q)\mathbf{U}(q)\, \mathrm{d}q & (6.100)\\ &= \int_0^{t_1} \dot{\phi}(t_2, q)\mathbf{U}(q)\, \mathrm{d}q + \int_{t_1}^{t_2} \dot{\phi}(t_2, q)\mathbf{U}(q)\, \mathrm{d}q. & (6.101) \end{aligned}$$

By making use of (6.94) in the first integral in equation (6.101) and approximating the second integral by the trapezoidal rule yields

$$\begin{aligned} \boldsymbol{\gamma}(t_2) &= \int_0^{t_1} \sum_{j=1}^{N_\phi} e^{-\alpha_j(t_2-t_1)} \alpha_j \phi_j e^{-\alpha_j(t_1-q)}\mathbf{U}(q)\, \mathrm{d}q \\ &+ \Big(\frac{t_2 - t_1}{2}\Big)\Big[\sum_{j=1}^{N_\phi} \alpha_j \phi_j \Big\{e^{-\alpha_j(t_2-t_1)}\mathbf{U}(t_1) + \mathbf{U}(t_2)\Big\}\Big]. & (6.102) \end{aligned}$$

Using (6.95) and letting $h_2 = t_2 - t_1$, equation (6.102) can be written as

$$\begin{aligned} \boldsymbol{\gamma}(t_2) &= \sum_{j=1}^{N_\phi} \mathbf{r}_j(t_2) \\ &= \sum_{j=1}^{N_\phi} e^{-\alpha_j(t_2-t_1)}\mathbf{r}_j(t_1) \\ &+ \Big(\frac{h_2}{2}\Big)\Big[\sum_{j=1}^{N_\phi} \alpha_j \phi_j \Big\{e^{-\alpha_j(t_2-t_1)}\mathbf{U}(t_1) + \mathbf{U}(t_2)\Big\}\Big]. & (6.103) \end{aligned}$$

Substituting (6.103) into (6.99) and rearranging, we have that

$$\mathbf{A}(t_2,t_2)\Big(1-\frac{h_2}{2}\sum_{j=1}^{N_\phi}\alpha_j\phi_j\Big)\mathbf{U}(t_2)=\mathbf{F}(t_2)$$
$$+\mathbf{A}(t_2,t_2)\sum_{j=1}^{N_\phi}e^{-\alpha_j(t_2-t_1)}\Big(\mathbf{r}_j(t_1)+\frac{h_2}{2}\alpha_j\phi_j\mathbf{U}(t_1)\Big), \qquad (6.104)$$

where $\mathbf{r}_j(t_1)$, $j=1,2,\cdots,N_\phi$ are determined by (6.97). Again $\mathbf{U}(t_2)$ is determined by solving (6.104) and then $\mathbf{r}_j(t_2)$ in (6.103) will be calculated. These values will be stored for the next time step. Similarly, it can be shown that for $t=t_i$,

$$\mathbf{A}(t_i,t_i)\Big(1-\frac{h_i}{2}\sum_{j=1}^{N_\phi}\alpha_j\phi_j\Big)\mathbf{U}(t_i)=\mathbf{F}(t_i)$$
$$+\mathbf{A}(t_i,t_i)\sum_{j=1}^{N_\phi}e^{-\alpha_j(t_i-t_{i-1})}\Big(\mathbf{r}_j(t_{i-1})+\frac{h_i}{2}\alpha_j\phi_j\mathbf{U}(t_{i-1})\Big),$$
$$i=2,3,\cdots,N, \qquad (6.105)$$

where $h_i=t_i-t_{i-1}$ and $\mathbf{r}_j(t_{i-1})$ is obtained from values at the previous time step t_{i-1}. After solving (6.105) for $\mathbf{U}(t_i)$, $\mathbf{r}_j(t_i)$ is obtained from the formula

$$\mathbf{r}_j(t_i)=\Big(e^{-\alpha_j(t_i-t_{i-1})}\mathbf{r}_j(t_{i-1})+\frac{h_i}{2}\alpha_j\phi_j\Big[e^{-\alpha_j(t_i-t_{i-1})}\mathbf{U}(t_{i-1})+\mathbf{U}(t_i)\Big]\Big) \qquad (6.106)$$

for $j=1,2,\cdots,N_\phi$. Therefore, the fully discrete formulation in the case of a linear viscoelastic, isotropic, homogeneous and synchronous solid can be obtained from equation (6.98) for $t=t_1$ and equation (6.105) for $t>t_1$. The advantage of this way of implementing the method is that only the displacement $\mathbf{U}$ and $\mathbf{r}_j$, $j=1,2,\cdots,N_\phi$, at the previous time step are involved in the computation of the displacement $\mathbf{U}$ at the current time step.

6.3 The Quasistatic Displacement Algorithm

In this section will define the algorithms for computing the ODE and the fully discrete formulations which are discussed in previous sections. The algorithms will be used in Chapter 7 in order to produce the numerical solutions of both formulations.

6.3.1 The ODE Algorithm

The details of the algorithms for computing the ODE formulation are presented as follows.

Algorithm 1 **[Main ODE Algorithm]**

Given: (i) the percentage of relative error,

(ii) a matrix $\mathbf{D} := \mathbf{D}_0\phi(t)$ where

$$\mathbf{D}_0 = \begin{pmatrix} \lambda_0+\mu_0 & \lambda_0 & 0 \\ \lambda_0 & \lambda_0+\mu_0 & 0 \\ 0 & 0 & \mu_0/2 \end{pmatrix} \text{ and}$$

$$\phi(t) = \phi_0 + \phi_1 e^{-\alpha_1 t} + \phi_2 e^{-\alpha_2 t} + \phi_3 e^{-\alpha_3 t},$$

(iii) the boundary condition.

Task: find the displacement $\mathbf{u}(t)$ given in (6.69).

Step 1 For TIME $= t_0 = 0, t_1, t_2, \cdots, T$ (time step loop)

Step 2 Read the beginning meshes and apply the boundary condition to the meshes.

Step 3 For OPTIMAL $= 1, 2, \cdots, 50$ (mesh refinement loop)

Step 4 Calculate the matrix $\widetilde{\mathbf{K}}$ and the vector $\widetilde{\mathbf{F}}$ as in Algorithm 2.

Step 5 Solve a linear system

$$\widetilde{\mathbf{K}}\mathbf{u}_{Eh} = \widetilde{\mathbf{F}}$$

by using preconditioned conjugate gradient (PCG),(Golub and Van Loan [14], Schwarz [33]) see Algorithm 3.

Step 6 Compute the error estimators as in Algorithm 4.

Step 7 If the error indicator > tolerance in the kth element then the kth element is refined

Step 8 If there is at least one element to be refined then apply the boundary condition to the element

go to step 4

Else

go to End For OPTIMAL

End If

End For OPTIMAL

Step 9 If TIME $>$ 0 then compute the quasistatic solution (see Algorithm 5).

End For TIME

Algorithm 2 [Element Algorithm]

For K=1, NE (NE = number of elements)

Step 1 Determined the matrix $\widehat{\mathbf{K}}$ and the vector $\widehat{\mathbf{F}}$ from the formulas

$$\begin{aligned} \widehat{\mathbf{K}} &= \frac{|J|}{2}\widehat{\mathbf{B}}^T\mathbf{D}\widehat{\mathbf{B}}, \\ \widehat{\mathbf{F}} &= \frac{|J|}{6}\begin{pmatrix} \mathbf{f} \\ \mathbf{f} \\ \mathbf{f} \end{pmatrix}, \end{aligned}$$

as described in Chapter 3, section 3.7.

Step 2 Compute the vector $\widehat{\mathbf{G}}$

$$\widehat{\mathbf{G}} = \frac{|\mathbf{x}_j - \mathbf{x}_i|}{2}\begin{pmatrix} g_1 \\ g_2 \end{pmatrix}.$$

Step 3 Apply the boundary condition to each element.

Step 4 Assemble $\widehat{\mathbf{K}}$ to form the matrix $\widetilde{\mathbf{K}}$.

Step 5 Assemble $\widehat{\mathbf{F}}$ to form the vector $\widetilde{\mathbf{F}}$.

End For K

Algorithm 3 [Preconditioned Conjugate Gradients Algorithm]

Given a symmetric positive definite $A \in \mathbb{R}^{n\times n}$ and $\mathbf{b} \in \mathbb{R}^n$, a symmetric positive definite preconditioner M, and an initial guess $\mathbf{x}_0$ ($A\mathbf{x}_0 \approx \mathbf{b}$), the following algorithm solves the linear system $A\mathbf{x} = \mathbf{b}$ (Golub and Van Loan [14]).

$k = 0$

$\mathbf{r}_0 = \mathbf{b} - A\mathbf{x}_0$

while ($\mathbf{r}_k >$ stopping tolerance)

Solve $M\mathbf{z}_k = \mathbf{r}_k$

$k = k + 1$

if $k = 1$

$\mathbf{p}_1 = \mathbf{z}_0$

else

$\beta_k = \dfrac{\mathbf{r}_{k-1}^T\mathbf{z}_{k-1}}{\mathbf{r}_{k-2}^T\mathbf{z}_{k-2}}$

$\mathbf{p}_k = \mathbf{z}_{k-1} + \beta_k\mathbf{p}_{k-1}$

end

$\alpha_k = \dfrac{\mathbf{r}_{k-1}^T\mathbf{z}_{k-1}}{\mathbf{p}_k^T A\mathbf{p}_k}$

$\mathbf{x}_k = \mathbf{x}_{k-1} + \alpha_k\mathbf{p}_k$

$\mathbf{r}_k = \mathbf{r}_{k-1} - \alpha_k A\mathbf{p}_k$

end

$\mathbf{x} = \mathbf{x}_k$

Algorithm 4 [Error Estimation Algorithm]

For a linear element, let

$$
\begin{aligned}
\mathbf{P}(x,y) &= [1,\ x,\ y], \quad \hat{\boldsymbol{\sigma}}_h = [\hat{\sigma}_{h11},\ \hat{\sigma}_{h22},\ \hat{\sigma}_{h12}]^T, \\
\tilde{\boldsymbol{\sigma}}^* &= [\tilde{\sigma}^*_{11},\ \tilde{\sigma}^*_{22},\ \tilde{\sigma}^*_{12}]^T, \quad \boldsymbol{\sigma}^* = [\sigma^*_{11},\ \sigma^*_{22},\ \sigma^*_{12}]^T, \\
\boldsymbol{\sigma} &= [\sigma_{11},\ \sigma_{22},\ \sigma_{12}]^T, \quad \mathbf{A}^1 = [A^1_1,\ A^1_2\ ,A^1_3]^T, \\
\mathbf{A}^2 &= [A^2_1,\ A^2_2,\ A^2_3]^T, \quad \mathbf{A}^3 = [A^3_1,\ A^3_2,\ A^3_3]^T.
\end{aligned}
$$

Step 1 Solve the following linear systems to obtain $\mathbf{A^1}$, $\mathbf{A^2}$, $\mathbf{A^3}$

$$\begin{aligned}
\sum_{i=1}^{NS} \mathbf{P}^T(x_i, y_i)\mathbf{P}(x_i, y_i)\mathbf{A^1} &= \sum_{i=1}^{NS} \mathbf{P}^T(x_i, y_i)\hat{\sigma}_{h11}, \\
\sum_{i=1}^{NS} \mathbf{P}^T(x_i, y_i)\mathbf{P}(x_i, y_i)\mathbf{A^2} &= \sum_{i=1}^{NS} \mathbf{P}^T(x_i, y_i)\hat{\sigma}_{h22}, \\
\sum_{i=1}^{NS} \mathbf{P}^T(x_i, y_i)\mathbf{P}(x_i, y_i)\mathbf{A^3} &= \sum_{i=1}^{NS} \mathbf{P}^T(x_i, y_i)\hat{\sigma}_{h12}.
\end{aligned}$$

Note NS is the total number of sampling points and (x_i, y_i) is a co-ordinate of sampling point.

Step 2 Compute $\|\tilde{\mathbf{e}}\|_{E(\Omega)} = \left(\sum_{K=1}^{NE} \|\tilde{\mathbf{e}}\|^2_{E(\Omega_K)}\right)^{1/2}$ by the following process.

Step 2.1 Calculate the elements of vector $\tilde{\boldsymbol{\sigma}}^*$ from the equations

$$\begin{aligned}
\tilde{\sigma}^*_{11} &= \mathbf{P}(x, y)\mathbf{A}^1 = A^1_1 + A^1_2 x + A^1_3 y, \\
\tilde{\sigma}^*_{22} &= \mathbf{P}(x, y)\mathbf{A}^2 = A^2_1 + A^2_2 x + A^2_3 y, \\
\tilde{\sigma}^*_{12} &= \mathbf{P}(x, y)\mathbf{A}^3 = A^3_1 + A^3_2 x + A^3_3 y.
\end{aligned}$$

Step 2.2 Calculate the elements of vector $\boldsymbol{\sigma}^*$ from the equations

$$\begin{aligned}
\sigma^*_{11} &= N_1\tilde{\sigma}^*_{11}(x_1, y_1) + N_2\tilde{\sigma}^*_{11}(x_2, y_2) + N_3\tilde{\sigma}^*_{11}(x_3, y_3), \\
\sigma^*_{22} &= N_1\tilde{\sigma}^*_{22}(x_1, y_1) + N_2\tilde{\sigma}^*_{22}(x_2, y_2) + N_3\tilde{\sigma}^*_{22}(x_3, y_3), \\
\sigma^*_{12} &= N_1\tilde{\sigma}^*_{12}(x_1, y_1) + N_2\tilde{\sigma}^*_{12}(x_2, y_2) + N_3\tilde{\sigma}^*_{12}(x_3, y_3).
\end{aligned}$$

Step 2.3 Evaluate the finite element stress $\hat{\boldsymbol{\sigma}}_h = \mathbf{D}\widehat{\mathbf{B}}\mathbf{u}_{Eh}$ and the error estimate $\mathbf{e}^*_\sigma = \boldsymbol{\sigma}^* - \hat{\boldsymbol{\sigma}}_h$.

Step 2.4 Compute (see Akin [1] for the weight w_i)

$$\|\tilde{\mathbf{e}}\|^2_{E(\Omega_K)} = \sum_{i=1}^{NG} w_i \mathbf{e}^{*T}_\sigma(\xi_i, \eta_i)\mathbf{D}^{-1}\mathbf{e}^*_\sigma(\xi_i, \eta_i)|J|.$$

Step 3 Calculate $\|\mathbf{e}\|_{E(\Omega)} = \left(\sum_{K=1}^{NE} \|\mathbf{e}\|^2_{E(\Omega_K)}\right)^{1/2}$ by the following process.

Step 3.1 Evaluate $\mathbf{e}_\sigma = \boldsymbol{\sigma} - \hat{\boldsymbol{\sigma}}_h$ using the known exact solution for the test problem.

Step 3.2 Compute

$$\|\mathbf{e}\|^2_{E(\Omega_K)} = \sum_{i=1}^{NG} w_i \mathbf{e}_\sigma^T(\xi_i,\eta_i)\mathbf{D}^{-1}\mathbf{e}_\sigma(\xi_i,\eta_i)|J|.$$

Step 4 Calculate the effective index

$$\theta = \frac{\|\tilde{\mathbf{e}}\|_{E(\Omega)}}{\|\mathbf{e}\|_{E(\Omega)}}.$$

Algorithm 5 [Quasistatic Algorithm]

Let

$$\begin{aligned}
\mathbf{u}_E &= [u_{E1}, u_{E2}]^T, \ \ \mathbf{u}_V = [u_{V1}, u_{V2}]^T, \\
\mathbf{B} &= u_{E1}[C_1,\ C_2,\ \cdots,\ C_{N_\phi}]^T,\ \mathbf{C} = u_{E2}[C_1,\ C_2,\ \cdots,\ C_{N_\phi}]^T, \\
H &= 2 \quad \text{(the time step) and } TV(0) = A = 0, \\
\mathbf{Q} &= [\mathbf{QF}, \mathbf{QS}]^T, \ \ \mathbf{P} = [\mathbf{PF}, \mathbf{PS}]^T, \\
\mathbf{W} &= [\mathbf{WF}, \mathbf{WS}]^T, \\
\mathbf{QF} &= [QF_1,\ QF_2,\ \cdots,\ QF_{N_\phi}]^T,\ \mathbf{QS} = [QS_1,\ QS_2,\ \cdots,\ QS_{N_\phi}]^T, \\
\mathbf{PF} &= [PF_1,\ PF_2,\ \cdots,\ PF_{N_\phi}]^T,\ \mathbf{PS} = [PS_1,\ PS_2,\ \cdots,\ PS_{N_\phi}]^T, \\
\mathbf{WF} &= [WF_1\ WF_2\ \cdots,\ WF_{N_\phi}]^T,\ \mathbf{WS} = [WS_1,\ WS_2,\ \cdots,\ WS_{N_\phi}]^T.
\end{aligned}$$

Step 1 Solve

$$f(\lambda) := 1 - \sum_{j=1}^{N_\phi} \frac{C_j}{\lambda + \alpha_j} = 0 \tag{6.107}$$

to obtain the eigenvalues λ by the following procedure.

Step 1.1 Set $C_j = \alpha_j \phi_j$.

Step 1.2 Verify that a root is in the interval $(-\alpha_{i-1}, -\alpha_i)$ by considering the condition $f(-\alpha_{i-1})f(-\alpha_i) < 0$.

Step 1.3 Determine the initial value for solving (6.107) by using the bisection method (see Burden and Faires [5], Chapra [6] or Gerald and Wheatley [13]).

Step 1.4 Solve (6.107) by using the Newton method (see Burden and Faires [5], Chapra [6] or Gerald and Wheatley [13]).

Step 2 Calculate the eigenvectors

$$(v_j)_k = \frac{C_j}{\lambda_k - \beta_j}, \quad j,k = 1,\cdots,N_\phi$$

and set the matrix $\mathbf{X}$,

$$\begin{aligned}\mathbf{X} &= [\mathbf{v}_1, \mathbf{v}_2, \cdots, \mathbf{v}_{N_\phi}] \\ &= \begin{bmatrix} \frac{\alpha_1\phi_1}{\lambda_1+\alpha_1} & \cdots & \frac{\alpha_1\phi_1}{\lambda_{N_\phi}+\alpha_1} \\ \vdots & \ddots & \vdots \\ \frac{\alpha_{N_\phi}\phi_{N_\phi}}{\lambda_1+\alpha_{N_\phi}} & \cdots & \frac{\alpha_{N_\phi}\phi_{N_\phi}}{\lambda_{N_\phi}+\alpha_{N_\phi}} \end{bmatrix}.\end{aligned}$$

Step 3 For $I = 0$, STEP-1

Step 4 For NODE = 1, M

Step 5 Determine the vectors $\mathbf{PF}$ and $\mathbf{PS}$ by solving

$$\begin{aligned}\dot{P}F_j &= \lambda_j PF_j + QF_j, \\ PF_j(0) &= 0\end{aligned}$$

and

$$\begin{aligned}\dot{P}S_j &= \lambda_j PS_j + QS_j, \quad j = 1,\cdots,N_\phi, \\ PS_j(0) &= 0\end{aligned}$$

using following process.

Step 5.1 Set $T1 = TV(I)$
and extract $\begin{bmatrix} PF_j(T1) \\ PS_j(T1) \end{bmatrix}$ and $\begin{bmatrix} u_{E1}(T1) \\ u_{E2}(T1) \end{bmatrix}$ of node M at time $= T1$ which is corresponding node M at time $= (I+1)H$.

Step 5.1.1 Solve $\mathbf{XQF}(T1) = \mathbf{B}$ and $\mathbf{XQS}(T1) = \mathbf{C}$ for $\mathbf{QF}(T1)$ and $\mathbf{QS}(T1)$, respectively.

Step 5.1.2 Compute

$$\begin{aligned} FK1_j &= H\Big\{\lambda_j PF_j(T1) + QF_j(T1)\Big\} \\ SK1_j &= H\Big\{\lambda_j SF_j(T1) + QS_j(T1)\Big\}. \end{aligned}$$

Step 5.2 Set $T2 = TV(I) + 0.5H$
and extract $\begin{bmatrix} u_{E1}(T2) \\ u_{E2}(T2) \end{bmatrix}$ of node M at time $= T2$ which is corresponding node M at time $= (I+1)H$.

Step 5.2.1 Solve $\mathbf{XQF}(T2) = \mathbf{B}$ and $\mathbf{XQS}(T2) = \mathbf{C}$ for $\mathbf{QF}(T2)$ and $\mathbf{QS}(T2)$, respectively.

Step 5.2.2 Compute

$$\begin{aligned} FK2_j &= H\Big\{\lambda_j\Big(PF_j(T1) + \frac{FK1_j}{2}\Big) + QF_j(T2)\Big\} \\ SK2_j &= H\Big\{\lambda_j\Big(PS_j(T1) + \frac{SK1_j}{2}\Big) + QS_j(T2)\Big\} \\ FK3_j &= H\Big\{\lambda_j\Big(PF_j(T1) + \frac{FK2_j}{2}\Big) + QF_j(T2)\Big\} \\ SK3_j &= H\{\lambda_j\Big(PS_j(T1) + \frac{SK2_j}{2}\Big) + QS_j(T2)\Big\}. \end{aligned}$$

Step 5.3 Set $T3 = TV(I) + H$.

Step 5.3.1 Solve $\mathbf{XQF}(T3) = \mathbf{B}$ and $\mathbf{XQS}(T3) = \mathbf{C}$ for $\mathbf{QF}(T3)$ and $\mathbf{QS}(T3)$, respectively.

Step 5.3.2 Compute

$$\begin{aligned} FK4_j &= H\Big\{\lambda_j\Big(PF_j(T1) + FK3_j\Big) + QF_j(T3)\Big\} \\ SK4_j &= H\Big\{\lambda_j\Big(PS_j(T1) + SK3_j\Big) + QS_j(T3)\Big\} \\ PF_j(T3) &= PF_j(T1) + \frac{1}{6}\Big(FK1_j + 2FK2_j + 2FK3_j + FK4_j\Big) \\ PS_j(T3) &= PS_j(T1) + \frac{1}{6}\Big(SK1_j + 2SK2_j + 2SK3_j + SK4_j\Big). \end{aligned}$$

Step 6 Calculate

$$\begin{aligned} \mathbf{WF}(T3) &= \mathbf{XPF}(T3) \\ \mathbf{WS}(T3) &= \mathbf{XPS}(T3). \end{aligned}$$

Step 7 Calculate the quasistatic solutions

$$\begin{aligned} u_{V1}(T3) &= u_{E1}(T3) + \sum_{j=1}^{N_\phi} WF_j(T3) \\ u_{V2}(T3) &= u_{E2}(T3) + \sum_{j=1}^{N_\phi} WS_j(T3). \end{aligned}$$

End For NODE

Step 8 Set $TV(I+1) = A + (I+1)H$

End For I

6.3.2 The Fully Discrete Algorithm

As detailed in section 6.2, now we defined the algorithms 6-8 to calculate the fully discrete formulation.

Algorithm 6 [Main Fully Discrete Algorithm]

Given: (i) the percentage of relative error,

(ii) a matrix **D** see Algorithm 1,

(iii) $H = 2$ (the time step).

Task: find the quasistatic solution form {(6.98),(6.105)}.

Step 1 For TIME = 0 , T

Step 2 At TIME = 0,

solve the problem of linear elasticity as given in Algorithm 1

Step 3 At TIME = t_1

Step 3.1 Set $h_1 = t_1$.

Step 3.2 Evaluate $\mathbf{K}_g$ and $\mathbf{F}_g$ in Algorithm 7 by solving the linear system

$$\mathbf{K}_g \mathbf{U}(t_1) = \mathbf{F}_g(t_1)$$

for $\mathbf{U}(t_1)$.

Step 3.3 Calculate $\mathbf{r}_j(t_1)$ in Algorithm 8.

Step 4 At TIME $= t_i > t_1$, $i = 2, 3, \ldots, N$,

Step 4.1 Set $h_i = t_i - t_{i-1}$.

Step 4.2 Evaluate $\mathbf{K}_g$ and $\mathbf{F}_g$ in Algorithm 7 and solve the linear system

$$\mathbf{K}_g \mathbf{U}(t_i) = \mathbf{F}_g(t_i)$$

for $\mathbf{U}(t_i)$.

Step 4.3 Calculate $\mathbf{r}_j(t_i)$ in Algorithm 8.

End For TIME

Algorithm 7 [Fully Discrete Element Algorithm]

For K = 1, NE

Step 1 Determine the matrix $\widehat{\mathbf{K}}$ and the vector $\widehat{\mathbf{F}}$ at each element in Algorithm 2.

Step 2 At TIME $= t_1$

Step 2.1 Extract $\mathbf{U}(0)$ and set $h_1 = t_1$.

Step 2.2 Determine

$$\widetilde{\mathbf{F}}^*(t_1) = \widehat{\mathbf{F}}(t_1) + \widehat{\mathbf{K}} \frac{h_1}{2} \sum_{j=1}^{N_\phi} \alpha_j \phi_j e^{-\alpha_j t_1} \mathbf{U}(0).$$

Step 3 At TIME $= t_i > t_1 \quad i = 2, 3, \cdots, N$,

Step 3.1 Extract $\mathbf{U}(t_{i-1})$, $\mathbf{r}_j(t_{i-1})$, $j = 1, 2, \cdots, N_\phi$ and set $h_i = t_i - t_{i-1}$.

Step 3.2 Determine

$$\widetilde{\mathbf{F}}^*(t_i) = \widehat{\mathbf{F}}(t_i) + \widehat{\mathbf{K}} \sum_{j=1}^{N_\phi} \alpha_j \phi_j e^{-\alpha_j (t_i - t_{i-1})} \Big[\mathbf{r}_j(t_{i-1}) + \frac{h_i}{2} \alpha_j \phi_j \mathbf{U}(t_{i-1}) \Big].$$

Step 4 Determine

$$\widetilde{\mathbf{K}}^* = \widehat{\mathbf{K}} \Big(1 - \frac{h_i}{2} \sum_{j=1}^{N_\phi} \alpha_j \phi_j \Big).$$

Step 5 Apply the boundary condition to each element.

Step 6 Assemble $\widetilde{\mathbf{K}}^*$ to form the matrix $\mathbf{K}_g$.

Step 7 Assemble $\widetilde{\mathbf{F}}^*$ to form the vector $\mathbf{F}_g$.

End For K

Algorithm 8 [$\mathbf{r}_j$ **Algorithm**]

For NODE = 1, M

Step 1 At TIME = t_1

Step 1.1 Extract $\mathbf{U}(0)$ and $\mathbf{U}(t_1)$.

Step 1.2 Compute

$$\mathbf{r}_j(t_1) = \frac{t_1}{2}\Big(\alpha_j\phi_j\Big[e^{-\alpha_j t_1}\mathbf{U}(0) + \mathbf{U}(t_1)\Big]\Big), \quad j = 1, 2, \cdots, N_\phi.$$

Step 2 At TIME = $t_i > t_1, \quad i = 2, 3, , \cdots, N,$

Step 2.1 Extract $\mathbf{U}(t_i)$, $\mathbf{U}(t_{i-1})$ and $\mathbf{r}_j(t_{i-1})$.

Step 2.2 Compute

$$\begin{aligned}\mathbf{r}_j(t_i) &= e^{-\alpha_j(t_i - t_{i-1})}\mathbf{r}_j(t_{i-1}) \\ &+ \frac{h_i}{2}\alpha_j\phi_j\Big[e^{-\alpha_j(t_i-t_{i-1})}\mathbf{U}(t_{i-1}) + \mathbf{U}(t_i)\Big], \quad j = 1, 2, \cdots, N_\phi.\end{aligned}$$

End For NODE

Chapter 7

Numerical Experiments

7.1 Introduction

In the previous chapter we proposed the *fully discrete formulation* and the *ODE formulation* consisting of ODE's for the time and an elasticity problem in space for treating problems of linear viscoelasticity. The aim of the present chapter is to illustrate the performance of the algorithms of the numerical formulations by computing the approximate solutions to two model "spike problems" for which the exact solutions(displacements) are known. The spike problems are so constructed that in certain zones of the region the exact solution has very high gradients. It is felt that such problems provide significant challenges for the numerical schemes that have been proposed. The effectiveness of each formulation is analysed by considering the percentage relative errors in terms of the discrete L_∞ norm, the L_2 norm and the energy norm. As the solution $\mathbf{u}$ of each problem is known, we are able to calculate these error norms which are defined as follows:

$$
\begin{aligned}
\|\mathbf{v}\|_{L_\infty(\Omega)} &= \max\{|\mathbf{v}(\mathbf{x}_i)| : \ \mathbf{x}_1, \mathbf{x}_2, \cdots, \mathbf{x}_M \text{ are the nodes of the mesh}\}, \\
\|\mathbf{v}\|^2_{L_2(\Omega)} &= \sum_{i=1}^{NE} \int_{\Omega_i} \mathbf{v}^T\mathbf{v} \ \mathrm{d}\Omega_i := \sum_{i=1}^{NE} \|\mathbf{v}\|^2_{L_2(\Omega_i)}, \\
\|\mathbf{v}\|^2_{E(\Omega)} &= \sum_{i=1}^{NE} \int_{\Omega_i} \boldsymbol{\epsilon}(\mathbf{v})^T\mathbf{D}\boldsymbol{\epsilon}(\mathbf{v}) \ \mathrm{d}\Omega_i := \sum_{i=1}^{NE} \|\mathbf{v}\|^2_{E(\Omega_i)}.
\end{aligned}
$$

The L_∞, L_2 and energy norms of the % relative errors in the displacement will be denoted by $\% R_{L_\infty}$, $\% R_{L_2}$ and $\% R_{en}$ where, respectively,

$$\% R_{L_\infty} := \frac{\|\mathbf{u}-\mathbf{u}_h\|_{L_\infty(\Omega)}}{\|\mathbf{u}\|_{L_\infty(\Omega)}} \times 100, \tag{7.1}$$

$$\% R_{L_2} := \frac{||\mathbf{u} - \mathbf{u}_h||_{L_2(\Omega)}}{||\mathbf{u}||_{L_2(\Omega)}} \times 100, \tag{7.2}$$

$$\% R_{en} := \frac{||\mathbf{u} - \mathbf{u}_h||_{E(\Omega)}}{||\mathbf{u}||_{E(\Omega)}} \times 100, \tag{7.3}$$

where $\mathbf{u}$ and $\mathbf{u}_h$ denote respectively the exact and approximate displacements.

7.2 The spike problem

We now construct our linear viscoelastic problems for which the displacements will be known. In order to do this we let the domains be the square

$$\Omega := \{x, y \in \mathbb{R} \mid 0 \leq x \leq 2, 0 \leq y \leq 2\}.$$

Each problem is cast in the domain Ω with $\mathbf{u} = \mathbf{0}$ on the boundary $\partial\Omega$ and it is assumed that the exact displacements have the form,

$$\mathbf{u}(\mathbf{x}, t) = \begin{bmatrix} u_1(\mathbf{x}, t) \\ u_2(\mathbf{x}, t) \end{bmatrix} = \begin{bmatrix} 0.25 \exp(-110[(x - x_0)^2 + (y - y_0)^2]) \\ 0.25 \exp(-110[(x - x_0)^2 + (y - y_0)^2]) \end{bmatrix}, \tag{7.4}$$

where $\mathbf{x} = [x, y]^T \in \Omega$ and (x_0, y_0) is the centre point of the spike domain. Starting with (7.4) the two spike problems are constructed as follows.

Example 1 The centre point (x_0, y_0) of the spike domain moves along line $x = y$ as time t increases and we define

$$x_0(t) = 0.35 + t, \quad 0 \leq t \leq 1, \tag{7.5}$$

$$y_0(t) = 0.35 + t, \quad 0 \leq t \leq 1. \tag{7.6}$$

Example 2 If the moving zone of the centre point of the spike problem is an ellipse, we define then the centre point as

$$x_0(t) = 1 + 0.6 \cos(2\pi t), \quad 0 \leq t \leq 1, \tag{7.7}$$

$$y_0(t) = 1 + 0.4 \sin(2\pi t), \quad 0 \leq t \leq 1. \tag{7.8}$$

Figures 7.1 and 7.2 illustrate one component of the displacement $\mathbf{u}$ in (7.4) at time $t = 1$ where the centres of spikes are given by {(7.5),(7.6)} and {(7.7),(7.8)} respectively. These figures show the displacements in the z direction and also exhibit the spike profiles. It is seen from (7.4) and demonstrated in each figure that at the boundary $\partial\Omega$ the displacement, $\mathbf{u}$, is virtually zero. This will be taken as the boundary condition for both displacement components.

In order to define the problems associated with (7.4) in the two cases, we obtain the body force $\mathbf{f}$ in each case by substituting the displacements into the equilibrium equation (3.21). We also assume, in (6.5), that the stress relaxation function is

$$\phi(t) \;:=\; 0.25 + 0.25e^{-0.5t} + 0.25e^{-t} + 0.25e^{-1.5t}.$$

To treat the linear elasticity problems which arise, the material properties will be taken to be Young's modulus $E = 1$ and Poisson's ratio $\nu = 1/4$.

The following sections present the numerical results for the linear viscoelasticity problem using both the ODE and fully discrete formulations detailed in sections 6.1 and 6.2, respectively.

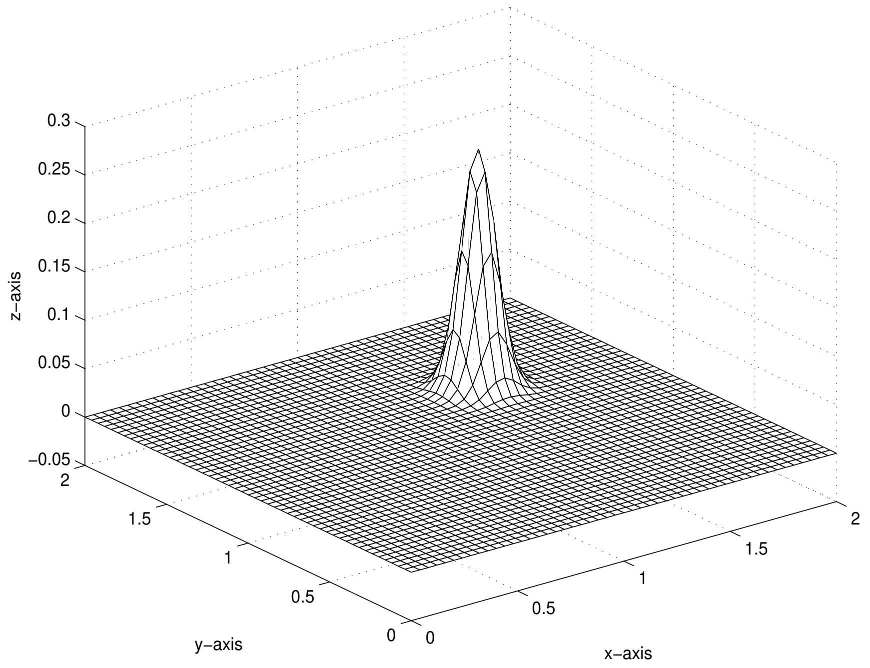

Figure 7.1: Example 1. The spike displacement, u_1, at $t = 1$.

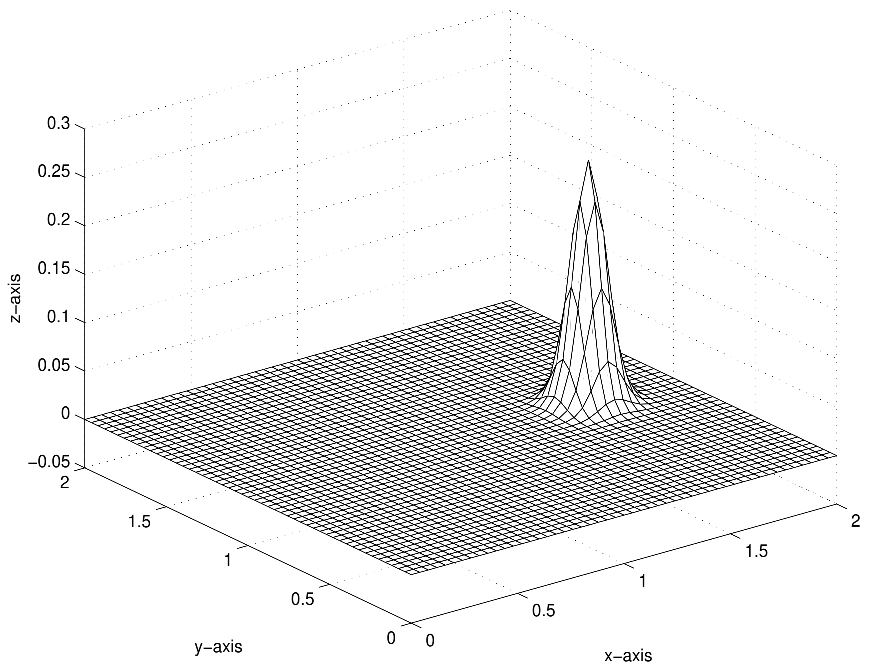

Figure 7.2: Example 2. The spike displacement, u_1 at $t = 1$.

7.3 Numerical results: Example 1

The numerical solutions of example 1 using the ODE formulation are reported first. As described in section 6.1 the ODE formulation is implemented by solving a linear elastic problem at each time step and then the elastic solutions are used as data in solving of ODEs for each point in the spatial mesh at which the viscoelastic displacements are required. The linear elasticity problem is solved by using the finite element method using a mesh consisting of triangular elements. As described in section 4.3 in order to get an optimal space mesh it is necessary to refine the mesh adaptively until a required percentage relative error tolerance condition is satisfied.

In these examples the percentage of relative error tolerance, measured in the energy norm, is set to 10%. Tables 7.1 (a)-(c) show the percentage errors in the numerical solutions of the linear elastic problem, which are reported as $\%\, R_{L_\infty}$, $\%\, R_{L_2}$, $\%\, R_{en}$, for various values of the time steps. It can be seen that, for each time level t, the relative errors are exactly the same throughout. This is due to the fact that the linear elastic problem is a spatial problem for which there is no temporal discretization error and all errors arise from the spatial discretization error. Furthermore, we got the optimal mesh at each time step because the $\%\, R_{en}$ is less than 5% as shown in Table 7.1 (c). This verifies that the finite element solutions are good approximations to the exact elastic solution given by (6.20). One component of the exact elastic solution u_{E1}, (6.20), at time $t = 1$ has a sharp feature as illustrated in Figure 7.3.

Table 7.1: The percentage relative error of linear elastic problem. The errors are generated by using the adaptive scheme and are measured in (a) L_∞ norm, (b) L_2 norm and (c) energy norm.

(a)

time, t	$\% R_{L_\infty}$ $\Delta t = 0.1$	$\Delta t = 0.05$	$\Delta t = 0.025$	$\Delta t = 0.0125$
0.0	0.4584	0.4584	0.4584	0.4584
0.2	0.5357	0.5357	0.5357	0.5357
0.4	0.6690	0.6690	0.6690	0.6690
0.6	0.7079	0.7079	0.7079	0.7079
0.8	0.7285	0.7285	0.7285	0.7285
1.0	0.6709	0.6709	0.6709	0.6709

(b)

time, t	$\% R_{L_2}$ $\Delta t = 0.1$	$\Delta t = 0.05$	$\Delta t = 0.025$	$\Delta t = 0.0125$
0.0	1.9498	1.9498	1.9498	1.9498
0.2	2.3934	2.3934	2.3934	2.3934
0.4	3.4379	3.4379	3.4379	3.4379
0.6	3.7872	3.7872	3.7872	3.7872
0.8	3.9097	3.9097	3.9097	3.9097
1.0	3.6421	3.6421	3.6421	3.6421

(c)

time, t	$\% R_{en}$ $\Delta t = 0.1$	$\Delta t = 0.05$	$\Delta t = 0.025$	$\Delta t = 0.0125$
0.0	4.3730	4.3730	4.3730	4.3730
0.2	4.3480	4.3480	4.3480	4.3480
0.4	4.3690	4.3690	4.3690	4.3690
0.6	4.4348	4.4348	4.4348	4.4348
0.8	4.4123	4.4123	4.4123	4.4123
1.0	4.3260	4.3260	4.3260	4.3260

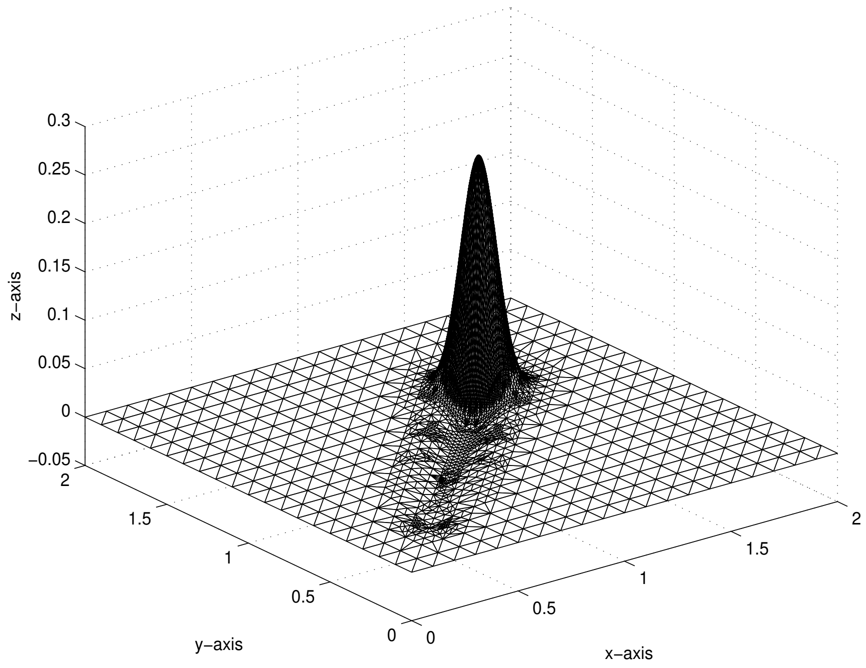

Figure 7.3: The exact elastic displacement, u_{E1}, at $t = 1$.

Figures 7.4-7.9 (a)-(b) demonstrate the adapted mesh and one component of the finite element elastic solution u_{Eh} at times t = 0, 0.2, 0.4, 0.6, 0.8 and 1.0, respectively. Figures 7.4-7.9 (b) track the movement of the spike with time and indicate that considerable refinement occurs in the region in which the displacements are changing rapidly. Comparing Figure 7.9 (b) with Figure 7.3, it can be seen that the finite element elastic solutions are good approximation to the exact elastic solutions.

(a)

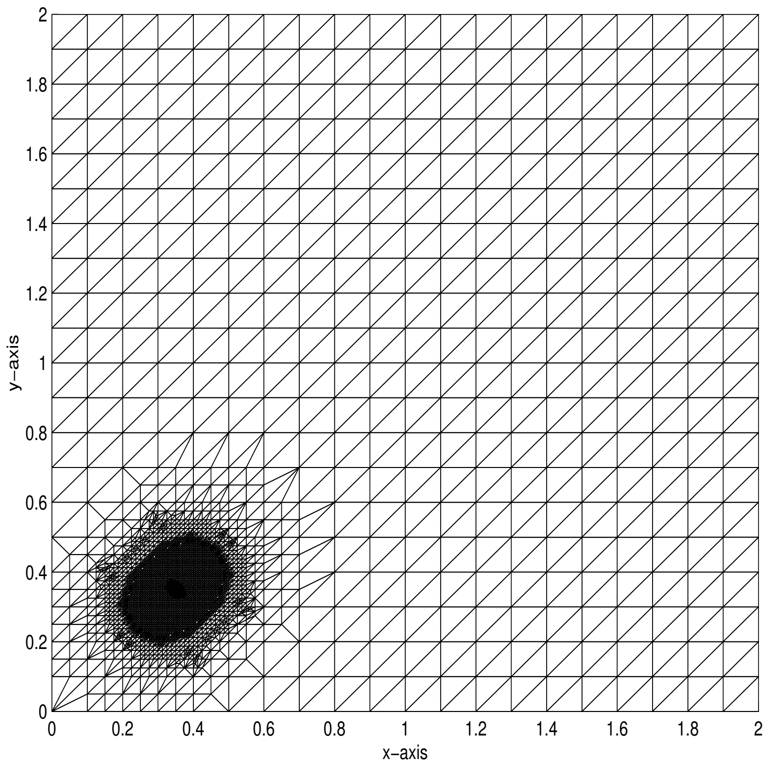

(b)

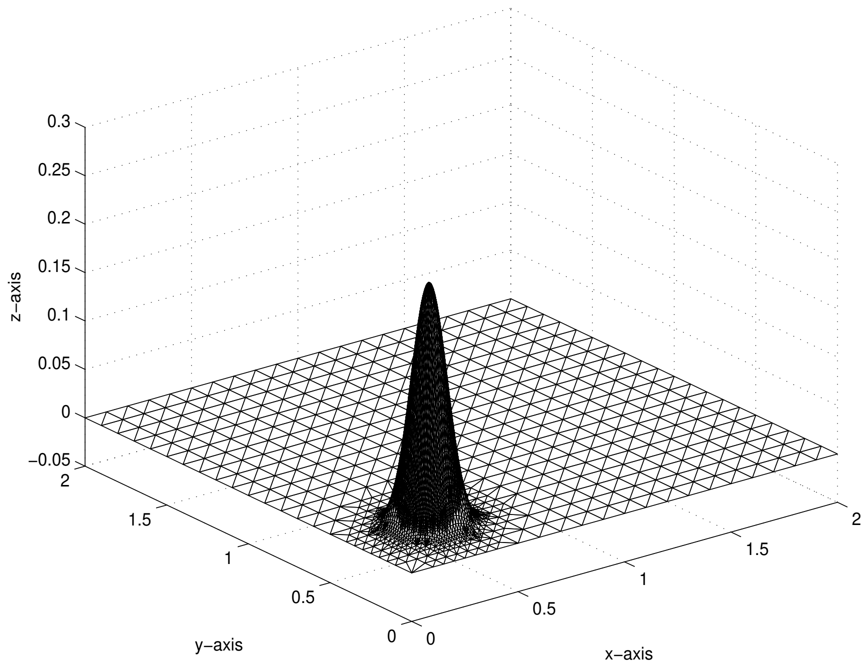

Figure 7.4: At time $t = 0$, (a) the adapted meshes and (b) the finite element solution u_{Eh1}.

(a)

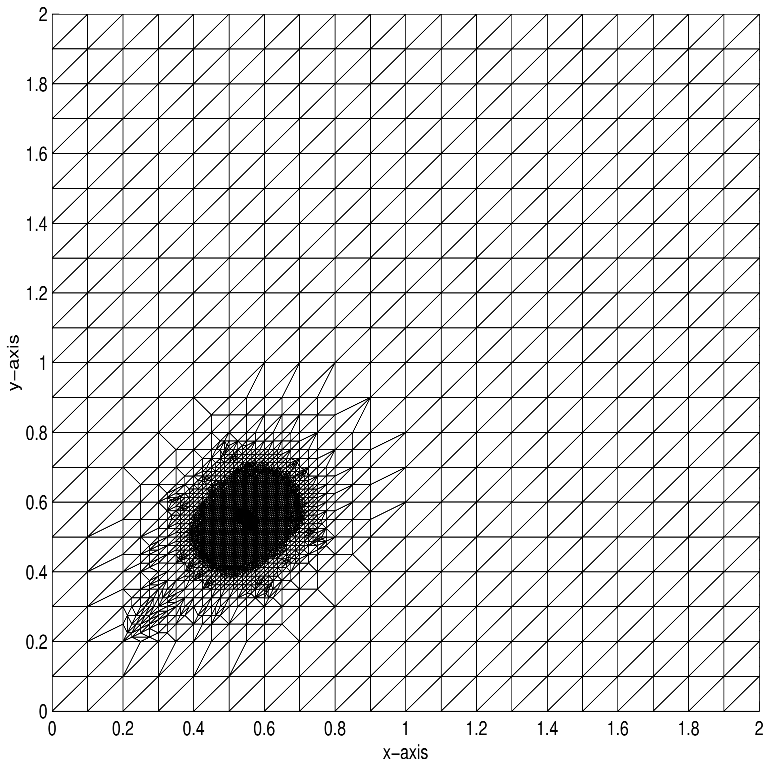

(b)

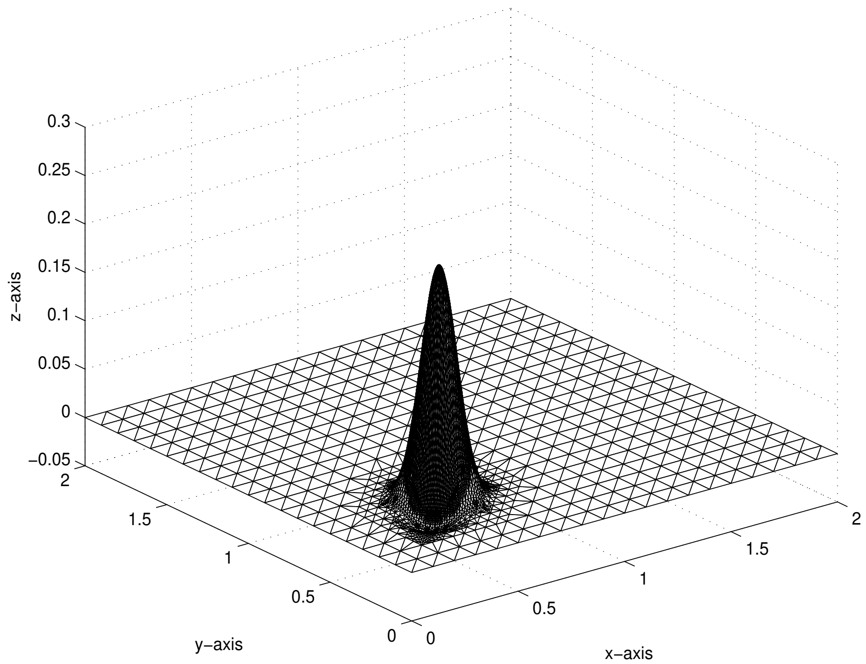

Figure 7.5: At time $t = 0.2$, (a) the adapted meshes and (b) the finite element solution u_{Eh1}.

(a)

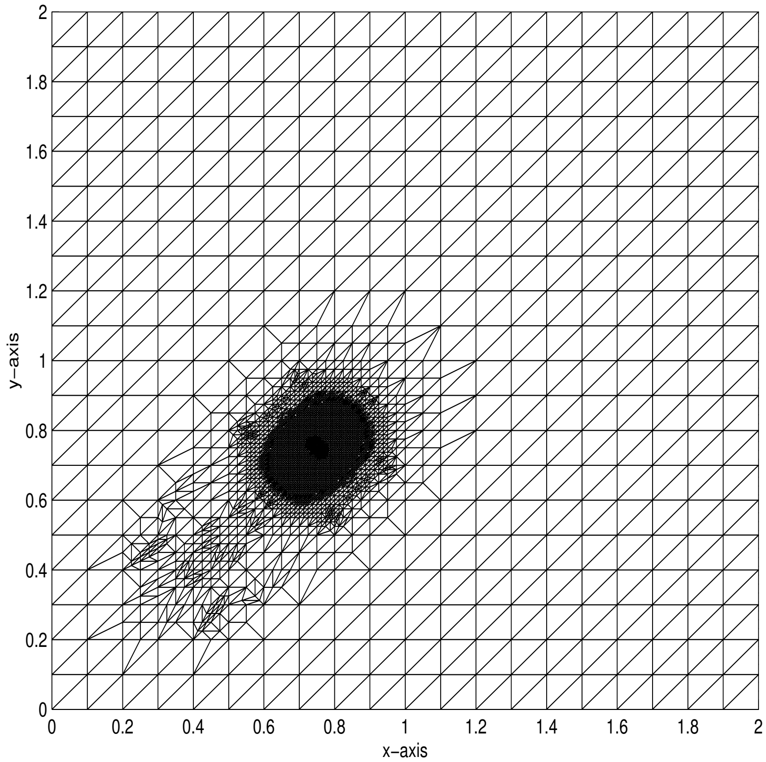

(b)

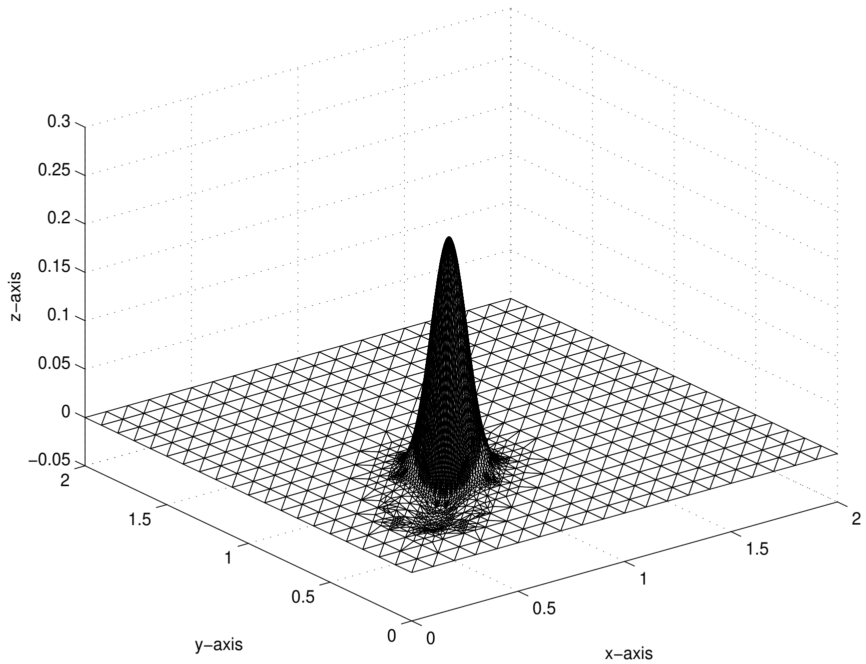

Figure 7.6: At time $t = 0.4$, (a) the adapted meshes and (b) the finite element solution u_{Eh1}.

(a)

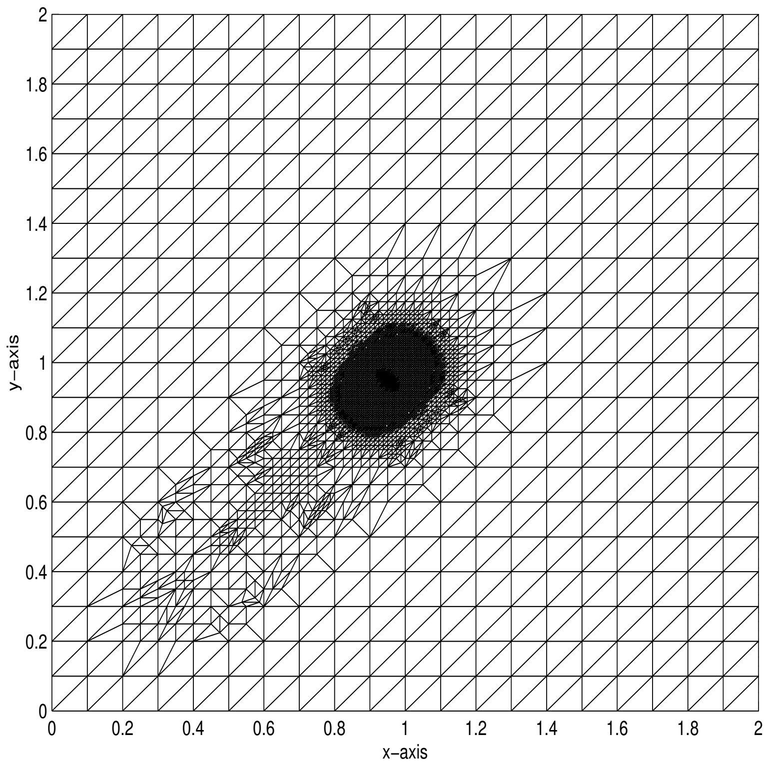

(b)

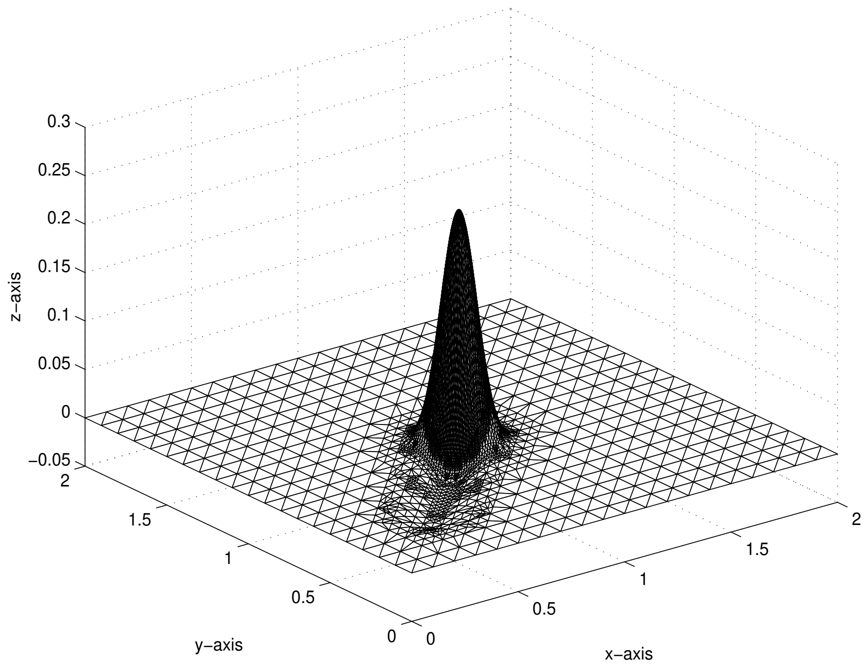

Figure 7.7: At time $t = 0.6$, (a) the adapted meshes and (b) the finite element solution u_{Eh1}.

(a)

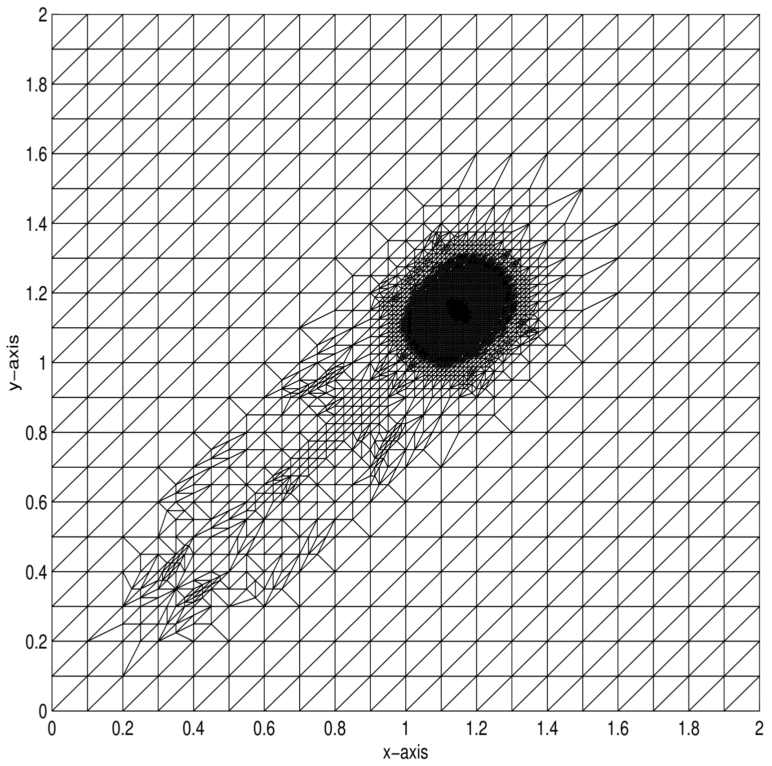

(b)

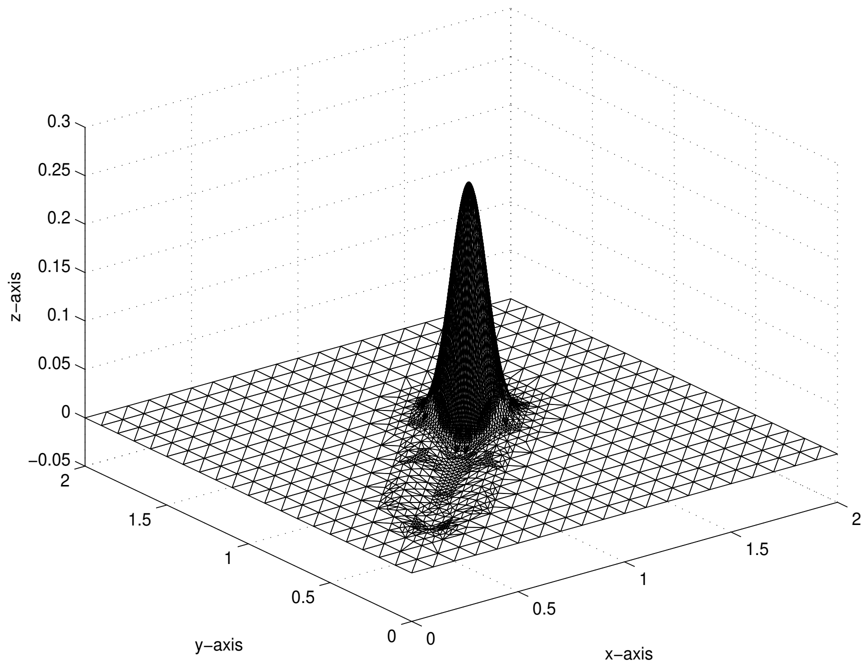

Figure 7.8: At time $t = 0.8$, (a) the adapted meshes and (b) the finite element solution u_{Eh1}.

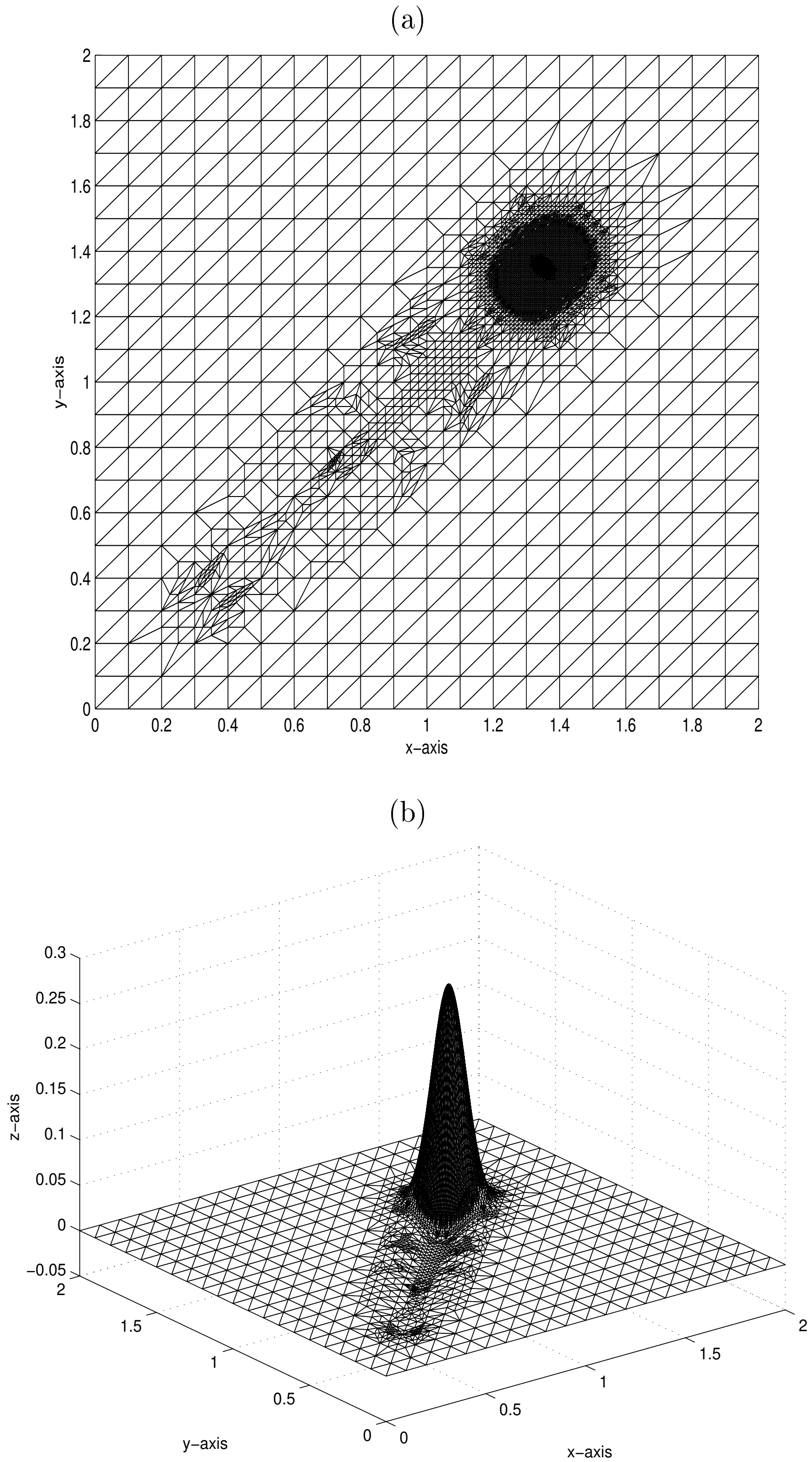

Figure 7.9: At time $t = 1$, (a) the adapted meshes and (b) the finite element solution u_{Eh1}.

Since the ODE formulation requires the elastic solution, the results of the ODE formulation using both the exact elastic and finite element elastic solutions are presented, in Tables 7.2 (a)-(c), in order to analyse separately temporal and spatial-temporal discretization errors with $\Delta t = 0.1$, 0.05, 0.025, 0.0125. For each time t, the $\%\, R_{L_\infty}$ using the exact elastic solution declines dramatically as the time step is decreased (see Table 7.2 (a)). This is because the $\% R_{L_\infty}$ values involve exact nodal displacement values and the decline in the errors is consistent with the $\mathcal{O}(\Delta t)^5$ error of the fourth-order Runge Kutta scheme. In contrast $\%\, R_{L_2}$ and $\%\, R_{en}$ do not decrease so rapidly as Δt decreases because the computation of the L_2 and energy norms involves integration over each element and this always involves a spatial discretization error. This means that, for small time steps, the spatial error is more dominant than the temporal error, while the temporal error dominates for large time steps.

The spike problem is then solved by using the fully discrete formulation given by (6.98) and (6.105) to compare with that of the ODE formulation. The meshes used at each time level are the same as those used in the ODE formulation. The $\%\, R_{L_\infty}$, $\%\, R_{L_2}$ and $\%\, R_{en}$ of the ODE and the fully discrete formulations are reported and are compared in Tables 7.3 (a)-(c). These show how the percentage relative errors change with varying the values of the time step. It can be seen from the Tables that as the value of the time step is decreased until $\Delta t = 0.025$, the percentage relative errors of both formulations are quite similar.

Table 7.2: Viscoelastic solutions: the percentage relative error generated by solving the ODE formulation with finite element and exact elastic solutions, respectively. The errors are measured in (a) L_∞ norm, (b) L_2 norm and (c) energy norm.

(a)

time,	$\% R_{L_\infty}$							
	Using finite element solution				Using exact elastic solution			
	time step, Δt				time step, Δt			
t	0.1	0.05	0.025	0.0125	0.1	0.05	0.025	0.0125
0.0	0.4584	0.4584	0.4584	0.4584	0.4584	0.4584	0.4584	0.4584
0.2	2.2552	0.5794	0.5735	0.5720	1.8359	0.0954	0.0024	0.0001
0.4	2.6524	0.7795	0.7608	0.7581	1.9435	0.0969	0.0024	0.0001
0.6	2.7584	0.8917	0.8603	0.8605	1.9435	0.0969	0.0024	0.0001
0.8	2.8369	0.9374	0.9275	0.9283	1.9435	0.0969	0.0024	0.0001
1.0	2.8023	0.9933	0.9877	0.9893	1.9435	0.0969	0.0024	0.0001

(b)

time,	$\% R_{L_2}$							
	Using finite element solution				Using exact elastic solution			
	time step, Δt				time step, Δt			
t	0.1	0.05	0.025	0.0125	0.1	0.05	0.025	0.0125
0.0	1.9498	1.9498	1.9498	1.9498	1.9498	1.9498	1.9498	1.9498
0.2	2.8443	2.1889	2.1962	2.1912	1.7844	0.2133	0.1794	0.1792
0.4	4.3190	3.4779	3.4979	3.4739	2.5386	0.2168	0.1792	0.1792
0.6	4.8681	4.0695	4.0986	4.0876	2.7506	0.2152	0.1815	0.1815
0.8	5.0703	4.3146	4.3393	4.3424	2.7486	0.2120	0.1783	0.1783
1.0	4.7276	3.9250	3.9362	3.9344	2.7476	0.2069	0.1730	0.1730

(c)

time,	$\% R_{en}$							
	Using finite element solution				Using exact elastic solution			
	time step, Δt				time step, Δt			
t	0.1	0.05	0.025	0.0125	0.1	0.05	0.025	0.0125
0.0	4.3730	4.3730	4.3730	4.3730	4.3730	4.3730	4.3730	4.3730
0.2	5.8444	4.3126	4.3141	4.3180	5.8252	4.3409	4.3288	4.3288
0.4	6.9069	4.3694	4.3690	4.4001	6.8559	4.3256	4.3081	4.3081
0.6	7.0603	4.5166	4.5026	4.5265	7.0843	4.3412	4.3242	4.3242
0.8	7.0548	4.5212	4.5196	4.5567	7.0519	4.2901	4.2733	4.2733
1.0	6.9447	4.4662	4.4479	4.4584	7.0030	4.2108	4.1939	4.1939

Table 7.3: Errors in the viscoelastic solutions: the percentage relative error generated by the ODE and the fully discrete formulations. The errors are measured in (a) L_∞ norm, (b) L_2 norm and (c) energy norm.

(a)

time,	$\% R_{L_\infty}$							
	Using ODE formulation				Using fully discrete formulation			
	time step, Δt				time step, Δt			
t	0.1	0.05	0.025	0.0125	0.1	0.05	0.025	0.0125
0.0	0.4584	0.4584	0.4584	0.4584	0.4584	0.4584	0.4584	0.4584
0.2	2.2552	0.5794	0.5735	0.5720	6.2930	1.4756	0.7006	0.5814
0.4	2.6524	0.7795	0.7608	0.7581	6.2063	1.6754	0.8914	0.7527
0.6	2.7584	0.8917	0.8603	0.8605	6.3367	1.7353	0.9474	0.8490
0.8	2.8369	0.9374	0.9275	0.9283	6.4218	1.7264	0.9378	0.8985
1.0	2.8023	0.9933	0.9877	0.9893	6.2708	1.6123	0.9274	0.9475

(b)

time,	$\% R_{L_2}$							
	Using ODE formulation				Using fully discrete formulation			
	time step, Δt				time step, Δt			
t	0.1	0.05	0.025	0.0125	0.1	0.05	0.025	0.0125
0.0	1.9498	1.9498	1.9498	1.9498	1.9498	1.9498	1.9498	1.9498
0.2	2.8443	2.1889	2.1962	2.1912	7.8353	2.6033	2.1865	2.1785
0.4	4.3190	3.4779	3.4979	3.4739	9.5695	3.6175	3.4141	3.4134
0.6	4.8681	4.0695	4.0986	4.0876	10.0776	4.1420	3.9598	3.9575
0.8	5.0703	4.3146	4.3393	4.3424	10.1701	4.3199	4.1408	4.1379
1.0	4.7276	3.9250	3.9362	3.9344	10.0011	3.8977	3.7132	3.6908

(c)

time,	$\% R_{en}$							
	Using ODE formulation				Using fully discrete formulation			
	time step, Δt				time step, Δt			
t	0.1	0.05	0.025	0.0125	0.1	0.05	0.025	0.0125
0.0	4.3730	4.3730	4.3730	4.3730	4.3730	4.3730	4.3730	4.3730
0.2	5.8444	4.3126	4.3141	4.3180	11.7002	5.0628	4.3319	4.3149
0.4	6.9069	4.3694	4.3690	4.4001	16.4712	5.2098	4.3922	4.3945
0.6	7.0603	4.5166	4.5026	4.5265	17.4910	5.0097	4.5031	4.5133
0.8	7.0548	4.5212	4.5196	4.5567	17.5665	5.0647	4.5230	4.5427
1.0	6.9447	4.4662	4.4479	4.4584	17.5709	4.9605	4.4510	4.4403

Figures 7.10-7.12 give a visual comparison of the behaviour of the relative errors for the ODE and the fully discrete formulations by plotting the $\% \, R_{L_\infty}$, $\% \, R_{L_2}$ and $\% \, R_{en}$ against the time. In each case the dash line represents the fully discrete solution, whilst the solid line represents the ODE solution. It can be seen that the relative errors of both formulations are significantly different at $\Delta t = 0.1$ as depicted in Figures 7.10-7.12 (a). This is due to the fourth-order Runge Kutta is being used in the ODE formulation for solving the system of ODEs whilst the fully discrete formulation uses the trapezoidal rule for approximating the hereditary integral. As a result the effectiveness of ODE formulation is better than the fully discrete formulation for large time steps. The values of $\% \, R_{L_\infty}$, $\% \, R_{L_2}$ and $\% \, R_{en}$ for both formulations decline markedly when the time step is decreased. It is also observed that the relative errors (in the given norms) behave in a similar way for both formulations, see Figures 7.10-7.12 (a)-(d).

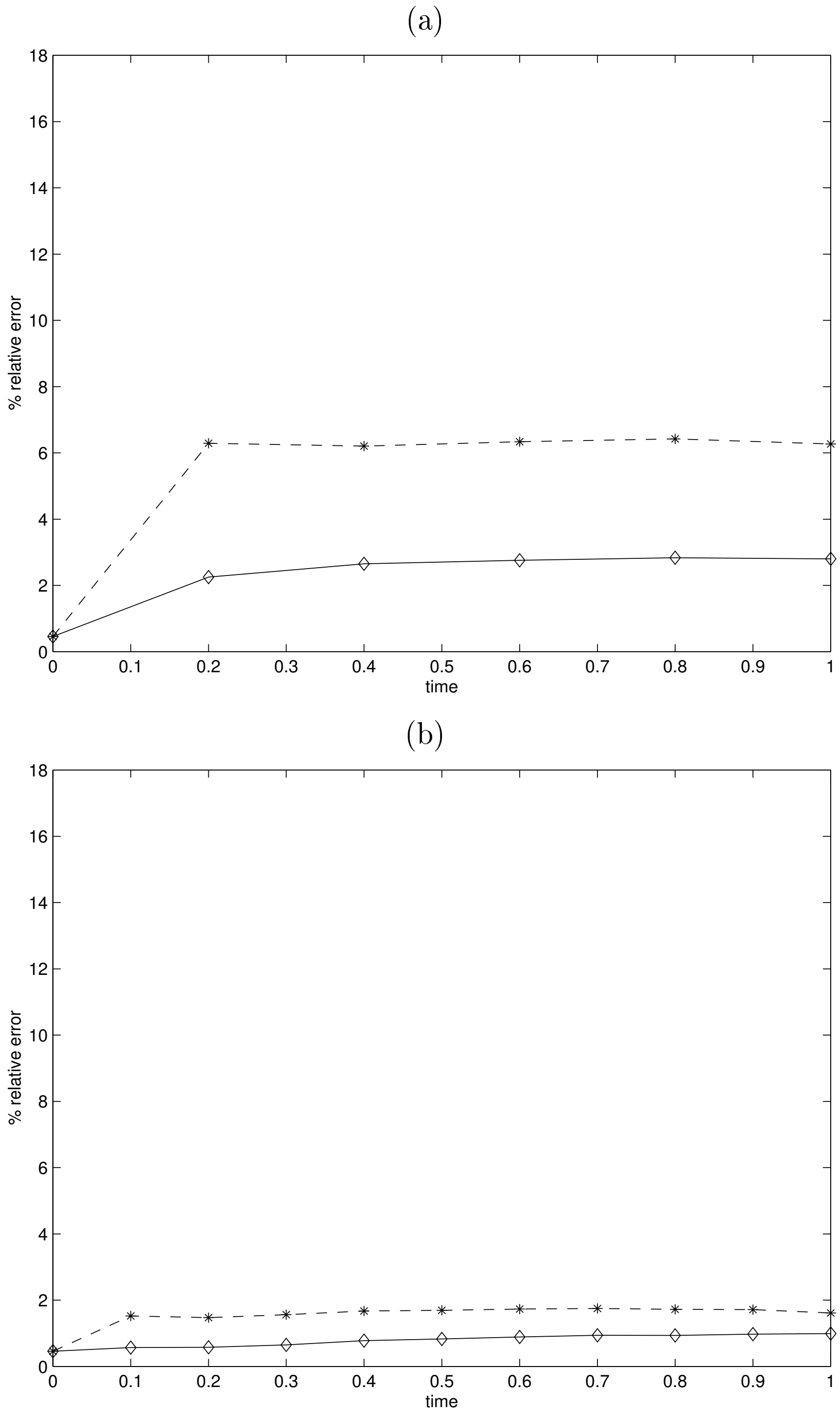

Figure 7.10

See caption on page 115

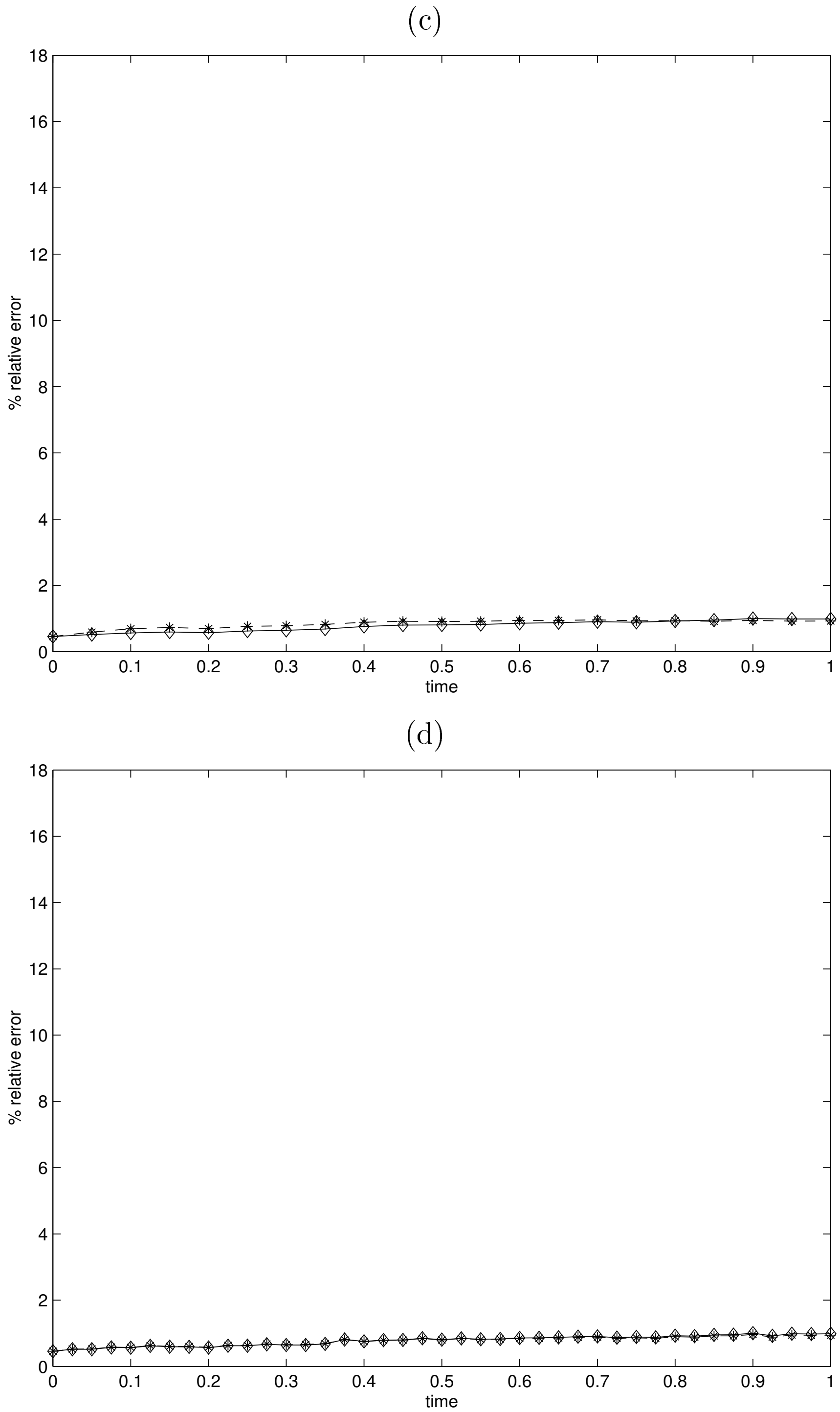

Figure 7.10: The evolution of the percentage relative error obtained using the ODE formulation(solid line marked with diamonds) and the fully discrete formulation (broken line marked with stars). The errors are measured in L_∞ norm and the time step is chosen to be (a) $\Delta t = 0.1$, (b) $\Delta t = 0.05$, (c) $\Delta t = 0.025$ and (d) $\Delta t = 0.0125$.

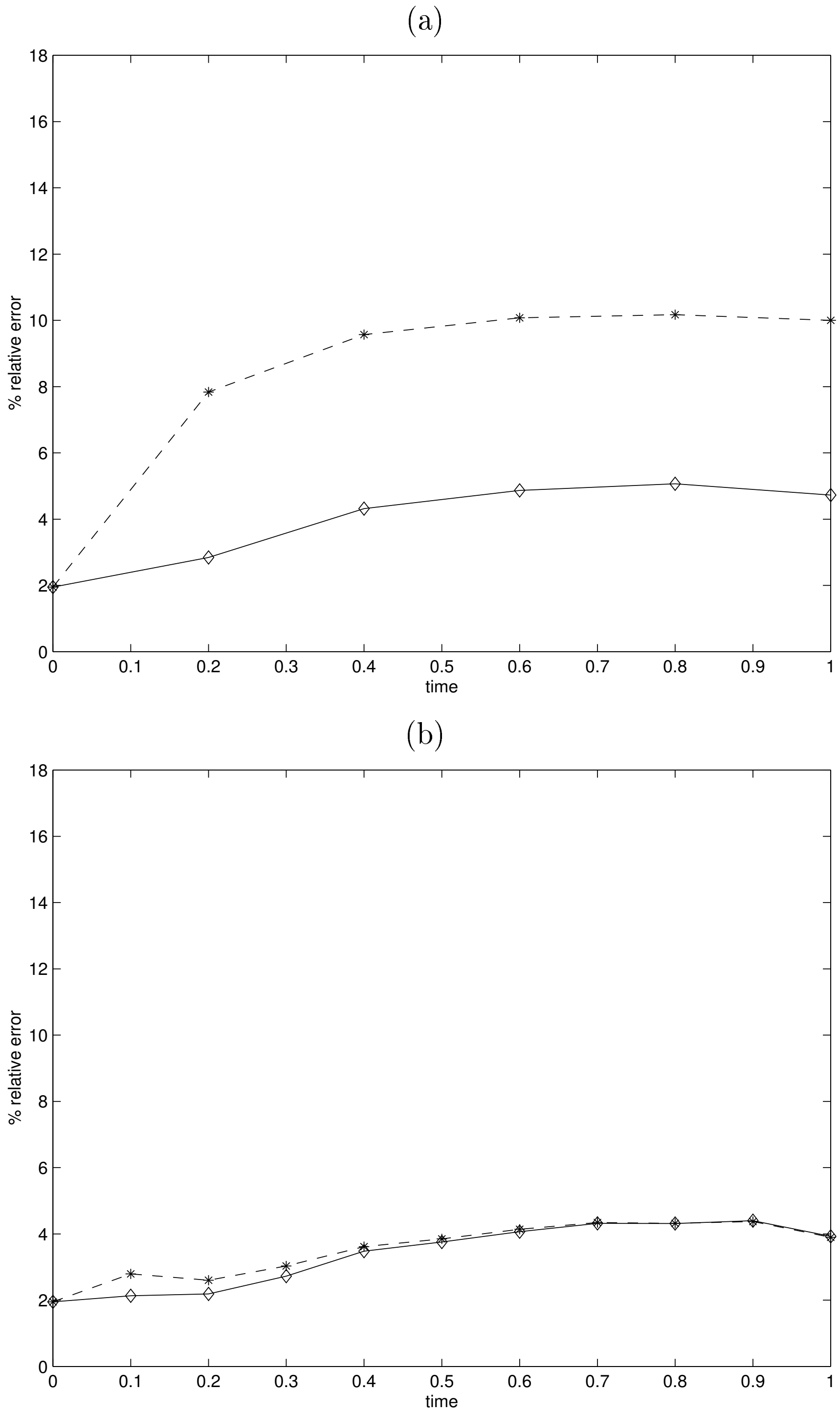

Figure 7.11

See caption on page 117

(c)

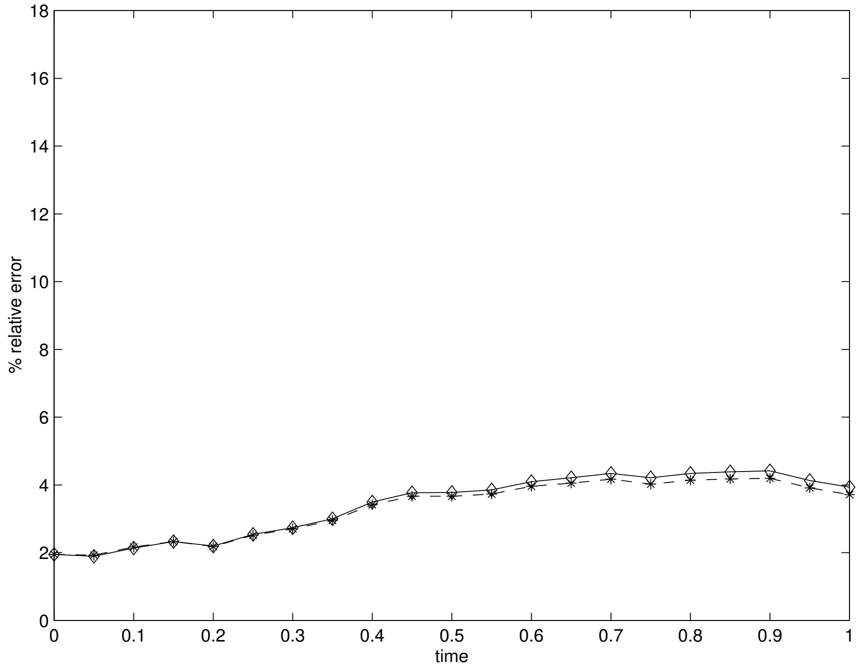

(d)

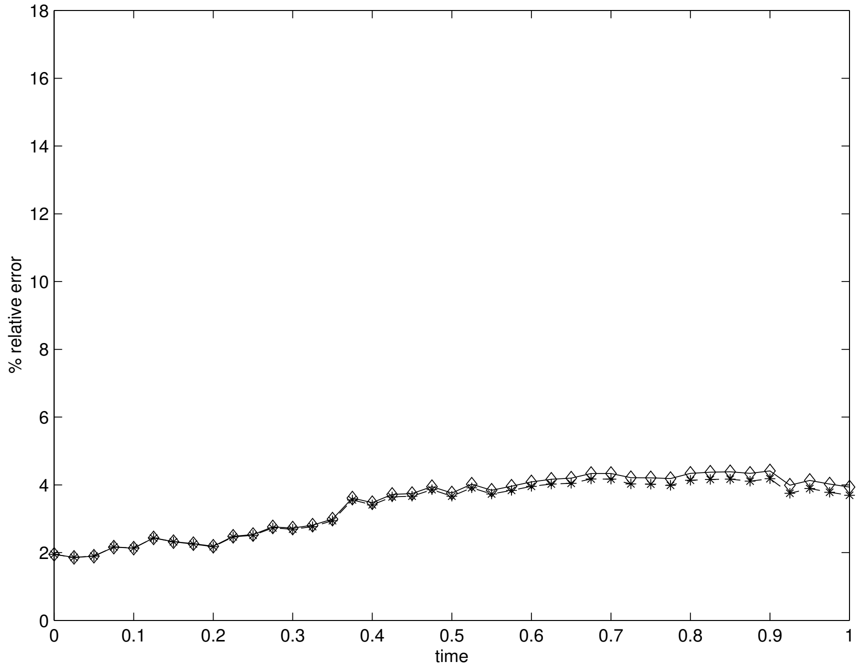

Figure 7.11: The evolution of the percentage relative error obtained using the ODE formulation(solid line marked with diamonds) and the fully discrete formulation (broken line marked with stars). The errors are measured in L_2 norm and the time step is chosen to be (a) $\Delta t = 0.1$, (b) $\Delta t = 0.05$, (c) $\Delta t = 0.025$ and (d) $\Delta t = 0.0125$.

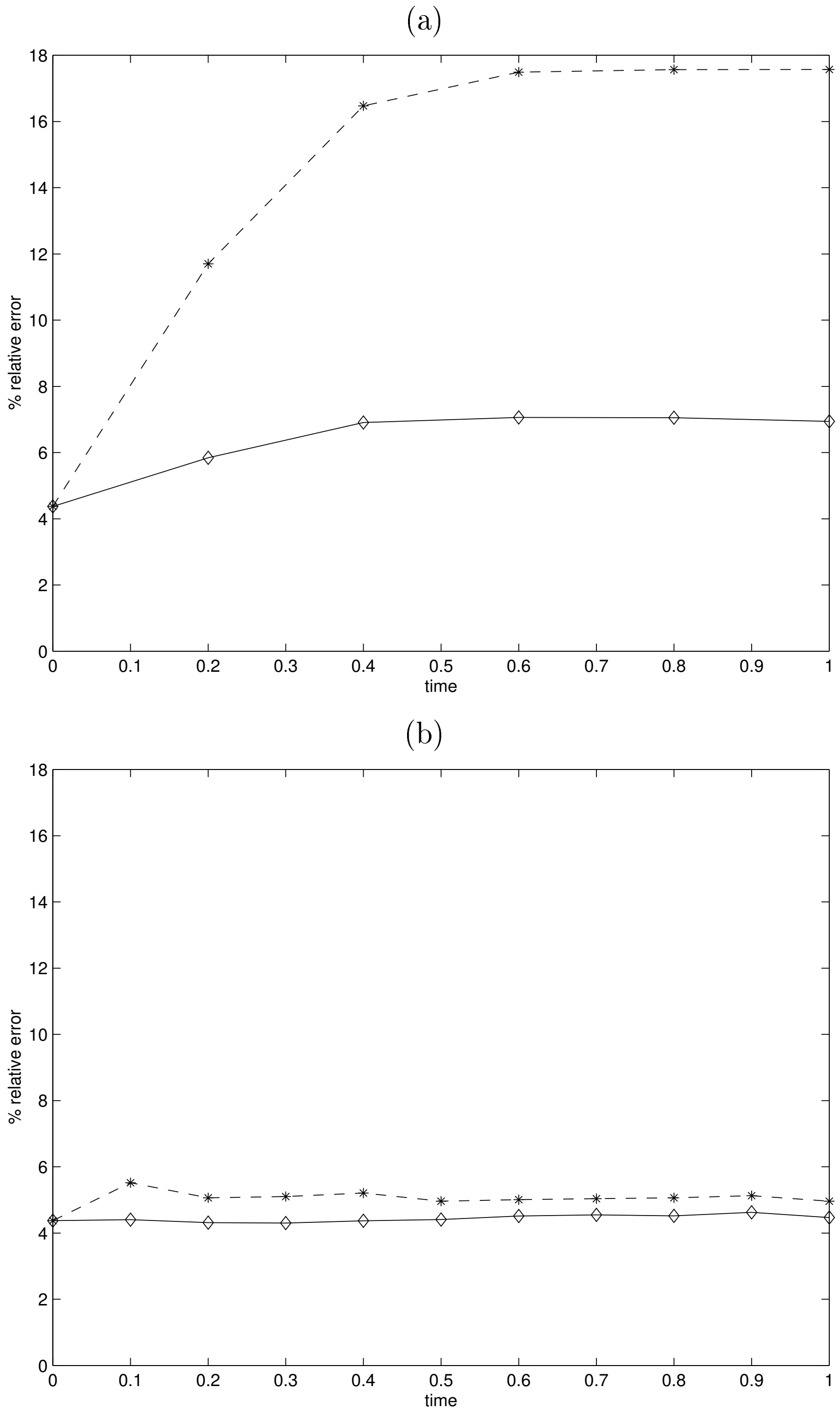

Figure 7.12

See caption on page 119

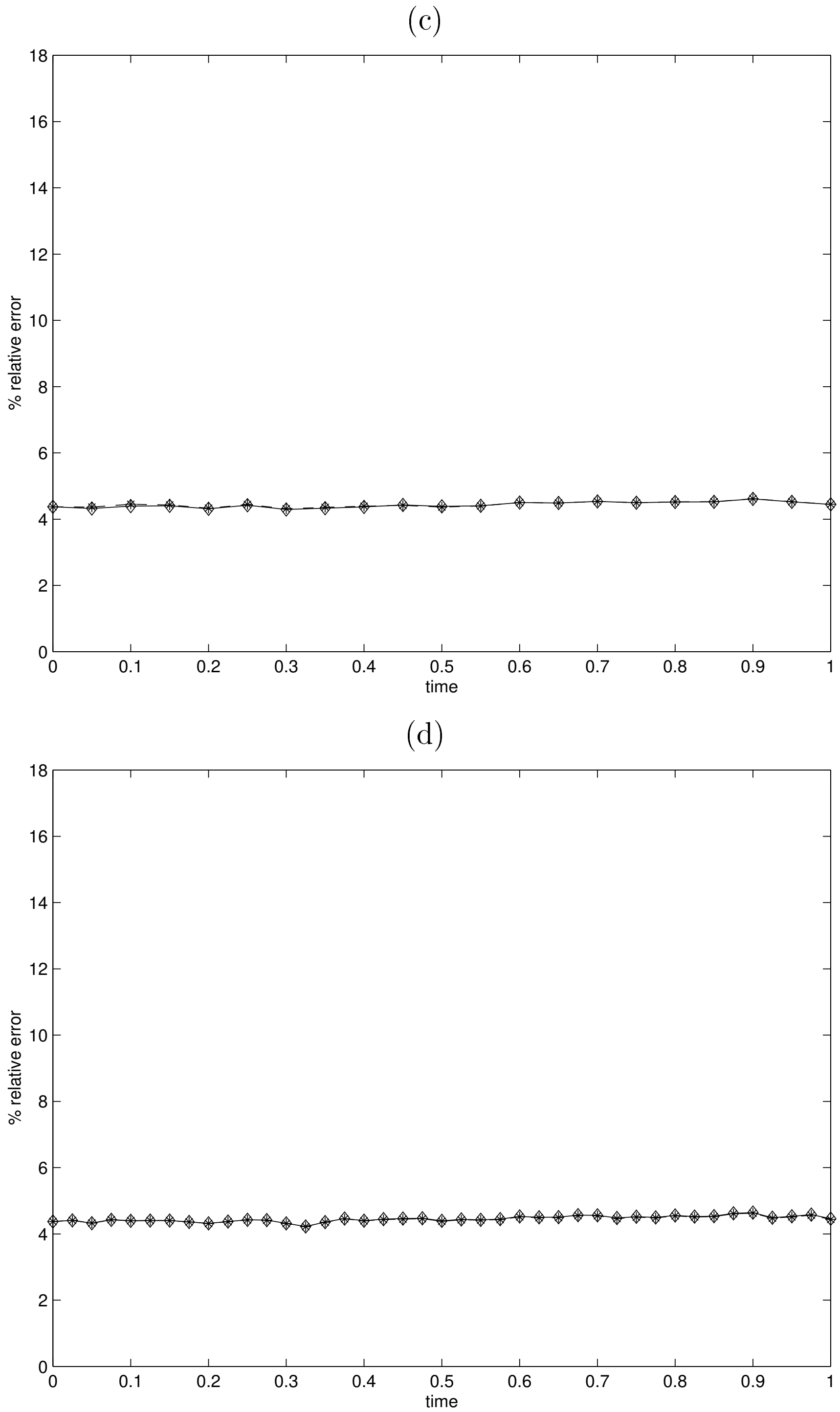

Figure 7.12: The evolution of the percentage relative error obtained using the ODE formulation(solid line marked with diamonds) and the fully discrete formulation (broken line marked with stars). The errors are measured in energy norm and the time step is chosen to be (a) $\Delta t = 0.1$, (b) $\Delta t = 0.05$, (c) $\Delta t = 0.025$ and (d) $\Delta t = 0.0125$.

7.4 Numerical results: Example 2

In this section we will consider the spike profile as it moves along the ellipse

$$\frac{(x_0-1)^2}{(0.6)^2}+\frac{(y_0-1)^2}{(0.4)^2}=1,$$

where 0.6 and 0.4 are the lengths of the major and minor axes. Apart from the different exact solution the details of the implementation are as in the previous example with the finite element solutions for the associated linear elastic problem being done using linear triangular elements. As described in section 7.3, the relative error measured in the energy norm for the elastic problem is set to 10% in order to ensure that optimal meshes are obtained. It is found that the relative error measured in the energy norm is less than 5% which confirms that the finite element solution is a sufficiently good approximation to the exact elastic solution. Tables 7.4 (a)-(c) show the errors in the finite element solution of the linear elastic problem for time step $\Delta t = 0.1,\ 0.05,\ 0.025$ and 0.0125. The results are presented to indicate the difficulties in solving the related elastic problems. The columns of each table are of course all the same as each elastic problem being solved just depends on the time t. It is only the approximate viscoelastic solution which is dependent on the time step Δt.

Table 7.4: The percentage relative error of linear elastic problem. The errors are generated by using the adaptive scheme and are measured in (a) L_∞ norm, (b) L_2 norm and (c) energy norm.

(a)

time, t	$\% R_{L_\infty}$			
	$\Delta t = 0.1$	$\Delta t = 0.05$	$\Delta t = 0.025$	$\Delta t = 0.0125$
0.0	0.5908	0.5908	0.5908	0.5908
0.2	0.6528	0.6528	0.6528	0.6528
0.4	0.6920	0.6920	0.6920	0.6920
0.6	0.6185	0.6185	0.6185	0.6185
0.8	0.5103	0.5103	0.5103	0.5103
1.0	0.3217	0.3217	0.3217	0.3217

(b)

time, t	$\% R_{L_2}$			
	$\Delta t = 0.1$	$\Delta t = 0.05$	$\Delta t = 0.025$	$\Delta t = 0.0125$
0.0	2.7872	2.7872	2.7872	2.7872
0.2	3.2515	3.2515	3.2515	3.2515
0.4	3.9016	3.9016	3.9016	3.9016
0.6	3.3344	3.3344	3.3344	3.3344
0.8	2.7260	2.7260	2.7260	2.7260
1.0	1.8127	1.8127	1.8127	1.8127

(c)

time, t	$\% R_{en}$			
	$\Delta t = 0.1$	$\Delta t = 0.05$	$\Delta t = 0.025$	$\Delta t = 0.0125$
0.0	4.3807	4.3807	4.3807	4.3807
0.2	4.3500	4.3500	4.3500	4.3500
0.4	4.3960	4.3960	4.3960	4.3960
0.6	4.3003	4.3003	4.3003	4.3003
0.8	4.1776	4.1776	4.1776	4.1776
1.0	4.1717	4.1717	4.1717	4.1717

Figures 7.13-7.18 (a)-(b) exhibit the corresponding adapted mesh and the finite element solutions of the linear elastic problem at times $t = 0$, 0.2, 0.4, 0.6, 0.8, and 1.0 respectively. These show the moving path of the spike profile and the mesh refinement that is obtained around the moving area, see Figures 7.13-7.18 (a). Figure 7.19 displays one component of the exact elastic solution u_{E1} at time $t = 1$. It can be seen that the finite element results are in good agreement with the exact elastic solution in which Figure 7.18 (b) is to be compared with Figure 7.19.

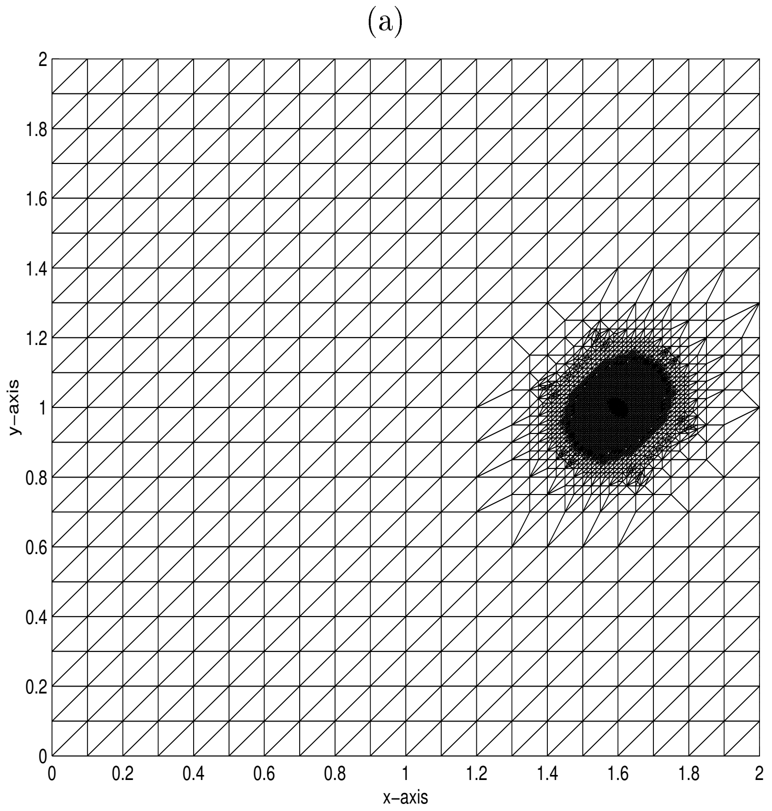

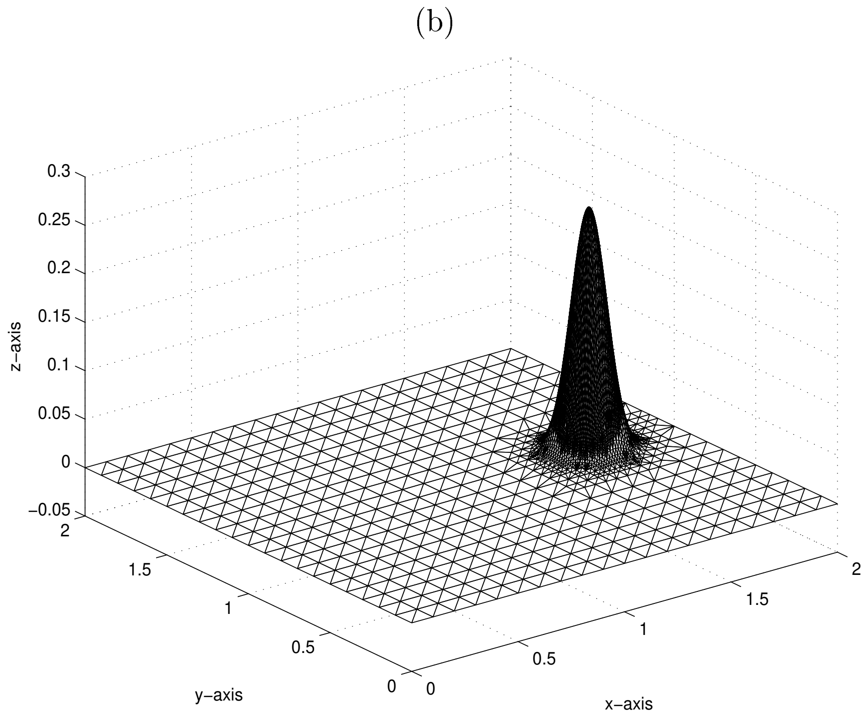

Figure 7.13: At time $t = 0$, (a) the adapted meshes and (b) the finite element solution u_{Eh1}.

(a)

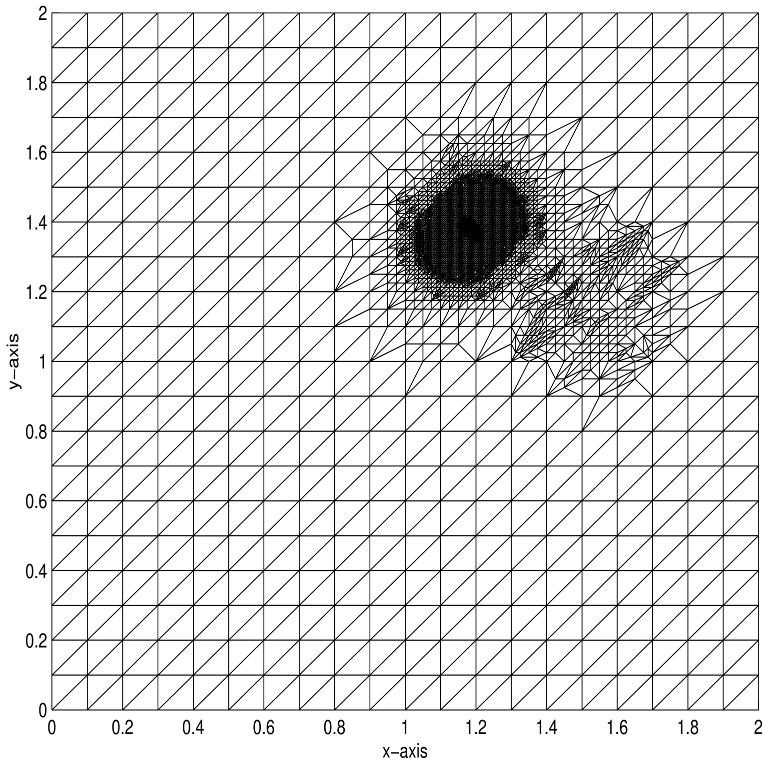

(b)

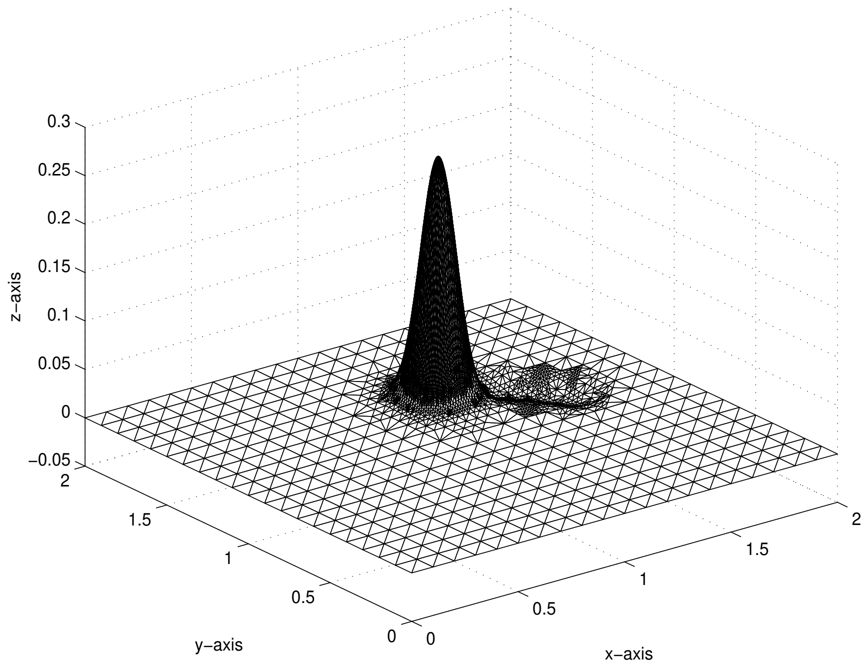

Figure 7.14: At time $t = 0.2$, (a) the adapted meshes and (b) the finite element solution u_{Eh1}.

(a)

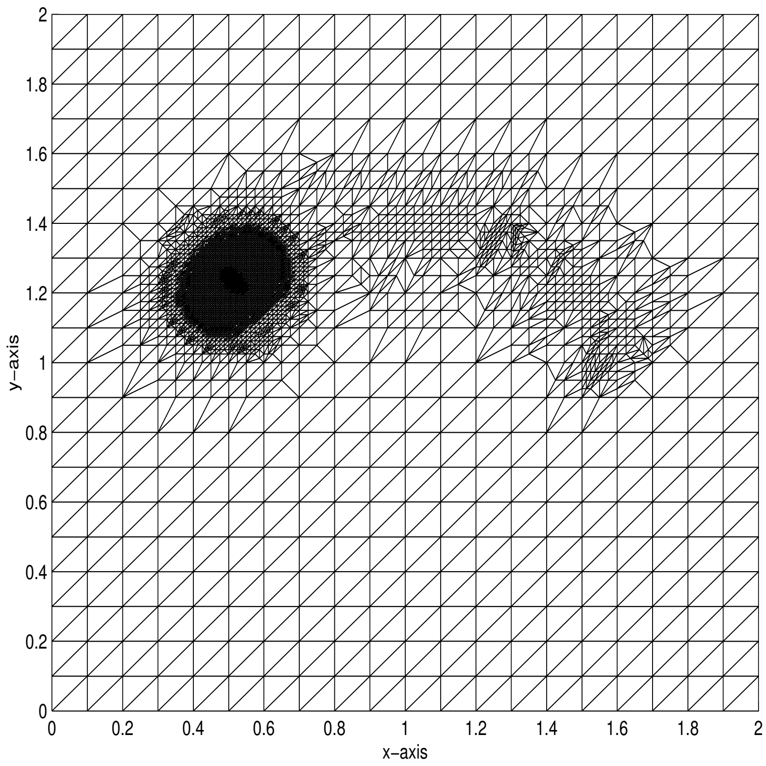

(b)

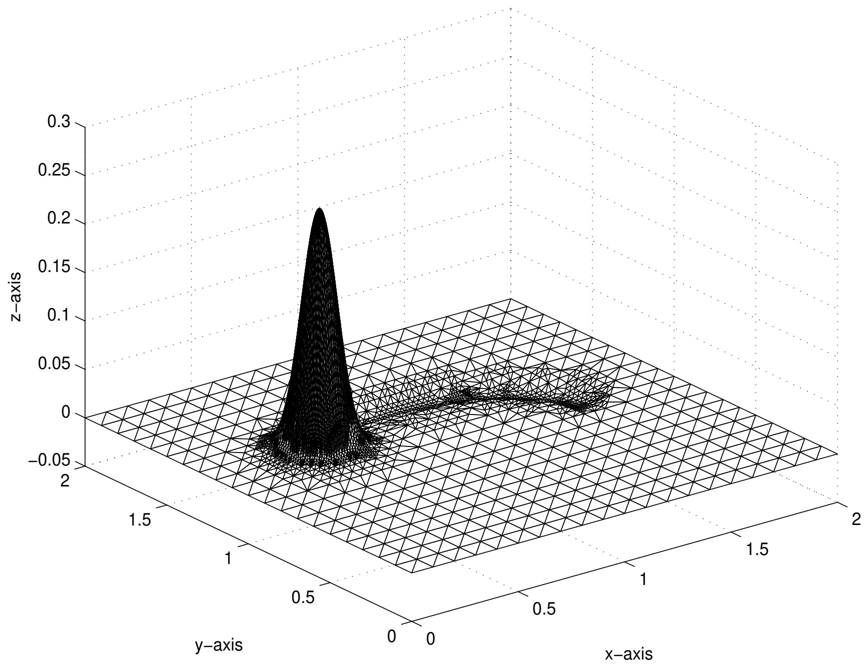

Figure 7.15: At time $t = 0.4$, (a) the adapted meshes and (b) the finite element solution u_{Eh1}.

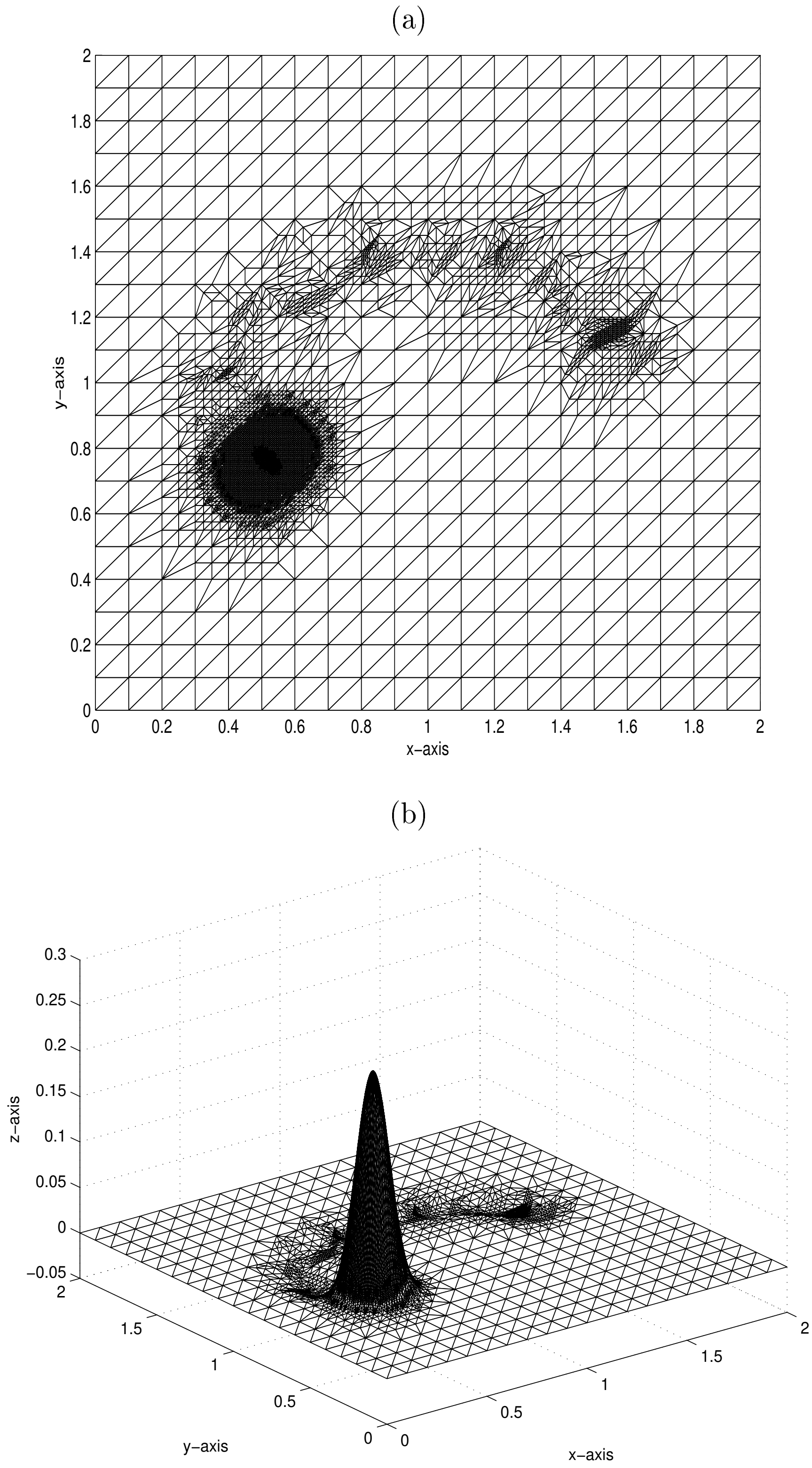

Figure 7.16: At time $t = 0.6$, (a) the adapted meshes and (b) the finite element solution u_{Eh1}.

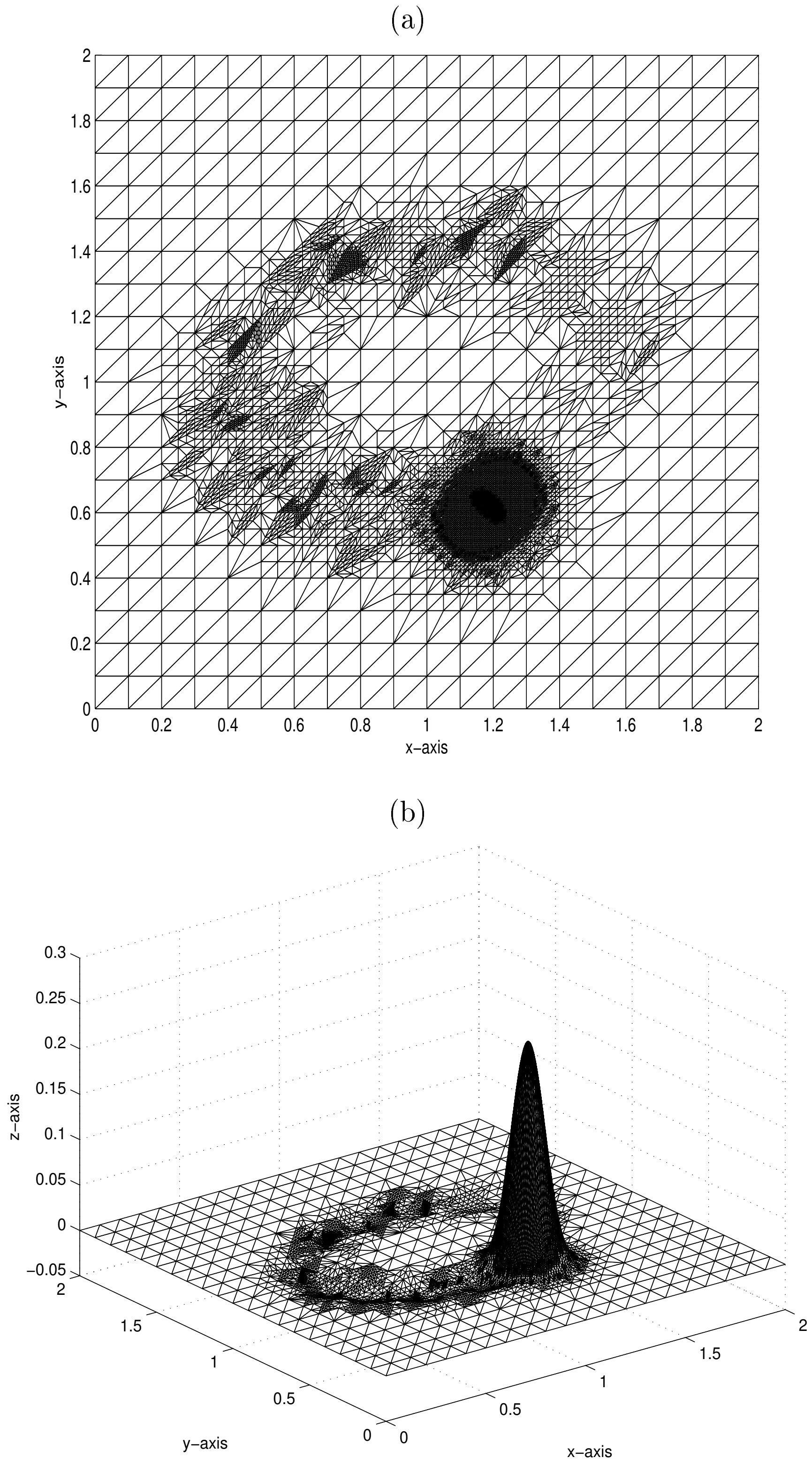

Figure 7.17: At time $t = 0.8$, (a) the adapted meshes and (b) the finite element solution u_{Eh1}.

(a)

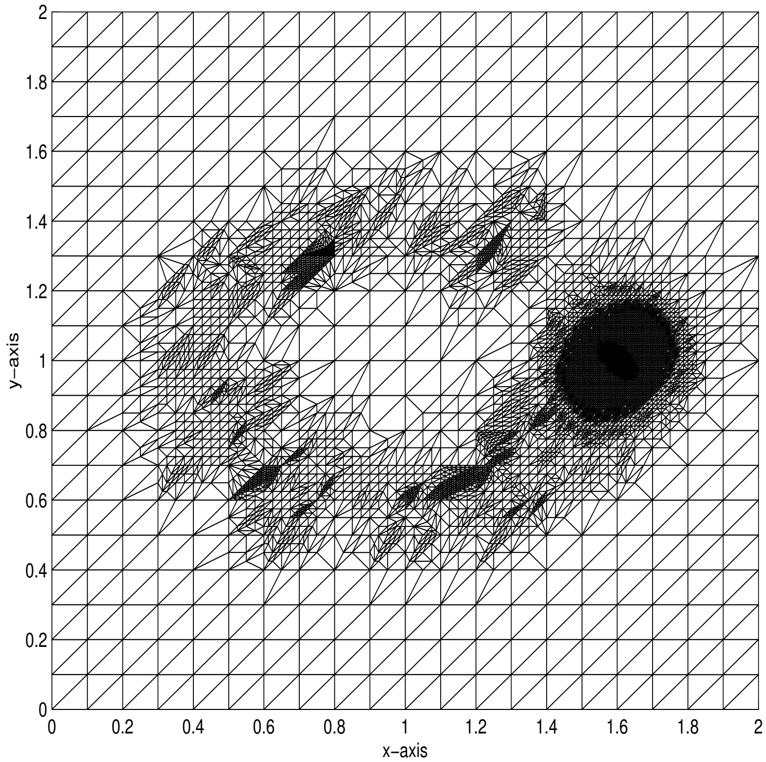

(b)

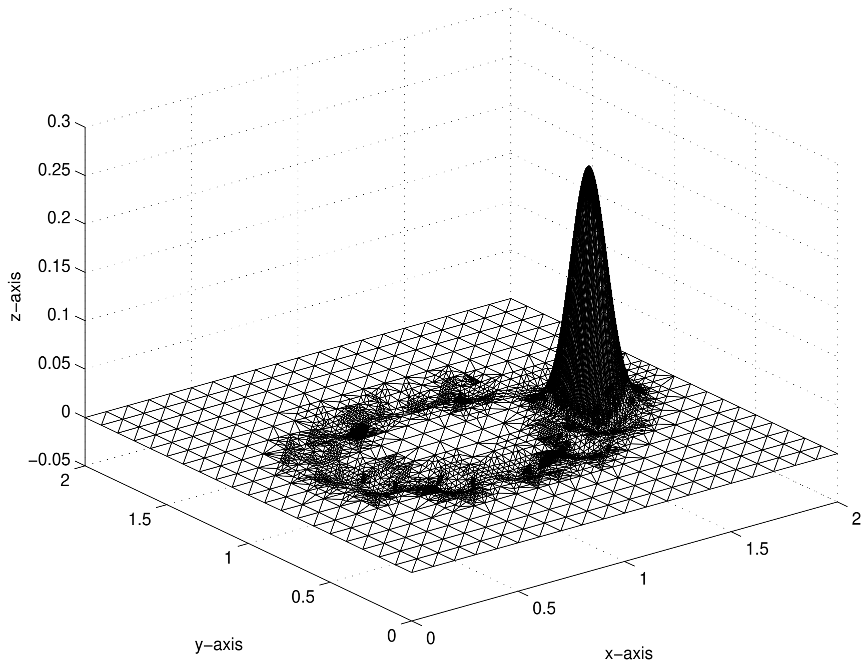

Figure 7.18: At time $t = 1$, (a) the adapted meshes and (b) the finite element solution u_{Eh1}.

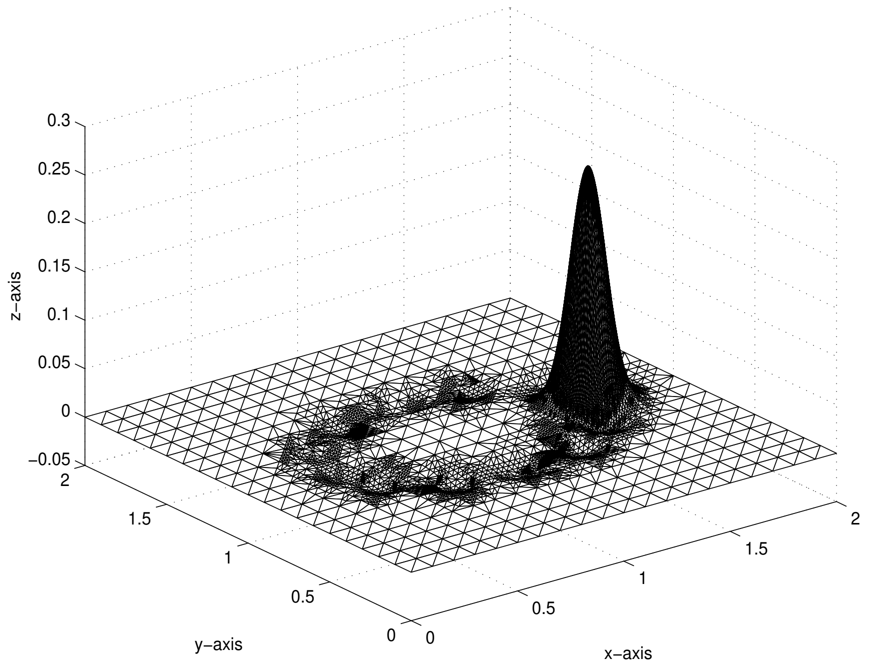

Figure 7.19: The exact elastic displacement, u_{E1}, at $t = 1$.

Tables 7.5 (a)-(c) show the results of the ODE formulation from using the finite element solution and the exact elastic solution with the errors in viscoelastic approximation measured in the (discrete) L_∞, L_2 and energy norms defined previously. The results show that when the exact elastic solution is used the time steps have to be quite small before the convergence rate expected with a Runge-Kutta scheme becomes apparent in the $\%R_{L_\infty}$ computation. When the finite element elastic solution is used instead the results with the $\%R_{L_\infty}$ computation are naturally higher with little improvement when Δt is made smaller than about 0.05 as the errors are dominated by the (spatial) finite element error in solving the elastic problems. The errors in the L_2 and the energy norms depend on the spatial discretization even with the exact elastic solution in these results; here "exact elastic solution" means the piecewise linear interpolant based on the exact model values. This is why the $\%R_{L_2}$ and the $\%R_{en}$ values computed using the exact elastic solution eventually do not decrease much as Δt is decreased further. The same trend is observed when the finite element elastic solution is used.

The results of Table 7.5 are similar to the results of Table 7.2 in Example 1.

Table 7.5: Viscoelastic solutions: the percentage relative error generated by solving the ODE formulation with finite element and exact elastic solutions, respectively. The errors are measured in (a) L_∞ norm, (b) L_2 norm and (c) energy norm.

(a)

time,	$\% R_{L_\infty}$							
	Using finite element solution				Using exact elastic solution			
	time step, Δt				time step, Δt			
t	0.1	0.05	0.025	0.0125	0.1	0.05	0.025	0.0125
0.0	0.5908	0.5908	0.5908	0.5908	0.5908	0.5908	0.5908	0.5908
0.2	5.8509	1.9426	0.7166	0.6940	5.5371	1.4099	0.1317	0.0031
0.4	6.7896	2.2935	0.7921	0.7840	6.1212	1.6344	0.1683	0.0016
0.6	6.0679	1.5647	0.9078	0.7819	5.7764	1.5107	0.1559	0.0016
0.8	7.8934	2.3060	1.5540	1.7019	6.1629	1.6813	0.1808	0.0031
1.0	7.0515	2.4065	2.3079	2.2328	5.6994	1.5682	0.1634	0.0003

(b)

time,	$\% R_{L_2}$							
	Using finite element solution				Using exact elastic solution			
	time step, Δt				time step, Δt			
t	0.1	0.05	0.025	0.0125	0.1	0.05	0.025	0.0125
0.0	2.7872	2.7872	2.7872	2.7872	2.7872	2.7872	2.7872	2.7872
0.2	6.7839	3.5452	3.1319	3.1278	6.1228	1.6554	0.2271	0.1768
0.4	7.6109	4.2637	3.6661	3.6577	6.7457	1.9740	0.2765	0.1667
0.6	6.4922	3.6529	3.3419	3.3265	5.7188	1.5911	0.1878	0.1633
0.8	8.5112	3.6560	3.3556	3.3927	7.0292	2.0846	0.2777	0.1350
1.0	8.3926	3.8734	3.4895	3.5159	7.2765	2.1309	0.2301	0.1273

(c)

time,	$\% R_{en}$							
	Using finite element solution				Using exact elastic solution			
	time step, Δt				time step, Δt			
t	0.1	0.05	0.025	0.0125	0.1	0.05	0.025	0.0125
0.0	4.3807	4.3807	4.3807	4.3807	4.3807	4.3807	4.3807	4.3807
0.2	8.4386	4.8835	4.3067	4.3159	8.4792	4.8603	4.2802	4.2718
0.4	10.0290	5.6585	4.4429	4.4043	10.1098	5.5062	4.2469	4.2051
0.6	11.5438	5.2034	4.4088	4.3925	11.3160	5.2058	4.1320	4.1200
0.8	11.9661	5.9568	5.2454	5.2927	10.4282	5.1804	3.9205	3.8820
1.0	13.0496	7.6141	6.9239	6.9517	11.7462	5.3570	3.8582	3.8131

The numerical results of the ODE formulation using the finite element solutions are compared with the numerical results of the fully discrete formulation in Tables 7.6 (a)-(c). The data from these tables can also be seen in Figures 7.20-7.22 where in each case the dashed line corresponds to the fully discrete scheme and the solid line corresponds to the ODE scheme. In all these cases the error as a result of the time discretization is seen to be 'large' when the time step is $\Delta t = 0.1$ or $\Delta t = 0.05$ (compare the graphs in (a),(b) with (c),(d) in each of the figures.) It is also evident that the ODE scheme is performing better in these large-time-step cases. For the smaller time steps ($\Delta t = 0.025$ and $\Delta t = 0.0125$) the values $\% R_{L_\infty}$, $\% R_{L_2}$ and $\% R_{en}$ do not change much by decreasing the time step Δt further due to the error being dominated by the spatial discretization error. When this is the case the errors are about the same for both the ODE and the fully discrete schemes.

Table 7.6: Errors in the viscoelastic solutions: the percentage relative error generated by solving the ODE formulation with finite element and exact elastic solutions. The errors are measured in (a) L_∞ norm, (b) L_2 norm and (c) energy norm.

(a)

time,	$\% R_{L_\infty}$							
	Using ODE formulation				Using fully discrete formulation			
	time step, Δt				time step, Δt			
t	0.1	0.05	0.025	0.0125	0.1	0.05	0.025	0.0125
0.0	0.5908	0.5908	0.5908	0.5908	0.5908	0.5908	0.5908	0.5908
0.2	5.8509	1.9426	0.7166	0.6940	6.8932	3.4592	1.2476	0.7450
0.4	6.7896	2.2935	0.7921	0.7840	6.8265	4.4347	1.1708	0.7636
0.6	6.0679	1.5647	0.9078	0.7819	9.8411	3.0493	1.0603	0.6993
0.8	7.8934	2.3060	1.5540	1.7019	6.5211	5.5109	2.1028	1.6617
1.0	7.0515	2.4065	2.3079	2.2328	11.8733	5.0836	2.1169	2.2100

(b)

time,	$\% R_{L_2}$							
	Using ODE formulation				Using fully discrete formulation			
	time step, Δt				time step, Δt			
t	0.1	0.05	0.025	0.0125	0.1	0.05	0.025	0.0125
0.0	2.7872	2.7872	2.7872	2.7872	2.7872	2.7872	2.7872	2.7872
0.2	6.7839	3.5452	3.1319	3.1278	10.1713	5.9094	3.2473	3.1194
0.4	7.6109	4.2637	3.6661	3.6577	8.9218	6.2559	3.7087	3.5896
0.6	6.4922	3.6529	3.3419	3.3265	13.0441	5.8491	3.2283	3.1804
0.8	8.5112	3.6560	3.3556	3.3927	9.8502	7.1334	3.4306	3.1684
1.0	8.3926	3.8734	3.4895	3.5159	14.9990	7.0923	3.4866	3.3515

(c)

time,	$\% R_{en}$							
	Using ODE formulation				Using fully discrete formulation			
	time step, Δt				time step, Δt			
t	0.1	0.05	0.025	0.0125	0.1	0.05	0.025	0.0125
0.0	4.3807	4.3807	4.3807	4.3807	4.3807	4.3807	4.3807	4.3807
0.2	8.4386	4.8835	4.3067	4.3159	11.4656	7.6605	4.5322	4.3190
0.4	10.0290	5.6585	4.4429	4.4043	13.1501	9.0811	4.8812	4.4057
0.6	11.5438	5.2034	4.4088	4.3925	16.4050	10.0679	4.4112	4.3838
0.8	11.9661	5.9568	5.2454	5.2927	14.9531	10.2746	5.7889	5.2170
1.0	13.0496	7.6141	6.9239	6.9517	22.9677	12.8785	7.2593	6.9194

(a)

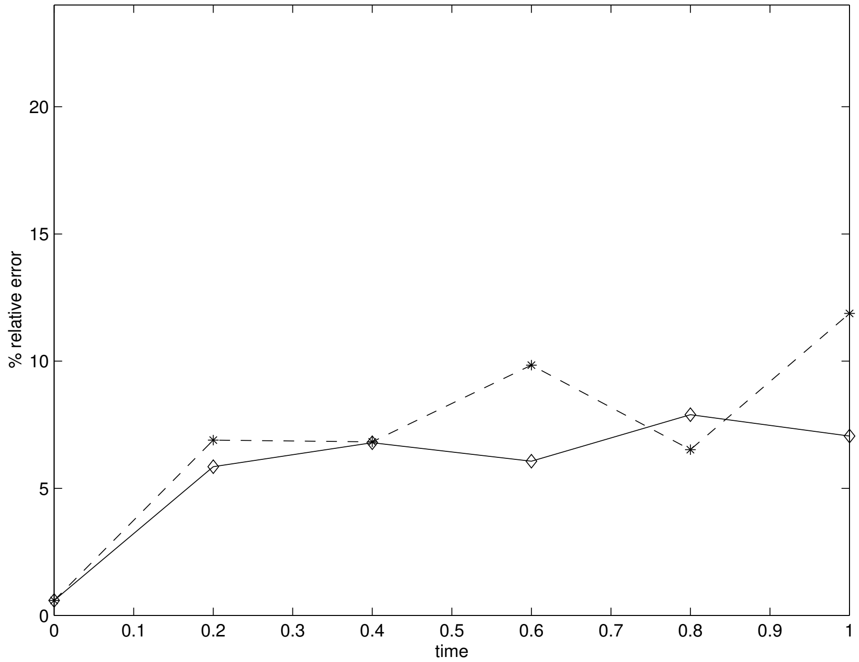

(b)

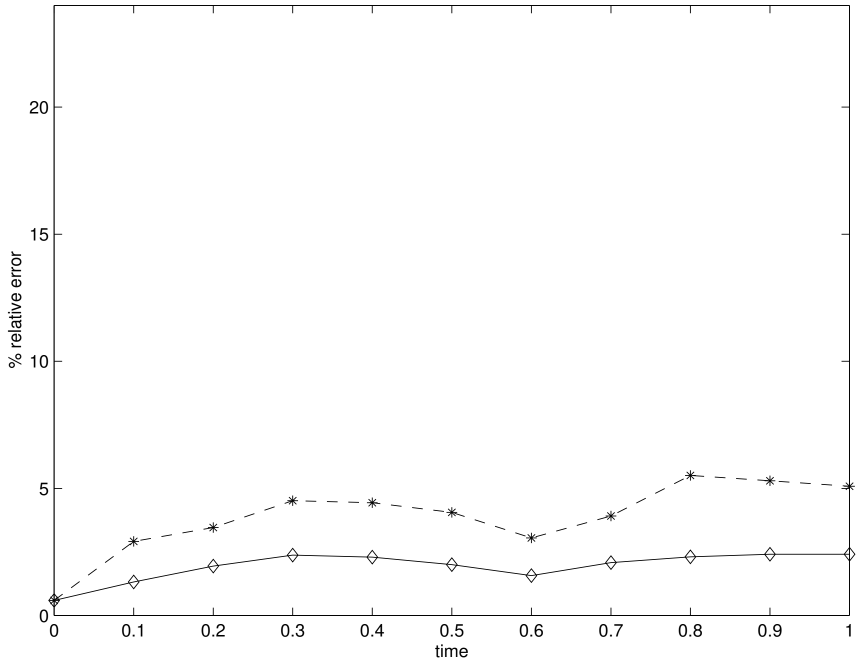

Figure 7.20

See caption on page 134

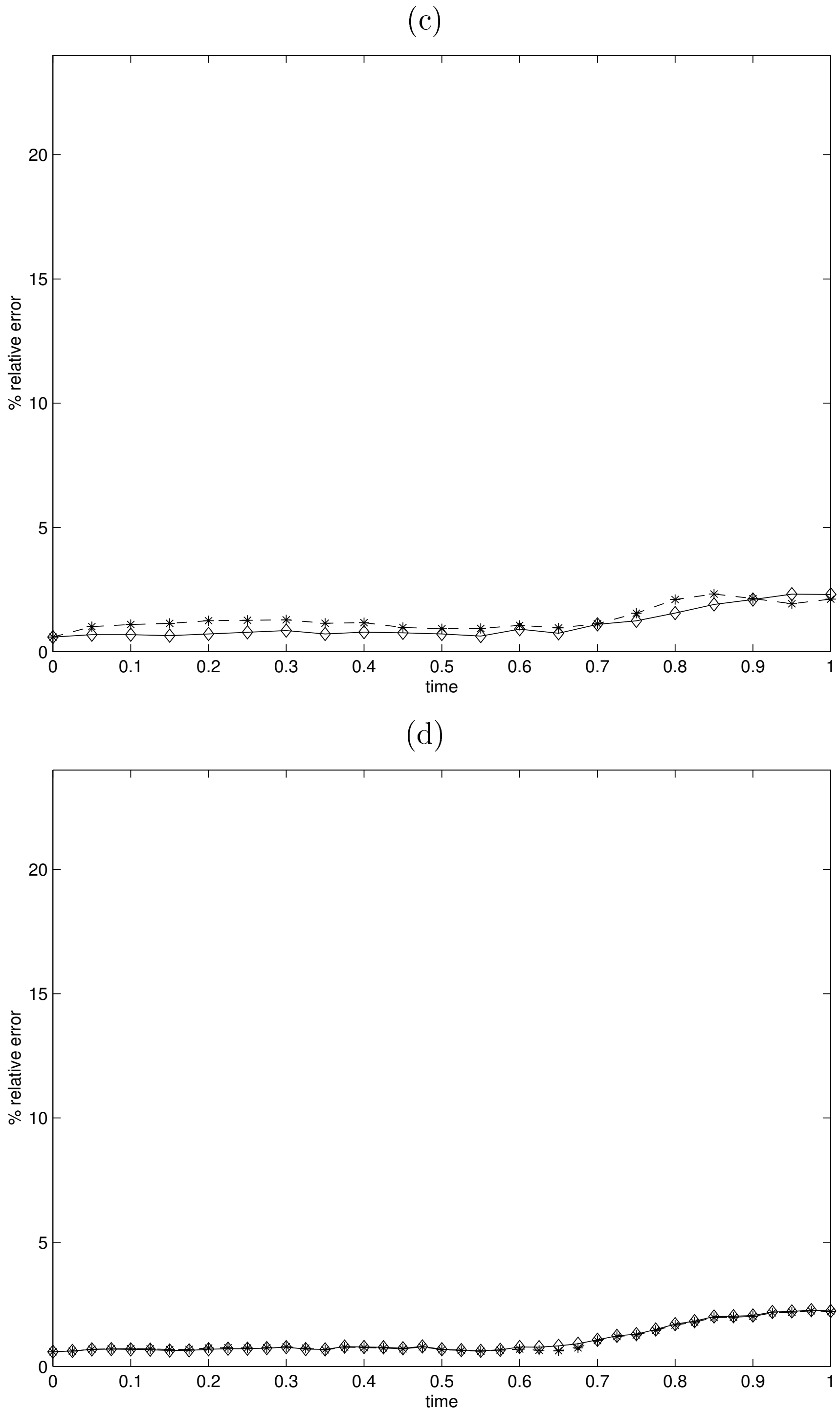

Figure 7.20: The evolution of the percentage relative error obtained using the ODE formulation(solid line marked with diamonds) and the fully discrete formulation (broken line marked with stars). The errors are measured in L_∞ norm and the time step is chosen to be (a) $\Delta t = 0.1$, (b) $\Delta t = 0.05$, (c) $\Delta t = 0.025$ and (d) $\Delta t = 0.0125$.

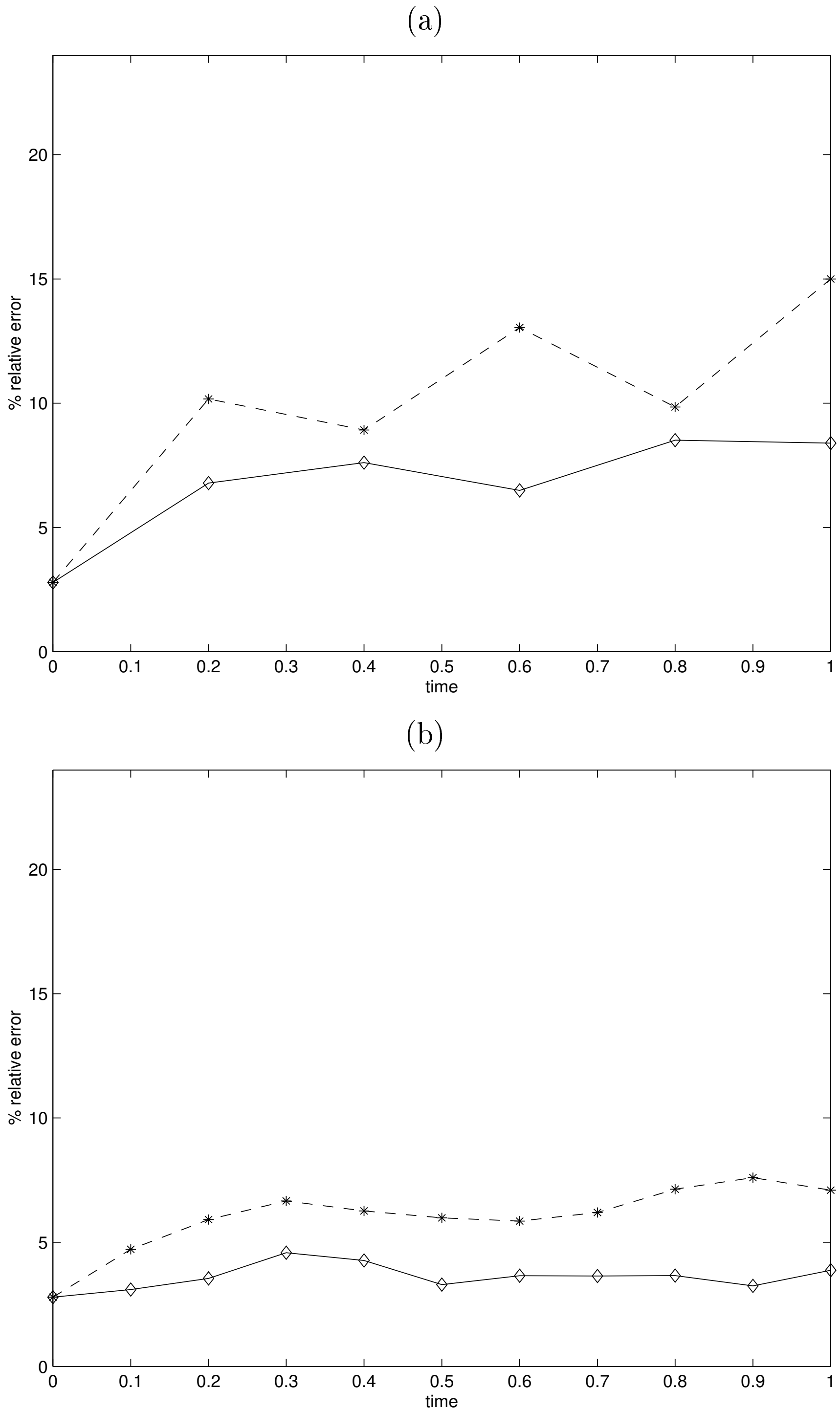

Figure 7.21

See caption on page 136

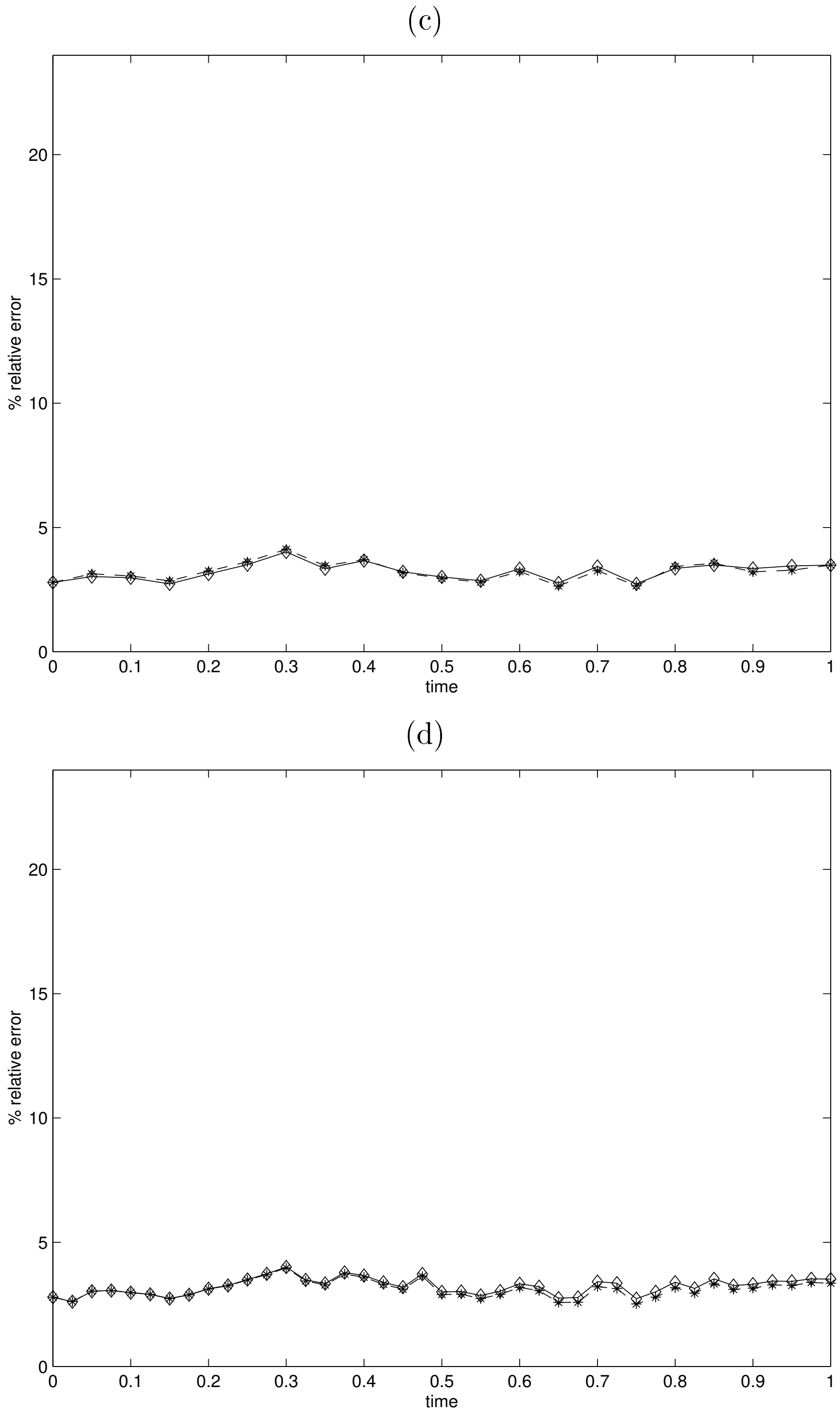

Figure 7.21: The evolution of the percentage relative error obtained using the ODE formulation(solid line marked with diamonds) and the fully discrete formulation (broken line marked with stars). The errors are measured in L_2 norm and the time step is chosen to be (a) $\Delta t = 0.1$, (b) $\Delta t = 0.05$, (c) $\Delta t = 0.025$ and (d) $\Delta t = 0.0125$.

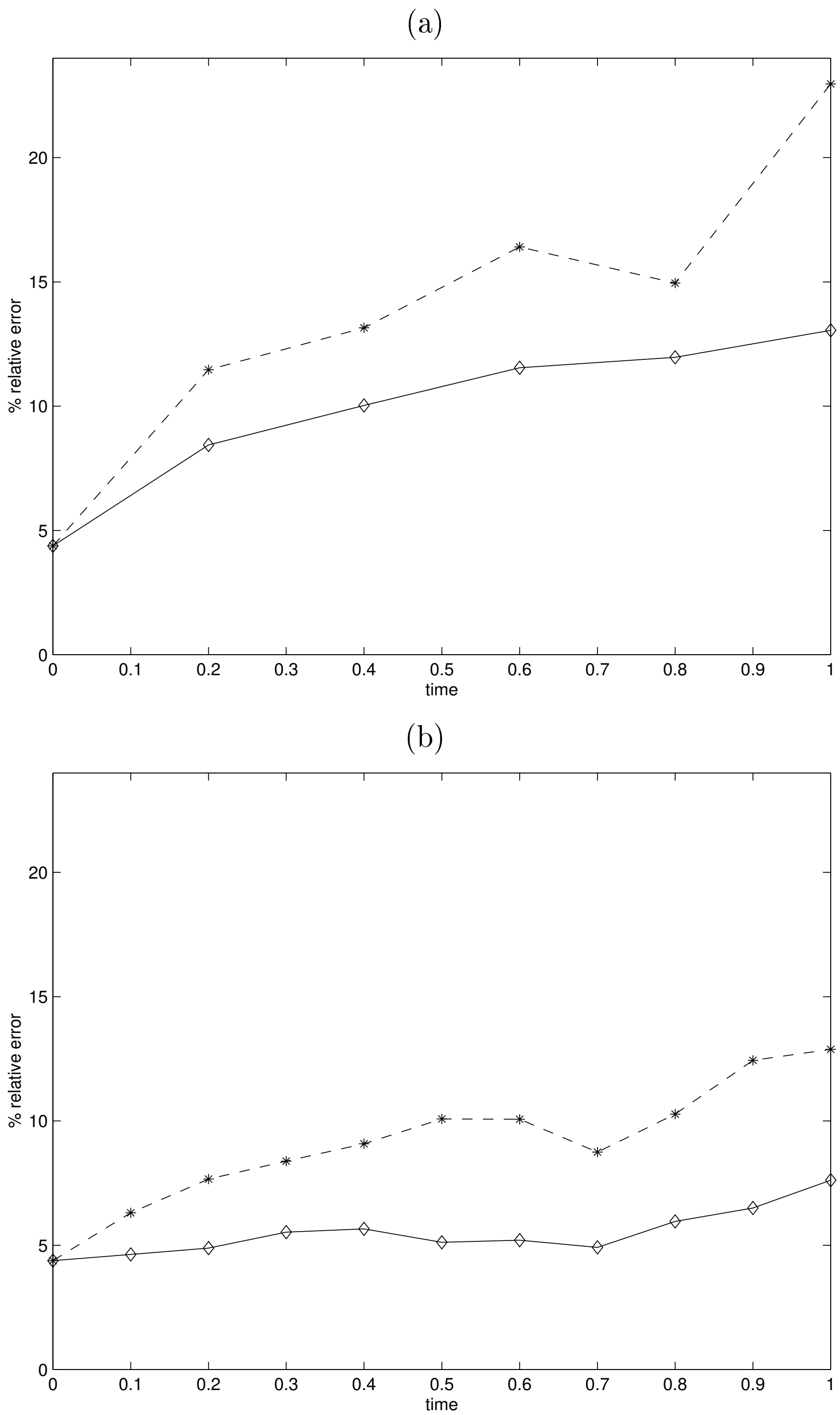

Figure 7.22

See caption on page 138

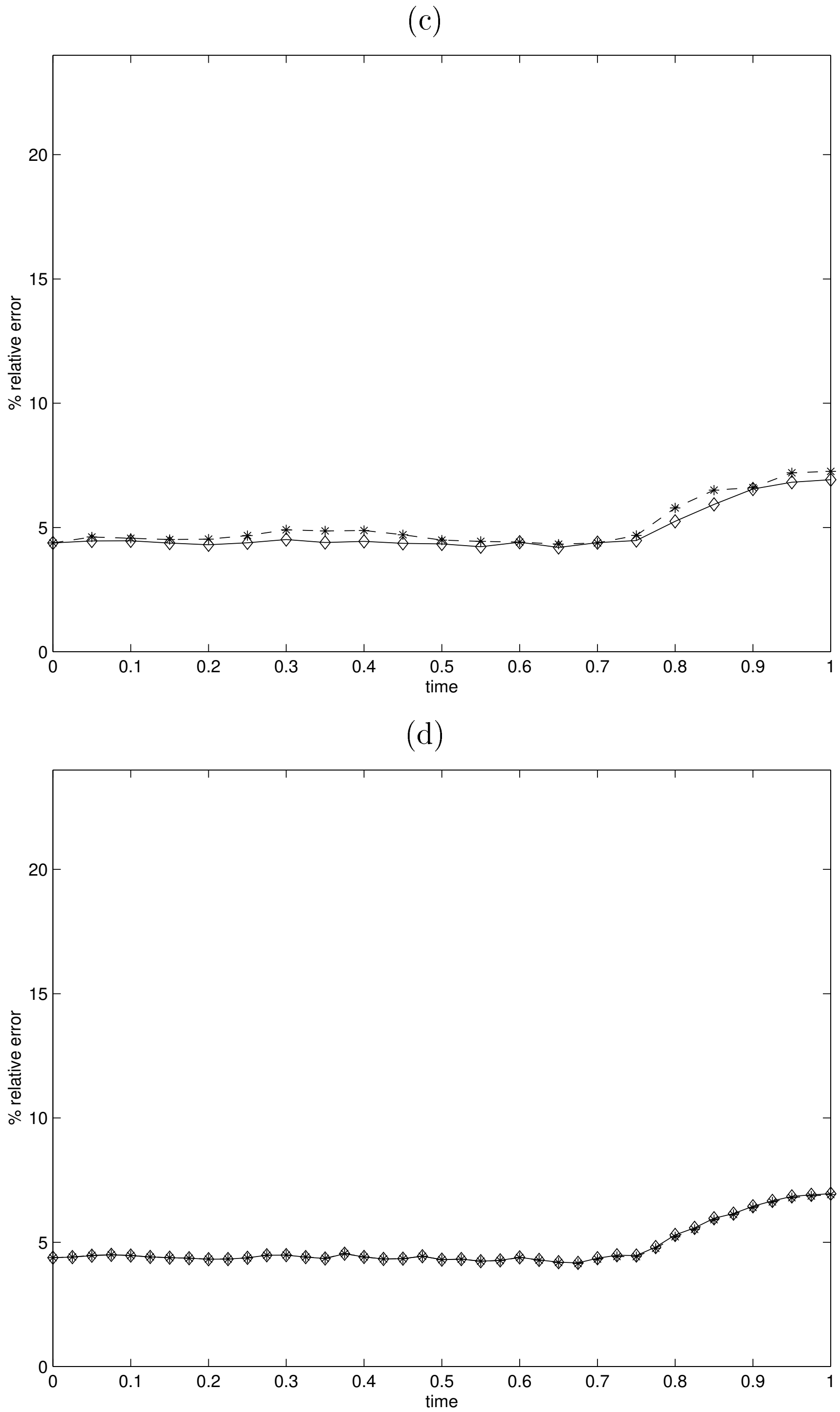

Figure 7.22: The evolution of the percentage relative error obtained using the ODE formulation(solid line marked with diamonds) and the fully discrete formulation (broken line marked with stars). The errors are measured in energy norm and the time step is chosen to be (a) $\Delta t = 0.1$, (b) $\Delta t = 0.05$, (c) $\Delta t = 0.025$ and (d) $\Delta t = 0.0125$.

Chapter 8

Conclusions

This thesis has been concerned with the numerical approximation of quasi-static linear viscoelastic problems involving homogeneous, non-ageing, synchronous, quasi-separable kernels and compressible solids. The object of this research has been to present numerical models of linear viscoelastic problems for this special case. The main contribution is the implementation and experimentation of a finite element/ ODE scheme for numerically solving this type of problem. The numerical results show that the scheme performs well in this context and compares favourably with the fully discrete scheme.

Both schemes outlined in sections 6.1 and 6.2 exploit the fact that the relaxation functions are quasi-separable. In this case a classical method allows the Volterra equation to be recast using the ODE form. The ODE formulation concerns the coupling of the finite element technique in space with ODE solvers in time to model the deformation of a certain class of viscoelastic materials. In section 6.2 we took the most general route to the time discretization of the linear viscoelastic problems by treating their semidiscrete analogues as Volterra equations. Then the fully discrete formulation is created by replacing the history integral with the trapezoidal rule for numerical integration.

The Dirichlet series choice for the relaxation functions, (6.5), has the advantage that the entire solution history can be stored in an efficient way. This is important in forming numerical schemes because the memory requirement, and operation counts, remain constant throughout the time stepping. This is not the case with general Volterra equations since the memory must be carried forward as the time stepping advances.

The numerical algorithms of the ODE and the fully discrete formulations have been described in section 6.3. It has been verified that they can effectively eliminate the solution history storage problem, in the sense that the fully discrete formulation produced the viscoelastic solutions, $\mathbf{u}(t_i)$, at current time step using the values of the previous $\mathbf{u}(t_{i-1})$ and the vector $\mathbf{r}_j(t_{i-1})$. Similarly, the ODE formulation needs to preserve the values of the two previous finite element solutions, $\mathbf{u}_{Eh}(t_{i-1})$ and $\mathbf{u}_{Eh}(t_{i-2})$, and the value of the previous vector $\mathbf{P}(t_{i-2})$ for computing the viscoelastic solutions $\mathbf{u}(t_i)$ at the current time step. It is obvious that the number of arithmetic operations and the storage requirement remain constant in time.

Finite element techniques are used for solving the weak formulation of the linear elasticity problem. An error indicator has been derived based on the work of Zienkiewicz and Zhu [48], [49] to estimate the error in the energy norm. The indicators identify those parts of the mesh which induce large errors. Using this information, the local mesh is then refined and the finite element computation is repeated. If necessary, this process can be repeated until an optimal mesh is obtained. In the numerical examples tested we conclude that the Z^2 error estimator (see page 46) is effective and that the finite element solutions are convergent.

The ODE and the fully discrete formulations have been tested on two demanding model viscoelastic problems for numerical verification. The numerical results of both formulations have been reported in terms of relative errors. In a series of numerical experiments it has been shown that the performance of the ODE formulation is better than the fully discrete formulation for large time steps. This is due, as detailed in section 7.3, to the fact that the fourth-order Runge Kutta is used in the ODE formulation for solving the system of ODEs and the fully discrete formulation uses the trapezoidal rule for approximating the hereditary integral. Both formulations, however, are competitive for very small time steps.

Much work is currently being undertaken in BICOM on the development of space-time finite element schemes for problems of viscoelasticity, and on *a posteriori* error estimates and adaptive meshing schemes for the case of linear viscoelasticity.

The ODE technique illustrated here is limited to the linear viscoelasticity case due to the need for quasi-separability in the expression for the relaxation function.

References

[1] J.E. Akin. *Finite Elements for Analysis and Design.* Academic Press, 1994.

[2] R.E. Bank. The efficient implementation of local mesh refinement algorithms. *in Adaptive Computational Methods for Partial Differential Equations*, (ed. Babuska, I., Chandra, J. and Flaherty, J.E.):74–81, Society for Industrial and Applied Mathematics, Philadelphia, 1983.

[3] D. Braess. *Finite Element Theory, Fast Solvers, and Applications in Solid Mechanics.* Cambridge University Press, 1997.

[4] S.C. Brenner and L.R. Scott. *The Mathematical Theory of Finite Element Methods.* Springer-Varlag, 1994.

[5] R.L. Burden and J.D. Faires. *Numerical Analysis.* Brooks/Cole Publishing Company, 1997.

[6] S.C. Chapra. *Numerical Methods for Engineers with Programming and Software Applications.* WCB/McGraw-Hill, 1998.

[7] R.M. Christensen. *Theory of Viscoelasticity, an Introduction.* Academic Press, 1971.

[8] P.G. Ciarlet. *Introduction to Numerical Linear Algebra and Optimisation.* Cambridge Univertisity Press, 1989.

[9] K. Eriksson, D. Estep, P. Hansbo, and Johnson. C. *Computational Differential Equations.* Cambridge University Press, 1996.

[10] G. Fairweather. *Finite Element Galerkin Methods for Differential Equations.* Marcel Dekker, 1978.

[11] W.N. Findley, J.S. Lai, and K. Onaran. *Creep and Relaxation of Nonlinear Viscoelastic Materials with an Introduction to Linear Viscoelasticity.* Dover Publications, 1976.

[12] W. Flügge. *Viscoelasticity.* Blaisdell Publishing Company, 1967.

[13] C.F. Gerald and P.O. Wheatley. *Applied Numerical Analysis.* Addison-Wesley Publishing Company, 1994.

[14] G.H. Golub and C.F. Van Loan. *Matrix Computations.* The Johns Hopkins University Press, 1996.

[15] S.C. Hunter. *Mechanics of Continuous Media.* John Wiley & Sons, 1976.

[16] V. Janvosky, S. Shaw, M.K. Warby, and J.R. Whiteman. Numerical methods for treating problems of viscoelastic isotropic solid deformation. *J. Comput. Appl. Math.*, 63:91–107, 1995.

[17] J.A. Kirby. *Superconvergence and Error Estimation of Finite Element Solutions to Fire-exposed Frame Problems.* PhD thesis, Department of Mathematical Sciences, Brunel University, Uxbridge, England, 2000.

[18] C.K. Lee and S.H. Lo. An automatic adaptive refinement finite element procedure for 2d elastostatic analysis. *International Journal for Numerical Methods in Engineering*, 35:1967–1989, 1992.

[19] X.D. Li and N.E. Wiberg. A posteriori error estimate by element patch post-processing, adaptive analysis in energy and l_2 norms. *Computers & Structures*, 53:907–919, 1994.

[20] P. Linz. *Analytical and Numerical Methods for Volterra Equations.* Society for Industrial and Applied Mathematics, Philadelphia, 1985.

[21] F.J. Lockett. *Nonlinear Viscoelastic Solids.* Academic Press, 1972.

[22] R.R. Long. *Mechanics of Solids and Fluids.* Prentice-Hall, Englewood Cliffs, N.J., 1961.

[23] M.J. Ludwig. *Adaptive Finite Element Methods with A Posteriori Error Estimates for Elliptic Problems.* M.Sc. Thesis, Department of Mathematical Sciences, Brunel University, Uxbridge, England, 1994.

[24] M.J. Ludwig. *Finite Element Error Estimation and Adaptivity for Problems of Elasticity.* PhD thesis, Department of Mathematical Sciences, Brunel University, Uxbridge, England, 1998.

[25] J.T. Marti. *Introduction to Sobolev Spaces and Finite Element Solution of Elliptic Boundary Value Problems.* Academic Press, 1986.

[26] J.T. Oden. *Mechanics of Elastic Structures.* John Wiley & Sons, 1967.

[27] J.T. Oden, L. Demkowicz, W. Rachowicz, and T.A. Westermann. Toward a unversal h-p adaptive finite element strategy, part 2. a posteriori error estimation. *Computer Methods in Applied Mechanics and Engineering*, 77:113–180, 1989.

[28] J.T. Oden and J.N. Reddy. *An introduction to the Mathematical Theory of Finite Elements.* McGraw-Hill, 1976.

[29] A.C. Pipkin. *Lectures on Viscoelasticity Theory.* Springer-Varlag, 1972.

[30] M.C. Rivara. Algorithms for refining triangular grids suitable for adaptive and multigrid techniques. *International Journal for Numerical Methods in Engineering*, 20:745–756, 1984.

[31] M.C. Rivara. Mesh refinement processes based on the generalized bisection of simplices. *SIAM Journal on Numerical Analysis*, 21:604–613, 1984.

[32] D. Ronald. *Viscoelastic Fluids, An Introduction to Their Properties and Behavior.* Marcel Dekker, 1976.

[33] H.R. Schwarz. *Finite Element Methods.* Academic Press, 1988.

[34] S. Shaw. *Finite Element and Discrete Time Methods for Continuum Problems with Memory and Applications to Viscoelasticity.* PhD thesis, Department of Mathematical Sciences, Brunel University, Uxbridge, England, 1993.

[35] S. Shaw, M.K. Warby, and J.R. Whiteman. Numerical techniques for problems of quasistatic and dynamic viscoelasticity. *The Mathematics of Finite Elements and Applications, Highlights. MAFELAP 1993*, pages 45–68. John Wiley & Sons, Chichester, 1994.

[36] S. Shaw, M.K. Warby, and J.R. Whiteman. *An Introduction to the Theory and Numerical Analysis of Viscoelasticity Problems.* BICOM, Brunel University, Uxbridge, England, 1997.

[37] S. Shaw, M.K. Warby, J.R. Whiteman, C. Dawson, and M.F. Wheeler. Numerical techniques for the treatment of quasistic viscoelastic stress problems in linear isotropic solids. *Computer Methods in Applied Mechanics and Engineering*, 118:211–237, 1994.

[38] S.L. Sobolev. *Partial Differential Equations of Mathematical Physics.* Dover Publications, 1964.

[39] A.J.M. Spencer. *Continuum Mechanics.* Longman Scientific and Technical, 1994.

[40] G. Strang and G.J. Fix. *An Analysis of the Finite Element Method.* Prentice-Hall, Englewood Cliffs, N.J., 1973.

[41] N.W. Tscgoegl. *The Phenomenological Theory of Linear Viscoelastic Behavior An Introduction.* Springer-Varlag, 1989.

[42] B. Venkatraman and S.A. Patel. *Structural Mechanics with Introductions to Elasticity and Plasticity.* McGraw-Hill, 1970.

[43] R. Wait and A.R. Mitchell. *Finite Element Analysis and Applications.* John Wiley & Sons, 1985.

[44] J.R. Whiteman. *Finite Element Course Notes.* BICOM, Brunel University, Uxbridge, England, 1998.

[45] J.R. Whiteman, A.E. Beagles, and M.K. Warby. Theoretical and practical aspects of finite elements in the context of some problems of solid mechanics. *Jber. d. Dt. Math.-Verein.*, 92:77–88, 1990.

[46] J.Z. Zhu and O.C. Zienkiewicz. Adaptive techniques in the finite element method. *Communications in Applied Numerical Methods*, 4:197–204, 1988.

[47] O.C. Zienkiewicz and J.Z. Zhu. A simple error estimator and adaptive procedure for practical engineering analysis. *International Journal for Numerical Methods in Engineering*, 24:337–357, 1987.

[48] O.C. Zienkiewicz and J.Z. Zhu. The superconvergent patch recovery and a posteriori error estimates. part 1: The recovery technique. *International Journal for Numerical Methods in Engineering*, 33:1331–1364, 1992.

[49] O.C. Zienkiewicz and J.Z. Zhu. The superconvergent patch recovery and a posteriori error estimates. part 2: Error estimates and adaptivity. *International Journal for Numerical Methods in Engineering*, 33:1365–1382, 1992.